Abstract

PASTEUR, ROGER DREW II. A Multiple-Inhibin Model of the Human Menstrual Cycle. (Under the direction of James F. Selgrade).

Inhibin is one of several hormones which collectively regulate the human female reproductive endocrine system. In recent years, physiologists have been able to separately assay two forms of inhibin. We begin by discussing the physiology and endocrinology that underlie the menstrual cycle. Then, we fit an existing delay differential equation model of the human menstrual cycle to new data describing average hormone levels of young women throughout the menstrual cycle. Next, we consider the existence and stability of equilibrium and periodic solutions, analyze bifurcations, and perform a sensitivity analysis. We compare and contrast these results to previously published results based on the same model but a different data set. Because the introduction of exogenous hormones, whether pharmacological or environmental, can have significant effects on the menstrual cycle, we model the effects of these external hormones. Next, we introduce an expanded model that more fully accounts for the actions of both forms of inhibin. We optimize the parameters to fit the data, then discuss the equilibrium and periodic solutions, bifurcations, and sensitivity for this new model and parameter set. Next, we use the model to consider the effects of exogenous pharmacological hormones. Finally, we discuss the effects on the menstrual cycle of age-related hormone production changes that occur during the peri-menopausal years. This leads to a second parameter set, with only a few variations from the first one, for which the model approximates the monthly hormonal fluctuations for a woman around age 40. In closing, we discuss future possibilities for this line of research.

A Multiple-Inhibin Model of the Human Menstrual Cycle

by
Roger Drew Pasteur, II

A dissertation submitted to the Graduate Faculty of
North Carolina State University
In partial fulfillment of the
Requirements for the degree of
Doctor of Philosophy

Applied Mathematics

Raleigh, North Carolina

June 10, 2008

APPROVED BY:

_____	_____
James F. Selgrade Advisory Committee Chair	John E. Franke
_____	_____
Robert H. Martin	Ernest L. Stitzinger

Dedication

To my wife Heather,

who has always supported me during

the past six years of graduate school,

and to my parents Roger & Pat Pasteur,

who gave me opportunities they never had.

Biography

Roger “Drew” Pasteur, II was born in the Raleigh-Durham metro area, although his family lived in Wilmington, North Carolina at the time. After moving to Wake County at age six, he attended public schools in Raleigh, and graduated from William G. Enloe High School in 1993. A mathematics major at the University of Florida, he graduated with honors at age twenty, then earned a master’s degree in math education the following year. After some additional classroom and internship work to become a Certified Athletic Trainer, Drew returned to the Raleigh area in 1998. He spent four years on the faculty of Fuquay-Varina High School, as a math teacher, head athletic trainer, and advisor to the Fellowship of Christian Athletes chapter, before resigning to pursue mathematics graduate work full-time at N.C. State University.

He earned a Master of Science degree in mathematics in 2004, followed by a Doctor of Philosophy in applied mathematics in 2008. While on a teaching assistantship at NCSU, Drew taught nearly 800 students, mostly in the engineering calculus sequence. In 2004, he received the math department’s Armstrong Maltbie award for excellence in teaching, and was nominated for a university-wide teaching award in the same year. He has accepted a tenure-track faculty position at the College of Wooster, a selective liberal arts college in Wooster, Ohio.

In 2003, he married Heather Harris, an alumna of nearby Meredith College, a year after they met in their church choir. They have one child, Daniel, who was born in 2007.

Acknowledgements

Although writing a dissertation is typically a solitary pursuit, the journey to the point of being ready to do so requires the assistance of many others. Without the knowledge, wisdom, and support of those around me, I could never have made it this far, so I am most grateful for their investments in me.

Upon arriving at NCSU six years ago, I quickly became part of a close-knit group of nine new graduate students in the mathematics department. With the exception of one rising star, John David, we were not the most promising students in our class, for a variety of reasons. Some had merely adequate, not exceptional, academic records, and several had graduated from small colleges with weak mathematics departments not known for sending students to graduate math programs. In my case, I had spent the previous five years in the high schools, away from college-level math, and had forgotten much of what I learned years before. Our weaknesses helped bring us together, as most of us met in a small, undergraduate-level real analysis class during the summer before our first year. Rather than competing for grades, we helped one another, to the benefit of all. This trend continued through multiple classes together over our first two years, and especially during a summer spent preparing together for the written Ph.D. qualifying exams (on which we collectively posted a 95% rate of passing on the first attempt). Even after we progressed to the point that we could no longer assist one another with the mathematics of individual research projects, we have still offered encouragement and support. We have shared in the joys of weddings and the birth of children,

celebrated one another's graduations and job-hunting successes, and helped each other overcome discouragement when things got difficult. Typically, about half of all students who begin pursuing a mathematics Ph.D. will eventually earn it; despite our weaker backgrounds, it appears that seven of the nine of us will complete our degrees, far outpacing what would have been expected. Of the two that did not finish, one left NCSU because of a call into vocational Christian ministry. My sincerest thanks are given to these eight colleagues who made this journey along with me:

- Jordan West Bostic (M.S. 2005, expected Ph.D. 2009)
- Prakash "Kang" Chanchana (M.S. 2004, Ph.D. 2007)
- John David (M.S. 2004, Ph.D. 2007)
- Desiree Jordan Howard
- Brad Hughes (M.S. 2004)
- Rebecca Smith Wills (M.S. 2004, Ph.D. 2007)
- Suthathip "Benz" Suanmali (M.S. 2005, Ph.D. 2007)
- Laurie Zack (M.S. 2005, Ph.D. 2007)

Besides these eight, there are other graduate students who came along later, but also became both helpful colleagues and trusted friends, including Rebecca Burton Kalhorn, Stacy Beun, April Alston, Ryan Siskind, Monique Taylor, James Cook, Julie Beier, Jon & Stacey Ernstberger, Brandy Benedict, Mike Allocca, and Ryan Therkelsen, and others.

The guidance of the math department faculty at NCSU has also been instrumental in my development as a mathematician. In particular, I wish to thank my research adviser, Dr. James Selgrade, for all of the time and energy he put into guiding me over the last three years. When I began working with him, I anticipated receiving technical instruction from an expert in dynamical systems and mathematical modeling. However, I was pleasantly surprised that Dr. Selgrade also became a professional mentor to me, guiding me not just in researching and writing a dissertation, but also in the job search process, as I sought out my first post-secondary faculty position. Because of his patience with, and appreciation of, my family and community responsibilities, I have been able to maintain a balanced life while a graduate student.

Other faculty and staff members have been most beneficial in other ways. Dr. Ernie Stitzinger was the face of the math department to me when I first applied to the program, and was the person I went to for advice until I began doing research with Dr. Selgrade; he always had an open door, a listening ear, and good counsel. During my first summer at NCSU, I was a student in Dr. John Franke's undergraduate analysis class. Through a combination of hard work and his outstanding teaching, I was very successful in learning material which had eluded me as an undergraduate, and that gave me confidence as I began graduate school. Dr. Bob Martin has been a role model to me, as he is a true gentleman, a faithful Christian, and an excellent teacher whose humor keeps a class lively. I also want to express my appreciation to Denise Seabrook, Di Bucklad, and Carolyn Gunton, three women who keep the math department running smoothly, and do so with a smile and a kind word.

A teaching assistantship sponsored by the math department helped make graduate school financially feasible, but was more than just a source of income for me. My experiences teaching at NCSU have made it clear that I do my best work in the classroom, helping undergraduates to learn mathematics. I am very grateful to Dr. John Griggs and Dr. Harvey Charlton, for the faith that they put in me, and the terrific opportunities that they gave me. In the first regular semester I was eligible to teach a class, I was entrusted with an engineering calculus class, and did my best not to disappoint. Being able to teach integral and multivariable calculus several times each gave me the chance to learn what practices worked best for me in a college classroom. Drs. Griggs and Charlton also allowed me to teach differential equations and linear algebra; these uncommon experiences were invaluable, and made my applications stand out, when I began applying for academic jobs last year. I also want to thank the nearly 800 men and women whom I have been privileged to teach at NCSU. Not only were they bright and motivated, but also personable and intellectually curious. Having such great students inspired me to want to excel as a classroom teacher.

Others in the field of education also remain in my mind as I near the end of this project. The faculty and staff of Fuquay-Varina High School, and particularly the two principals I worked under, Charles Rose and Gerald Pickett, were understanding and supportive when I made the difficult decision to leave their faculty to pursue a doctoral degree. The FVHS family continues, to this day, to welcome me as one of their own whenever I visit the campus. As a teenager, several of my teachers at Enloe High School made a lasting impact on me: Craig Baker used

athletics as a vehicle to teach life lessons, Joel Adams' love for music taught me the value of passion for one's subject area, Ron Robinson prepared me to excel in calculus and beyond, and Doug Alexander made it clear that personal faith does have a place in public education. Earlier still, participation on a state champion MATHCOUNTS team at Ligon Middle School, led by Barbara Sydnor, helped spur my interest in non-routine mathematics problems.

My family has been a continual source of inspiration and encouragement throughout my time at NCSU. My wife Heather has supported me, both emotionally and financially, and never wavered in her belief in me; she has been an incredible blessing to me! From the time I was a small child, my parents have taught me to be devoted to my education, and to pursue it diligently, but also to keep a sense of balance, as there is more to life than work. That advice has been more helpful than ever, as I have juggled the multiple responsibilities of classes, research, teaching, family, church leadership roles, and community involvement. I would also be remiss if I failed to mention my young son Daniel. While he will not remember his father working on this dissertation, his gentle touch and bright smile have motivated me to press ahead on the days when I have become frustrated with my research.

Finally, I want to give glory to my Lord and Savior, Jesus Christ, apart from whom I can do nothing. "Whatever you do, work at it with all your heart, as working for the Lord, not for men…" Colossians 3:23 (NIV)

Table of Contents

List of Tables

List of Figures

Chapter 1

Introduction

The human endocrine system has a complexity that is surpassed only by the nervous system. In the human female reproductive endocrine system, there are three sources of hormone production: the hypothalamus, the pituitary gland and the ovaries. The hormones produced in these three locations are involved in regulation of one another. Together, they control the processes surrounding ovulation and menstruation, primarily via feedback from the ovaries to the pituitary (Speroff et al., 1999). While substantial medical research has been done in the hope of fully understanding the interactions among these hormones, science has not yet achieved that goal. Many of the regulatory aspects among sexual hormones are well-understood physiologically, but relatively little research has been done in the area of mathematically modeling the hormone interactions (Reinecke and Deuflhard, 2007).

The oral introduction of external hormones as a pharmaceutical treatment is now common, for reasons including contraception, treatment of irregular or abnormal menstrual cycles, and to suppress unwanted effects of menopause. There is also rising concern over the potentially dangerous effects of unintentional intake of hormones, particularly xenoestrogens, from food (Davis et al., 1993) and drinking water (Rudel et al., 1998). Because breast cancer risk is related to total lifetime exposure to bioavailable

estrogens, there is significant anxiety regarding the long-term dangers of exposure to these estrogenic compounds, regardless of their source (Davis et al., 1993). Given that there are individual variations in menstrual dynamics, a deterministic mathematical model is unlikely to predict with certainty the results of external influences on the reproductive endocrine system. However, such a model could provide insight that might suggest a particular course of action in new clinical medical research studies.

Over the last three decades, significant progress has been made in mathematically modeling this system. Some previous models for this system, such as (Plouffe and Luxenburg, 1992), were based on general-use computer software. More recent research often involved large-scale models, such as (Reinecke and Deuflhard, 2007), and would not have been possible without high-speed computers. Also relatively recently, two forms of the ovarian hormone inhibin have been identified and separately assayed (Groome et al., 1996). With limited clinical data available regarding the two forms of inhibin, previous models have considered only total inhibin, rather than separately including its two forms. By incorporating both inhibins in the model separately, a model can better reflect the biological reality of the system. Both forms of inhibin have the same regulatory effect, which is to limit production of follicle-stimulating hormone (Welt et al., 1999). However, they are most active at different points in the menstrual cycle, as one is elevated during the follicular phase of the cycle, and the other is elevated during the luteal phase.

The line of research continued by this dissertation began with separate dynamical compartment models of the ovarian (Selgrade and Schlosser, 1999) and pituitary (Schlosser and Selgrade, 2000) hormone processes. Each of these models used time-dependent, periodic input functions to represent the behavior of the portion of the system not being modeled. In (Clark et al., 2003), these two models were merged to create a model based on a system of nonlinear delay differential equations. The system had dimension 13, with four equations for the pituitary gland and nine for the ovaries, plus three auxiliary equations. Parameters were estimated to fit the model to average hormone values from clinical data (McLachlan et al., 1990), allowing this system to predict the bloodstream concentrations of five hormones (two pituitary and three ovarian) throughout the cycle, without using time-dependent external functions. Clark et al. (2003) found that this model showed the existence of two periodic stable solutions for this system, one representing a normal menstrual cycle and the other representing an abnormal cycle, possibly associated with polycystic ovarian syndrome (PCOS).

In Chapter 2, a brief explanation of the interactions among the reproductive hormones is given. These interactions are inherent in the models used thereafter. In Chapter 3, we consider more recent data sets which include both inhibins (Groome et al., 1996) (Welt et al., 1999). For one such data set, we estimate the parameters to fit the model of Clark et al. (2003) to these data. Beginning from this optimized parameter set, we explore the system dynamics in Chapter 4. The existence and stability of equilibrium

and periodic solutions are discussed, and bifurcations of some parameters are explored. Also in this chapter, a sensitivity analysis is performed, identifying which parameters have the greatest proportional effects on the output. Finally, the effects of external hormones are modeled, both for short-term and longer-term exposures.

In Chapter 5, the model is expanded to six hormones, to include separately the effects of both forms of inhibin. This involves minor changes to the pituitary hormone model, as well as significant modifications and additions to the ovarian model. After expanding the model, the parameter estimation process must be repeated. With an increased number of parameters and an additional hormone profile to fit, this process is more difficult. In Chapter 6, we consider the dynamics of this new system, including equilibria, periodic solutions, bifurcations, and sensitivity.

The clinical data on which this dissertation is based (Welt et al., 1999) includes hormone profiles for two groups of women, one in their twenties and early thirties, the other in their mid-thirties to mid-forties. Well before menopause, the level of inhibin production begins to drop (Welt et al., 1999) (Speroff et al., 1999); this has effects on the levels of other sexual hormones at some points during the cycle. In Chapter 7, these changes are quantified in the model. Two largely similar parameter sets are identified, fitting the data for the two groups of women, with a minimal number of differing parameters to represent the effects of aging. Chapter 8 discusses future work in this line of research, including additional investigations related to the aging process.

Chapter 2

Biological Background

2.1 The Feedback Loop of the Hypothalamus, Pituitary Gland, and Ovaries

Reproductive endocrinology is largely based on activity in two glands at the base of the brain – the hypothalamus and the pituitary gland – as well as in the gonads. In females, the gonads are the ovaries, while in males, they are the testes (Speroff et al., 1999). Because this paper is describing the reproductive system of women, we will not discuss male physiology in detail. Each of the aforementioned endocrine glands produces one or more hormones; together all of these hormones jointly control ovulation. The hypothalamus produces gonadotropin-releasing hormone (GnRH). The pituitary gland synthesizes two gonadotropins, follicle-stimulating hormone (FSH) and luteinizing hormone (LH) (Speroff et al., 1999). Using acetate and cholesterol as a starting point, the ovaries synthesize multiple steroid hormones, including estradiol (E_2), progesterone (P_4), and even testosterone, which is more commonly associated with male reproductive development and physiology. The ovaries also produce non-steroidal hormones, including relaxin, oxytocin, activin and two forms of inhibin, via different chemical pathways (Speroff et al., 1999) (Zeleznik and Pohl, 2006) (Baird, 1984). The primary chemical pathways involved in synthesis of estradiol and progesterone are shown in Figure 2.1.

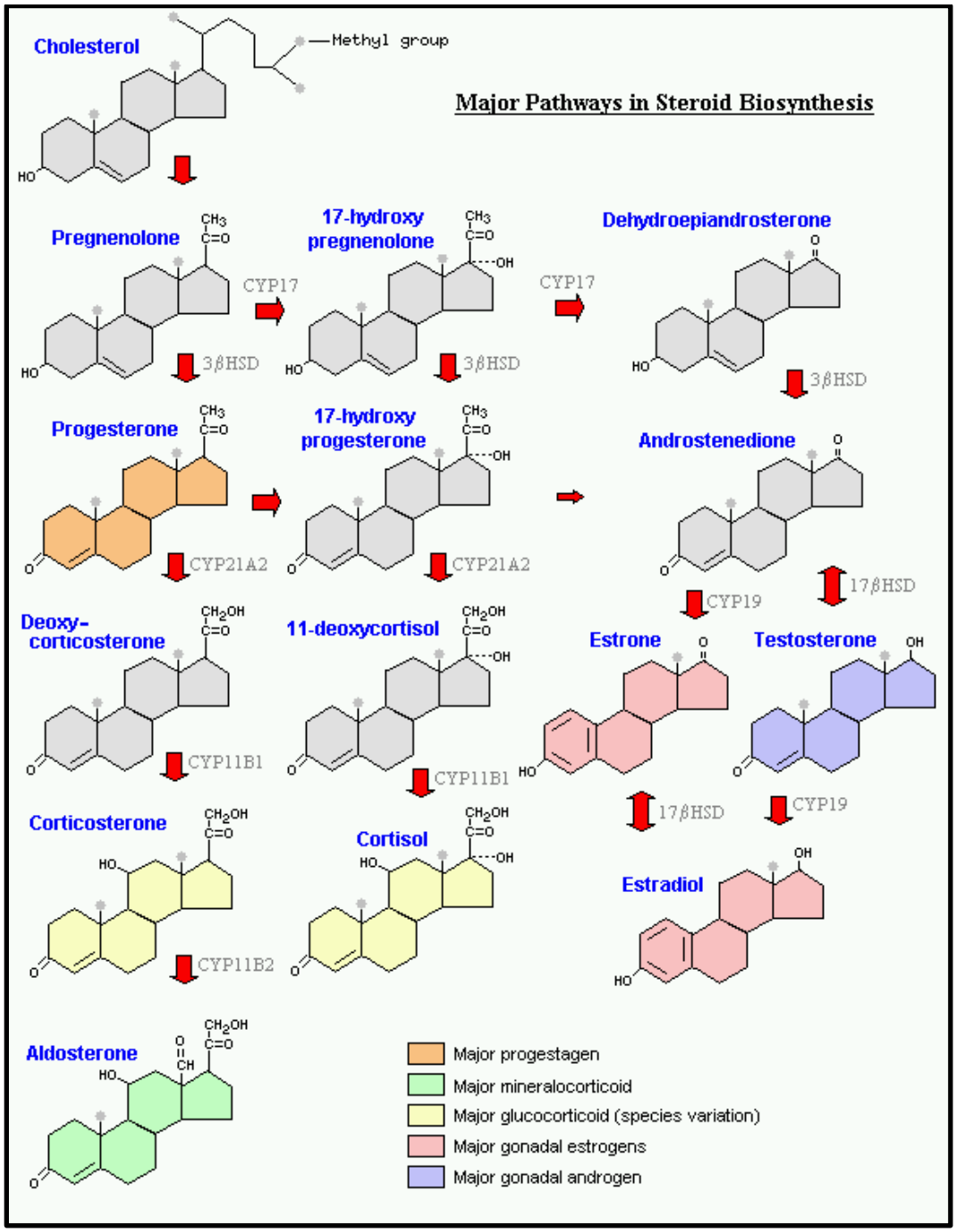

Figure 2.1 – Steroid Biosynthesis Pathways
(Reproduced by permission of R. A. Bowen, Colorado State University)

There is a system of positive and negative feedback loops among these glands that allows them to regulate one another. Because GnRH is produced in small amounts and has a very short half-life of only 2-4 minutes, the general circulatory system would be ineffective in supplying sufficient concentrations of GnRH to mediate gonadotropin synthesis (Speroff et al., 1999). An alternate mechanism resolves this issue; portal circulatory vessels conduct GnRH directly to the anterior pituitary, where it induces the production of LH and FSH. Secretion of GnRH is pulsatile in nature, with peaks roughly every 1-4 hours, varying based on the stage of the menstrual cycle. There are also significant frequency differences among individuals (Speroff et al., 1999).

The presence of GnRH in the anterior portion of the pituitary gland stimulates synthesis of both FSH and LH. The amounts produced are pulsatile, varying along with the GnRH concentration in the pituitary (Speroff et al., 1999). The ratio of FSH to LH produced is also variable, depending at least partially on the frequency of the GnRH pulses (Baird, 1984). As gonadotropins are synthesized, some are held in reserve, rather than being immediately released into the bloodstream. GnRH has three effects on the pituitary, with regard to LH and FSH production: increasing synthesis of gonadotropins to be held in reserve, causing movement of gonadotropins from the reserve pool to a pool available for immediate secretion, and promoting release of the gonadotropins (Speroff et al., 1999). The anterior pituitary also produces a third gonadotropin, called prolactin, which does not appear to have significant effects on the menstrual cycle (Speroff et al., 1999).

Once in the bloodstream, LH and FSH circulate throughout the body. They have significant effects on hormone production in the ovaries. FSH is important for the growth and development of ovarian follicles, and also stimulates production of estradiol from androgens (Baird, 1984) (Dorrington and Armstong, 1975). A high level of LH causes increased blood flow to the ovaries. LH also stimulates the conversion of pregnenolone from cholesterol, which is an early step in the production of the steroid hormones (Baird, 1984). Thus, both LH and FSH are necessary for proper ovarian function.

After being secreted into the bloodstream, the ovarian hormones have effects on the pituitary. As its name would suggest, the primary action of inhibin is to inhibit production of FSH (Speroff et al., 1999). However, inhibin does not suppress LH synthesis, and may even do the opposite (Bauer-Dantoin et al., 1995). Progesterone promotes the release of both FSH and LH into the bloodstream, while estradiol suppresses their release. Estradiol and progesterone have the opposite effects on the synthesis of LH, as progesterone causes it to decrease, while high levels of estradiol, beyond some threshold level, cause a sharp increase in LH production (Speroff et al., 1999). Estradiol appears to regulate the amplitude of LH pulses, while progesterone regulates their frequency (Yen, 1999). The steroid hormones also have indirect effects on GnRH synthesis in the hypothalamus (Speroff et al., 1999).

2.2 The Menstrual Cycle

The serum levels of the female reproductive hormones are not at equilibrium, but rather fluctuate in a predictable, periodic manner, accompanied by other repetitive physiological changes, including ovulation. Together these dynamic interactions control the menstrual cycle. The most common period for the human menstrual cycle is 28 days, but a relatively small percentage of women have a cycle of exactly 28 days, as there is substantial variation among healthy, fertile women (Speroff et al., 1999) (Vollman, 1977) (Treloar et al., 1967). This cycle will repeat hundreds of times in a typical woman's life. Menstruation, a period of vaginal bleeding lasting four days on average, occurs as the lining of the uterus is shed during each cycle (Speroff et al., 1999) (Hadley, 1992).

Menarche, the beginning of menstruation, occurs on average at age 12.5, as a part of puberty. Its occurrence is related to reaching a threshold level of body fat (Yen, 1999), as a healthy pregnancy cannot occur with low levels of body fat. Initially, a girl's menstrual cycle is usually irregular, without ovulation; the period is often longer than that of a young adult woman (Speroff et al., 1999). Most women's cycles become regular within a year or two, with a period between 24 and 35 days. Pregnancy and oral contraceptives both interrupt the menstrual cycle, as can a variety of health conditions. The cycle is eventually terminated naturally at menopause; in the years leading up to that point, cycles typically increase in duration, and may again become irregular and anovulatory (Yen, 1999) (Vollman, 1977) (Treloar et al., 1967).

By convention, the beginning of menstruation is considered the first day of the menstrual cycle. A classic 28-day cycle can be separated into two roughly equal parts, called the follicular phase and the luteal phase. These two phases are separated by ovulation, the rupture of a large, mature follicle, releasing an ovum for possible fertilization. If fertilization does not occur, then there is a smooth transition from the end of the luteal phase of one cycle to the start of the follicular phase of the next cycle.

At puberty, each ovary contains roughly 250,000 *oocytes*, immature egg cells which are contained in a single layer of granulosa cells. Together the oocyte and surrounding epithelial cells are called a primordial follicle. Out of these many follicles, only a few hundred will fully develop and release an egg for possible fertilization (Hadley, 1992). All of the other follicles will eventually undergo a degeneration process called *atresia*, until there are no active follicles remaining, at which point menopause occurs (Speroff et al., 1999). Throughout the years between menarche and menopause, there is constant low-level follicular growth during all stages of the menstrual cycle (Baird, 1984). Furthermore, the follicular processes of growth and atresia are unaffected by pregnancy or anovulatory menstrual cycles (Speroff et al., 1999). However, during each cycle, usually only one follicle will grow and develop to the point of ovulation. The incidence of fraternal twins is an example of the possibility of complete simultaneous development of multiple follicles. The growth process leading up to ovulation lasts approximately 85 days, only the latter portion of which is affected by hormonal processes (Oktay et al., 1998).

Shortly before menstruation, that is, a few days before a cycle begins, several developing follicles in each ovary move into an advanced, *antral* stage of development, based on slowly rising FSH levels, with each such follicle having the possibility of ovulation during the upcoming cycle (Pache et al., 1990). During the first half of the follicular phase, one follicle becomes dominant and begins to grow exponentially, while all of the other cohort follicles begin to undergo atresia (Baird, 1984). In many other species of mammals, multiple follicles simultaneously develop, so multiple births are the expected result. The physiological mechanisms of primates through which exactly one dominant follicle is typically selected during each cycle remain unknown (Zeleznik and Pohl, 2006).

Through most of the follicular phase, FSH levels are elevated; this is a necessary condition for follicular development. As it grows, the primary follicle secretes large amounts of estradiol, leading to an exponential rise in bloodstream estradiol levels (Baird, 1984). The increase of circulating estradiol levels inhibits pituitary release of FSH, causing a decline in bloodstream FSH levels. This has the effect of shutting down the growth processes of immature antral follicles (Speroff et al., 1999). By the time that this occurs, there are large amounts of FSH present inside of the primary follicle, so it is less dependent on circulating FSH (Baird, 1984). In the late follicular phase, there is an increase in the frequency of LH (and presumably GnRH) pulses. This increased frequency

appears to promote estradiol synthesis, even though the amplitude of the LH pulses is lower than at other times during the cycle (Speroff et al., 1999).

Late in the follicular phase, once the bloodstream level of estradiol remains above a threshold for approximately 36-48 hours, there is a change in the effect of estradiol on the anterior pituitary. At levels below this critical concentration, estradiol suppresses release of LH, but at sustained higher levels, it promotes this release (Speroff et al., 1999) (Young and Jaffe, 1976). Because estradiol concentrations are low throughout most of the follicular phase, a large amount of LH is stored after production. This reserve of LH is emptied over about two days, in response to high estradiol levels, leading to a high peak concentration of LH in the bloodstream, on average to eight times the baseline level (Welt et al., 1999). Not only does the anterior pituitary secrete a large amount of LH at this time, but it also secretes a substantial amount of FSH. Because FSH has been elevated throughout the follicular phase, this surge is not as pronounced, but it is still substantial, and is important for ovulation and preparation of the *corpus luteum*, the ruptured follicle without the ovum.

While progesterone concentrations are low throughout the follicular phase, they are slowly rising at mid-cycle, and progesterone plays a role in triggering the FSH surge (Speroff et al., 1999). There is also a mid-cycle surge of inhibin B, which may be caused by a release from the ruptured follicle at the time of ovulation (Speroff et al., 1999). Given that ovulation occurs on average 34 hours after estradiol levels peak (Pauerstein et

al., 1978), this hypothesis is supported by data that show inhibin B bloodstream concentrations peaking two days after estradiol peaks. However, (Muttuknrishna et al., 2000) suggests than inhibin A is mainly produced by the primary follicle/corpus luteum, while inhibin B is largely secreted by immature pre-antral follicles, casting doubt on the assertation of Speroff et al. (1999).

Following the LH surge, the luteal phase lasts approximately two weeks. It is characterized by high levels of progesterone, released by the corpus luteum in preparation for a potential pregnancy (Baird, 1984). One key luteal phase function of progesterone is preparation of the uterine walls for implantation of a fertilized egg. Bloodstream progesterone levels are elevated throughout this stage, peaking in the mid-luteal phase. There is also a secondary peak in estradiol during this phase, but with a significantly lower amplitude than the follicular phase peak. While inhibin B is elevated throughout the follicular phase and peaks again just after ovulation, levels of inhibin A are low during the follicular phase. Circulating inhibin A concentrations begin rising in the mid-follicular phase, then generally increase until they peak in the mid-luteal phase, with a secondary peak occurring on the same day as the LH surge. During the luteal phase, inhibin A and estradiol are primarily responsible for suppressing FSH, but inhibin B does not play a significant role (Welt et al., 1999) (Yen, 1999).

Unless fertilization of the egg occurs, the corpus luteum regresses rapidly during the late follicular phase, leading to declines in the levels of estradiol, progesterone, and

inhibin A. The decrease in pituitary suppression by inhibin A and estradiol allows for a slow increase in FSH during the luteal-follicular transition, beginning about two days before menstruation (Speroff, et al., 1999) (Yen, 1999). The slow rise of FSH causes development beyond the pre-antral stage for a new group of follicles. Menstruation is the external marker of the beginning of the next cycle. Once FSH reaches a critical level, inhibin B synthesis will increase, limiting the size of the FSH rise (Welt et al., 1997). Thus, inhibin B and FSH have a reciprocal feedback loop.

2.3 Changes in Peri-Menopause

Menopause, the permanent end of menstruation due to a loss of ovarian function, typically occurs in the late forties or early fifties. With no follicular activity in the ovaries, post-menopausal women have an acyclic hormone profile. As compared to younger, fertile women, women who have reached menopause produce less of the ovarian hormones (most notably estradiol), and more of the pituitary hormones LH and FSH (Speroff et al., 1999). However, for most women, there is not an abrupt end to menstruation. Instead, for 90 percent of women, menopause is preceded by a stage of menstrual irregularity called the perimenopausal transition (McKinlay et al., 1992).

Perimenopause lasts, on average, for 4-5 years, with intermittent anovulatory menstrual periods. Even earlier, menstrual cycle length begins to increase; this duration increase mostly comes from a longer follicular phase. The same general pattern occurs

regardless of the age at which perimenopause occurs, whether it is early or late (Speroff et al., 1999). Perimenopausal women have lower levels of inhibin B throughout the cycle and lower inhibin A during the luteal phase, as compared to younger women. Related effects are an increase in follicular phase FSH concentration and, closer to menopause, slight increases in estradiol during the late follicular phase (Welt et al., 1999) (Muttukrishna et al., 2000). Circulating levels of LH also begin increasing several years before menopause. During the last year before menopause, bloodstream concentrations of estradiol begin to drop substantially (Rannevik et al., 1995).

Post-menopausal women have very low levels of estradiol, and very high levels of both LH and FSH, as compared to young women (Speroff et al., 1999). After menopause, the ovaries are no longer producing estradiol (Baird, 1984), so the circulating estrogen has largely been produced by peripheral conversion of androstenedione (Speroff et al., 1999). Progesterone concentrations also fall drastically, due to the lack of follicular activity (Baird, 1984), and older women have circulating levels of inhibin that are insufficient to detect.

With these hormonal changes, particularly the lack of circulating estrogen, there are a variety of negative consequences commonly experienced by post-menopausal women. These include an increased risk of cardiovascular disease and/or osteoporosis, *vasomotor flushes* ("hot flashes"), and vaginal atrophy (Speroff et al., 1999). The most significant of these dangers is cardiovascular disease, a leading cause of death among

older women. Hormone replacement therapies, involving low-dose, long-term administration of either estrogen alone or estrogen with progestin, can be valuable in reducing the likelihood of heart disease and osteoporosis, as well as decreasing the other uncomfortable, but less dangerous, effects of estrogen deprivation (Speroff et al., 1999). However, hormone replacement therapy is not without risks, most notably an increased possibility of breast cancer, which varies with the type and duration of hormones administered (Beral et al., 2003). For this reason, the benefits and risks of post-menopausal estrogen therapy must be weighed on a case-by-case basis by physicians, in consultation with their post-menopausal patients.

Chapter 3

The Five-Hormone Model

3.1 Explanation of the Existing Model

In modeling any complicated physical or biological system, there are two conflicting objectives: making the model descriptive, and keeping it simple. The more components that are introduced, the larger the model becomes, increasing the difficulty of obtaining either analytical or numerical results. Simplifying assumptions, if chosen well, can decrease the complexity of a model and allow for greater mathematical understanding of it, without sacrificing too much of the physical or biological reality.

In creating their original models for the human female reproductive endocrine system (Selgrade and Schlosser, 1999) (Schlosser and Selgrade, 2000), Selgrade and Schlosser did not explicitly include the GnRH and the hypothalamus. Schlosser and Selgrade (2000) lumped the effects of the hypothalamus and pituitary together in tracking gonadotropin synthesis, release, and clearance. Additionally, short-term pulsatile changes in FSH and LH release, based on GnRH pulses, were not included.

It appears likely that not all FSH and LH produced by the pituitary are immediately secreted. Instead, there are reserves of these gonadotropins retained in the pituitary, in which FSH and LH are stored for subsequent release (Speroff et al., 1999). Schlosser and

Selgrade (2000) proposed a four-compartment model for the pituitary hormones. The four compartments represent the bloodstream concentrations of FSH and LH, and the pituitary reserves of FSH and LH. As is typical with compartment modeling, each compartment is represented by a differential equation, where the rate of change in the compartment's mass equals the rate of mass inflow minus the rate of mass outflow. For each gonadotropin, there are three processes to track: synthesis of hormone, release of hormone from the reserve pool into the bloodstream, and clearance from the bloodstream. The equations for reserve pool LH and bloodstream LH, with slightly different notation than (Schlosser and Selgrade, 2000) and (Harris, 2001) are as follows:

$$\begin{aligned} \frac{\mathrm{d}}{\mathrm{dt}} RP_{LH} &= \text{LH synthesis rate} - \text{LH release rate} \\ \frac{\mathrm{d}}{\mathrm{dt}} LH &= \frac{\text{LH release rate}}{\text{Volume of dispensation}} - \text{LH clearance rate} \end{aligned} \tag{3.1}$$

$$\begin{aligned} \text{LH synthesis rate}\left(E_2, P_4\right) &= \frac{v_{0,LH} + v_{1,LH} \dfrac{\left(E_2(t-d_E)/Km_{LH}\right)^a}{1+\left(E_2(t-d_E)/Km_{LH}\right)^a}}{1+\dfrac{P_4(t-d_P)}{Ki_{LH,P}}} \\ \text{LH release rate}\left(E_2, P_4, RP_{LH}\right) &= k_{LH} \cdot \frac{1+c_{LH,P}\cdot P_4(t)}{1+c_{LH,E}\cdot E_2(t)} \cdot RP_{LH}(t) \\ \text{LH clearance rate}\left(LH\right) &= r_{LH} \cdot LH(t) \end{aligned} \tag{3.2}$$

The design behind these equations is explained in detail in (Schlosser and Selgrade, 2000). However, there are a few points worth explaining. After a change occurs in circulating levels of E_2 and/or P_4, both of which regulate LH synthesis, there is a

delay before a corresponding change in the rate of LH synthesis occurs. For this reason, there are delays in the LH synthesis term. However, there are no delays in the release term, as hormones stored in the reserve pool are immediately available for secretion. This model considers the high levels of E_2 during the late follicular phase as leading to greatly increased LH production in the pituitary, and the numerator of the LH synthesis term includes a nonlinear *Hill function* to model this effect. A Hill function is used in biological or chemical situations when a process depends on a catalyst attaining a threshold level. In this case, the catalyst is E_2, and the threshold level is the parameter Km_{LH}. As E_2 rises above this level, LH synthesis greatly increases. However, there is some biological evidence to indicate that only the rate of LH release, not production, increases drastically in the late follicular phase. To reflect this, the model may need to be changed in the future, shifting the Hill function from the synthesis term to the release term. Finally, the time delay d_E in estradiol's effect on LH synthesis is likely small, but we will include it. Previously, it was included in (Schlosser and Selgrade, 2000) and (Harris, 2001), but removed in (Clark et al., 2003).

There is a similar system of equations for the synthesis, release, and clearance of FSH. Estradiol, progesterone, and the inhibins all play a role in regulation of FSH. This model also includes quadratic inhibition of E_2 on FSH release. Using newer data sets that differentiate between the two inhibins, we will attempt to reduce the E_2 inhibition to a linear effect, which is more realistic biologically. The FSH equations are as follows:

$$\begin{aligned}\frac{\mathrm{d}}{\mathrm{dt}} RP_{FSH} &= \text{FSH synthesis rate} - \text{FSH release rate} \\ \frac{\mathrm{d}}{\mathrm{dt}} FSH &= \frac{\text{FSH release rate}}{\text{Volume of dispensation}} - \text{FSH clearance rate}\end{aligned} \tag{3.3}$$

$$\begin{aligned}\text{FSH synthesis rate}\left(Ih\right) &= \frac{v_{FSH}}{1+\frac{Ih(t-d_{Ih})}{Ki_{FSH,Ih}}} \\ \text{FSH release rate}\left(E_2, P_4, RP_{FSH}\right) &= k_{FSH} \cdot \frac{1+c_{FSH,P} \cdot P_4(t)}{1+c_{FSH,E} \cdot \left(E_2(t)\right)^2} \cdot RP_{FSH}(t) \\ \text{FSH clearance rate}\left(FSH\right) &= a_{FSH} \cdot FSH(t)\end{aligned} \tag{3.4}$$

Out of (3.1) through (3.4), we get a four-dimensional system (based on derivatives of $RP_{LH}, LH, RP_{FSH},$ and FSH) that describes the bloodstream concentrations of the gonadotropins LH and FSH. Because LH and FSH have no direct effects on one another, this system can be dissected into a two-dimensional system for LH and a separate two-dimensional system for FSH. In (Schlosser and Selgrade, 2000), time-dependent input functions are used to represent the concentrations of the ovarian hormones E_2, P_4, and Ih, with the functions chosen to approximate the data from (McLachlan et al., 1990).

The bloodstream levels of the ovarian hormones are modeled in (Selgrade and Schlosser, 1999). The model for the ovarian hormones takes a different form than that of the pituitary hormones, largely because ovarian hormones are cleared from the bloodstream quickly, making it unnecessary to separately track synthesis, release, and clearance. Instead, a nine-stage model is used to represent the capacity of the ovaries to

produce hormones at each stage. There are three stages for the follicular phase, two for the time around ovulation, and four for the luteal phase.

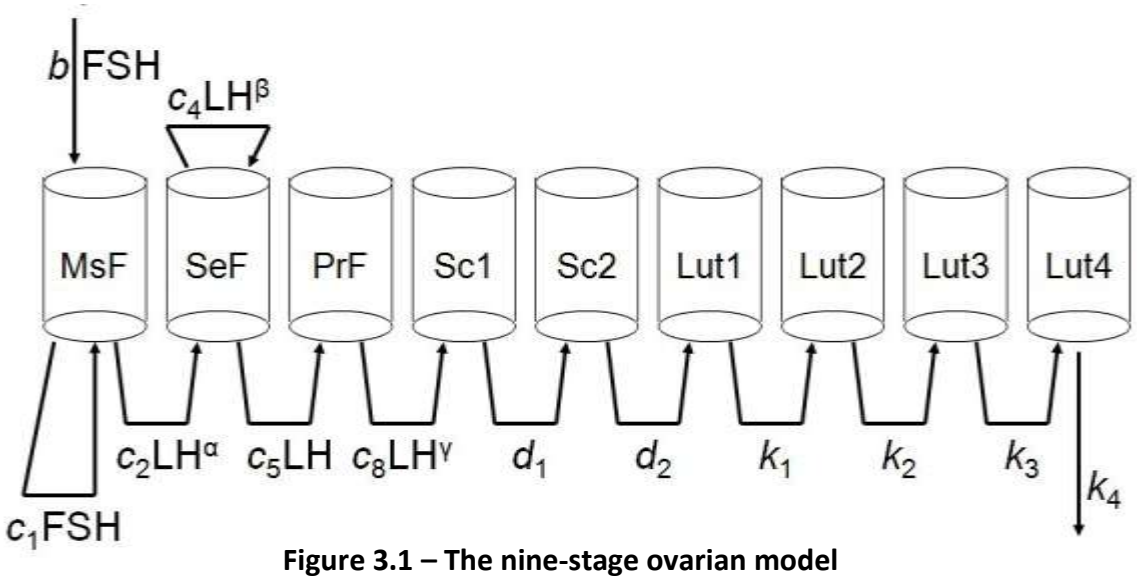

Figure 3.1 – The nine-stage ovarian model

This leads to nine ordinary differential equations which have no delays, and are linear with respect to the state variables. Production of E_2, P_4, and Ih are each modeled with a constant baseline level plus a linear combination of the stage values.

$$\frac{d}{dt}MsF = b \cdot FSH + \left(c_1 \cdot FSH - c_2 \cdot LH^{\alpha}\right) \cdot MsF$$
$$\frac{d}{dt}SeF = c_2 \cdot LH^{\alpha} \cdot MsF + \left(c_4 \cdot LH^{\beta} - c_5 \cdot LH\right) \cdot SeF$$
$$\frac{d}{dt}PrF = c_5 \cdot LH \cdot SeF - c_8 \cdot LH^{\gamma} \cdot PrF$$
$$\frac{d}{dt}Sc1 = c_8 \cdot LH^{\gamma} \cdot PrF - d_1 \cdot Sc1$$
$$\frac{d}{dt}Sc2 = d_1 \cdot Sc1 - d_2 \cdot Sc2$$
$$\frac{d}{dt}Lut1 = d_2 \cdot Sc2 - k_1 \cdot Lut1$$
$$\frac{d}{dt}Lut2 = k_1 \cdot Lut1 - k_2 \cdot Lut2$$
$$\frac{d}{dt}Lut3 = k_2 \cdot Lut2 - k_3 \cdot Lut3$$
$$\frac{d}{dt}Lut4 = k_3 \cdot Lut3 - k_4 \cdot Lut4 \qquad (3.5)$$

Additionally, there are three auxiliary equations that relate the ovarian hormone concentrations to the masses of the nine ovarian stages:

$$E_2 = e_0 + e_1 \cdot SeF + e_2 \cdot PrF + e_3 \cdot Lut4$$
$$P_4 = p_0 + p_1 \cdot Lut3 + p_2 \cdot Lut4 \qquad (3.6)$$
$$Ih = h_0 + h_1 \cdot PrF + h_2 \cdot Lut2 + h_3 \cdot Lut3 + h_4 \cdot Lut4$$

Because the production of ovarian hormones depends on the circulating concentrations of LH and FSH, Selgrade and Schlosser in (Selgrade and Schlosser, 1999) again used time-dependent input functions, approximating the data in (McLachlan et al., 1990), for LH and FSH.

In (Harris, 2001) and (Clark et al., 2003), the LH, FSH, and ovarian systems were merged, creating a 13-dimensional system without time-dependent input functions. The three ovarian auxiliary equations, given by (3.6), are also needed.

$$
\begin{aligned}
\frac{d}{dt}RP_{LH} &= \frac{v_{0,LH} + v_{1,LH}\dfrac{\left(E_2(t-d_E)/Km_{LH}\right)^a}{1+\left(E_2(t-d_E)/Km_{LH}\right)^a}}{1+\dfrac{P_4(t-d_P)}{Ki_{LH,P}}} - k_{LH}\cdot\frac{1+c_{LH,P}\cdot P_4}{1+c_{LH,E}\cdot E_2}\cdot RP_{LH} \\
\frac{d}{dt}LH &= \frac{1}{v}\cdot k_{LH}\cdot\frac{1+c_{LH,P}\cdot P_4}{1+c_{LH,E}\cdot E_2}\cdot RP_{LH} - r_{LH}\cdot LH \\
\frac{d}{dt}RP_{FSH} &= \frac{v_{FSH}}{1+\dfrac{Ih(t-d_{Ih})}{Ki_{FSH,Ih}}} - k_{FSH}\cdot\frac{1+c_{FSH,P}\cdot P_4}{1+c_{FSH,E}\cdot E_2^2}\cdot RP_{FSH} \\
\frac{d}{dt}FSH &= \frac{1}{v}\cdot\frac{1+c_{FSH,P}\cdot P_4}{1+c_{FSH,E}\cdot E_2^2}\cdot RP_{FSH} - a_{FSH}\cdot FSH \\
\frac{d}{dt}MsF &= b\cdot FSH + \left(c_1\cdot FSH - c_2\cdot LH^{\alpha}\right)\cdot MsF \\
\frac{d}{dt}SeF &= c_2\cdot LH^{\alpha}\cdot MsF + \left(c_4\cdot LH^{\beta} - c_5\cdot LH\right)\cdot SeF \\
\frac{d}{dt}PrF &= c_5\cdot LH\cdot SeF - c_8\cdot LH^{\gamma}\cdot PrF \\
\frac{d}{dt}Sc1 &= c_8\cdot LH^{\gamma}\cdot PrF - d_1\cdot Sc1 \\
\frac{d}{dt}Sc2 &= d_1\cdot Sc1 - d_2\cdot Sc2 \\
\frac{d}{dt}Lut1 &= d_2\cdot Sc2 - k_1\cdot Lut1 \\
\frac{d}{dt}Lut2 &= k_1\cdot Lut1 - k_2\cdot Lut2 \\
\frac{d}{dt}Lut3 &= k_2\cdot Lut2 - k_3\cdot Lut3 \\
\frac{d}{dt}Lut4 &= k_3\cdot Lut3 - k_4\cdot Lut4
\end{aligned}
\tag{3.7}
$$

3.2 Published Data Sets

In (Selgrade and Schlosser, 1999), (Schlosser and Selgrade, 2000), (Selgrade, 2001), (Harris, 2001), and (Clark et al., 2003), the McLachlan data set (McLachlan et al., 1990) was used. This data set gave mean daily bloodstream hormone levels (including LH, FSH, E_2, P_4, and Ih) for 33 normally cycling women, centered to the day of the LH surge. Because of the substantial sample size, there appears to be relatively little "noise" in the data, except at the beginning and end of the cycle. This noise occurs due to the variation among the cycle lengths of individual women, since all the data were centered to the mid-cycle LH surge. However, because separate assays for inhibin A and inhibin B were not yet available, the data includes only total inhibin.

The first available comparable data set including separate measurements of both inhibins was (Groome et al., 1996). In attempting to expand the existing five-hormone model to include both inhibins, we began by working with this data set. However, the sample size in (Groome et al., 1996) was only six women, leading to substantial noise, and related difficulty in using these data.

A newer hormonal data set including both inhibins was published in (Welt et al., 1999). This study included 23 women between the ages of 20 and 34 years old. While the aggregate hormone profiles are not as smooth as in (McLachlan et al., 1990), they are substantially less noisy than those in (Groome et al., 1996). This study also included

a second, separate group of 21 women aged 35 to 46 years old, allowing for comparisons between the two age groups, which are discussed in Chapter 7.

3.3 Fitting the Unmerged Model to the Welt Data

After writing the equations, the next step in the modeling process is to determine values for the unknown parameters which make the model fit the data. In the existing menstrual cycle model, there are a small number of coefficients that are known, based on previous physiological research, but the vast majority are unknown. Because of the complexity of the full merged model given by (3.7) and (3.6), it is advantageous to begin by dealing with smaller portions of the model, to get first estimates for the unknown parameters.

We begin by fitting the LH system (3.8), which has two equations and twelve parameters. Because of the delays, we use MATLAB's delay differential equation solver *dde23* to compute solutions. Two coefficients are known from the literature: $v = 2.5$ Liters is the volume of dispensation that the hormones circulate throughout, and $r_{LH} = 14 \text{ day}^{-1}$ is the clearance rate of LH. For the delays, we do not have exact values, but do know reasonable ranges: at most one day for d_E, and between 0.5 and 2 days for d_P. The other eight parameters will be chosen to make the model best fit the LH data.

$$\frac{d}{dt}RP_{LH} = \frac{v_{0,LH} + v_{1,LH}\dfrac{\left(E_2(t-d_E)/Km_{LH}\right)^a}{1+\left(E_2(t-d_E)/Km_{LH}\right)^a}}{1+\dfrac{P_4(t-d_P)}{Ki_{LH,P}}} - k_{LH}\cdot\frac{1+c_{LH,P}\cdot P_4}{1+c_{LH,E}\cdot E_2}\cdot RP_{LH} \qquad (3.8)$$

$$\frac{d}{dt}LH = \frac{1}{v}\cdot k_{LH}\cdot\frac{1+c_{LH,P}\cdot P_4}{1+c_{LH,E}\cdot E_2}\cdot RP_{LH} - r_{LH}\cdot LH$$

The parameter estimation process is a problem in bounded nonlinear optimization. The model is designed in such a way that all parameters should be nonnegative. Additionally, each of the delay length parameters has a range of values that are biologically reasonable. Finally, the Hill function exponent must be an integer. We wish to find the parameter set which minimizes the differences between the daily LH data points and the model predictions for LH on each day. We are generally using the standard least-squares measurement of error. However, the desired data fit is more qualitative than quantitative. This is primarily because of individual differences and noise in the data. For example, the LH surge peaks at eight times the baseline level, on average, but it is not critical that our model hits this data point perfectly. For this reason, when we subsequently refer to an optimized parameter set, this does not imply that we have obtained a global (or even local) minimum of least-squares error. Rather we have obtained a "best" fit of some sort, the measure of which may be quantitative or qualitative.

The MATLAB function *fminsearch*, a local optimization routine using the Nelder-Mead algorithm, was the primary optimization tool used. Because cases of the optimization routine making a parameter negative were rare, we dealt with the bounds by modifying the cost function (making the cost value extremely large if a parameter violated a bound) rather than using a bounded optimization routine. This did not solve the problem of how best to deal with any integer parameters, which were left fixed in the optimization routines and adjusted manually between *fminsearch* runs.

Because *fminsearch* looks for local minima, while we are searching for a global minimum, the use of this tool is insufficient to achieve our objectives, given that there are likely multiple local minima in a multidimensional parameter space. A variety of techniques were used to help solve this problem. One of the most basic involves manually adjusting parameters, based on understanding of the model, until a reasonable hormone profile is achieved, then allowing the optimization routine to fine-tune them. Another method used was repeatedly running the optimization routine from a randomized initial parameter set, chosen by allowing each parameter to vary from its previous value by up to a set percentage, then optimizing; if the optimized parameter set has a lower error total than the previous parameter set, then it replaces it. A similar technique, changing only one parameter at a time, and that by a nonrandom percentage, was also helpful. Sensitivity analysis, finding the proportionate effect (not just on total error, but on a variety of hormone plot features) was also very helpful in identifying key

parameters which heavily influence certain aspects of the system. Late in this research, we became aware of pattern search algorithms for global optimization, which may prove to be superior in future extensions of this research.

In fitting the LH system (3.8) to the Welt data (Welt et al., 1999), we assume the data to have a period of 28 days. Thus, our time-dependent input functions are also 28-day periodic. However, for plots of one period (where the time *t*, in days, is bounded by $0 \le t \le 28$) the abbreviated forms shown in (3.9) are sufficiently accurate.

$$\begin{aligned} E_2(t) &= 55 + 110 \cdot e^{-\frac{(t+6)^2}{15}} + 60 \cdot e^{-\frac{(t-11)^2}{15}} + 135 \cdot e^{-\frac{(t-13)^2}{4}} + 110 \cdot e^{-\frac{(t-22)^2}{15}} + 60 \cdot e^{-\frac{(t-39)^2}{15}} \\ P_4(t) &= 0.4 + 17.5 \cdot e^{-\frac{(t+7)^2}{21}} + 17.5 \cdot e^{-\frac{(t-21)^2}{21}} \end{aligned} \tag{3.9}$$

Each of these input functions has a constant term that represents the baseline bloodstream concentration, the lowest level during the menstrual cycle. Added to this baseline are negative exponential terms that create symmetric curved peaks of varying amplitude, duration, and timing. The input function graphs are shown in Figure 3.2.

In most cases, the initial conditions $RP_{LH}(0)$ and $LH(0)$ are inconsequential in the LH model, having no effect beyond the first 24-48 hours. However, to make the output curves as smooth as possible, we ran the model simulation for three periods (84 days), and took the middle period as our model output. The best fit of the model given by (3.8) to the LH data was achieved with the parameter set given in Table 3.1. In Figure 3.3, the model prediction of LH is compared with the data.

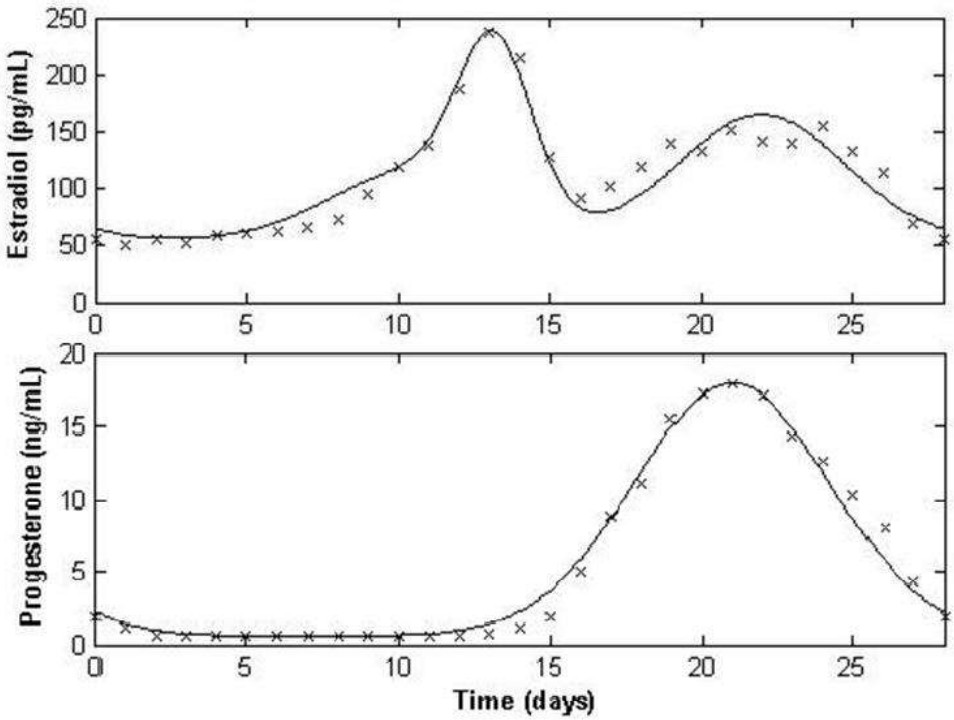

Figure 3.2 – Input Functions for E_2 and P_4, compared to data

Table 3.1 – LH system parameter values

Parameter	Value	Unit		Parameter	Value	Unit
$v_{0,LH}$	617	IU/day		$c_{LH,P}$	0.251	mL/ng
$v_{1,LH}$	$1.56 \cdot 10^{5}$	IU/day		$c_{LH,E}$	$4.94 \cdot 10^{-3}$	mL/pg
Km_{LH}	364	mL/pg		d_E	0.20	day
$Ki_{LH,P}$	23.5	mL/ng		d_P	1.04	day
k_{LH}	2.42	day^{-1}		r_{LH}	14	day^{-1}
a	8	(none)		v	2.5	L

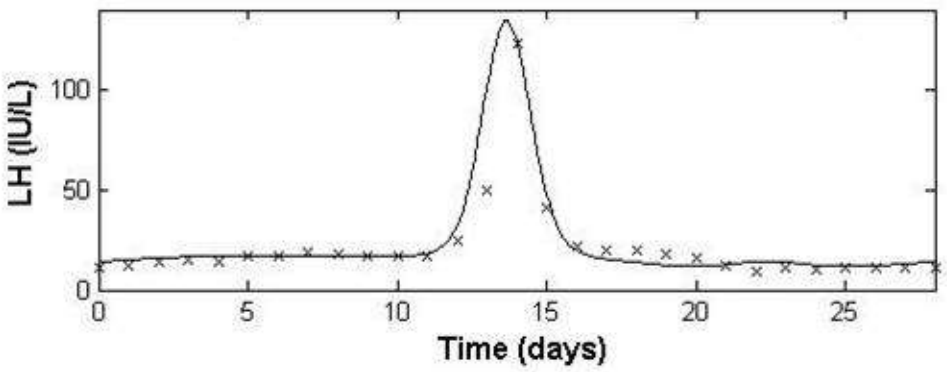

Figure 3.3 – LH model plot with data

The FSH system (3.10) has a similar form to that of the LH system. The most striking differences are the lack of a Hill function in the synthesis term, and the quadratic (rather than linear) inhibitory effect of E_2 on LH release.

$$\begin{aligned} \frac{d}{dt} RP_{FSH} &= \frac{v_{FSH}}{1+\frac{Ih(t-d_{Ih})}{Ki_{FSH,Ih}}} - k_{FSH} \cdot \frac{1+c_{FSH,P} \cdot P_4}{1+c_{FSH,E} \cdot E_2^2} \cdot RP_{FSH} \\ \frac{d}{dt} FSH &= \frac{1}{v} \cdot \frac{1+c_{FSH,P} \cdot P_4}{1+c_{FSH,E} \cdot E_2^2} \cdot RP_{FSH} - a_{FSH} \cdot FSH \end{aligned} \tag{3.10}$$

In addition to the input functions for E_2 and P_4, a time-dependent inhibin (Ih) input function is also needed. In the McLachlan data (McLachlan et al., 1990), there was only data for total inhibin. In the newer Welt data (Welt et al., 1999), there are separate measurements of inhibin A and inhibin B. Given that the profile of the total inhibin from the McLachlan data closely matches that of inhibin A in the Welt data, we will use (only)

inhibin A for this purpose. The profile of the inhibin input function, based on the Welt inhibin A data, is given by (3.11) and shown in Figure 3.4.

$$Ih(t) = 0.5 + 10 \cdot e^{-\frac{(t+8.5)^2}{30}} + 10 \cdot e^{-\frac{(t-19.5)^2}{30}} \tag{3.11}$$

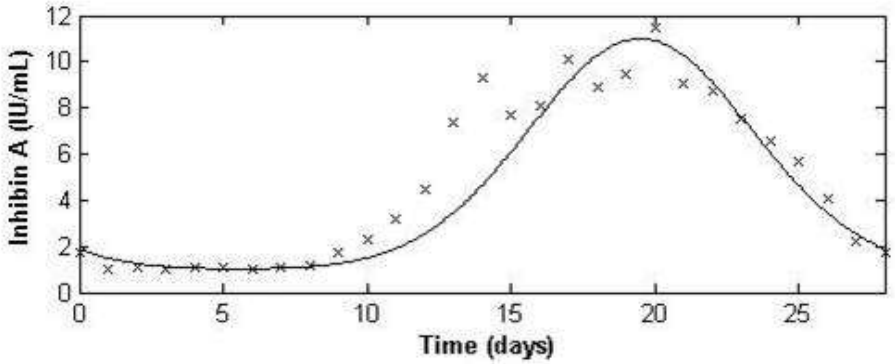

Figure 3.4 – Input function for inhibin, compared to inhibin A data

There are eight parameters in the FSH system, two of which (a_{FSH} and v) are biological constants. Additionally, a reasonable range for the delay d_{Ih} is 1.0 to 2.5 days. The optimal parameter set is shown in Table 3.2, and the model FSH prediction is compared with the FSH data in Figure 3.5.

Table 3.2 – FSH system parameter values

Parameter	Value	Unit		Parameter	Value	Unit
v_{FSH}	282	IU/day		$c_{FSH,E}$	$1.56 \cdot 10^{-3}$	mL^2/pg^2
$Ki_{FSH,Ih}$	8.32	IU/mL		d_{Ih}	2.5	day
k_{FSH}	1.88	day^{-1}		a_{FSH}	8.21	day^{-1}
$c_{FSH,P}$	30.6	mL/ng		v	2.5	L

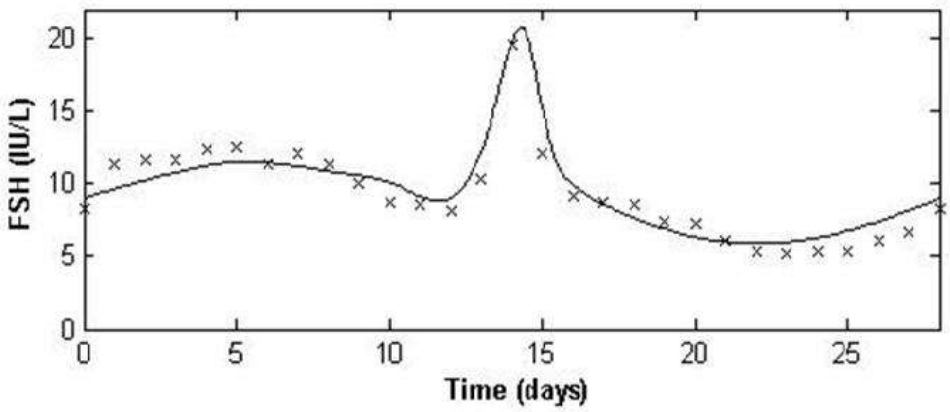

Figure 3.5 – FSH model plot with data

For the nine-stage ovarian model given by (3.5), we need time-dependent input functions for LH and FSH. As with the other input functions, these will have a period of 28 days. Abbreviated versions are given by (3.12), and shown in Figure 3.6.

$$\begin{aligned} LH(t) &= 10 + 100 \cdot e^{-\frac{(t-14)^2}{0.8}} + 12 \cdot e^{-\frac{(t-13.5)^2}{50}} \\ FSH(t) &= 4 + 8.5 \cdot e^{-\frac{(t-5)^2}{40}} + 11 \cdot e^{-\frac{(t-14)^2}{1}} + 4.5 \cdot e^{-\frac{(t-16.5)^2}{20}} + 8.5 \cdot e^{-\frac{(t-5)^2}{40}} \end{aligned} \tag{3.12}$$

The nine-dimensional system (3.5) has 15 parameters, but no delays, so we use the MATLAB ordinary differential equation solver *ode15s*, rather than the delay differential equation solver *dde23*. The three auxiliary equations given by (3.6) have an additional 12 parameters, for a total of 27. Aside from being nonnegative, the only constraint on these parameters is that the fractional exponents α, β, and γ should be at most one, as they are intended to weaken LH effects on the ovarian stages.

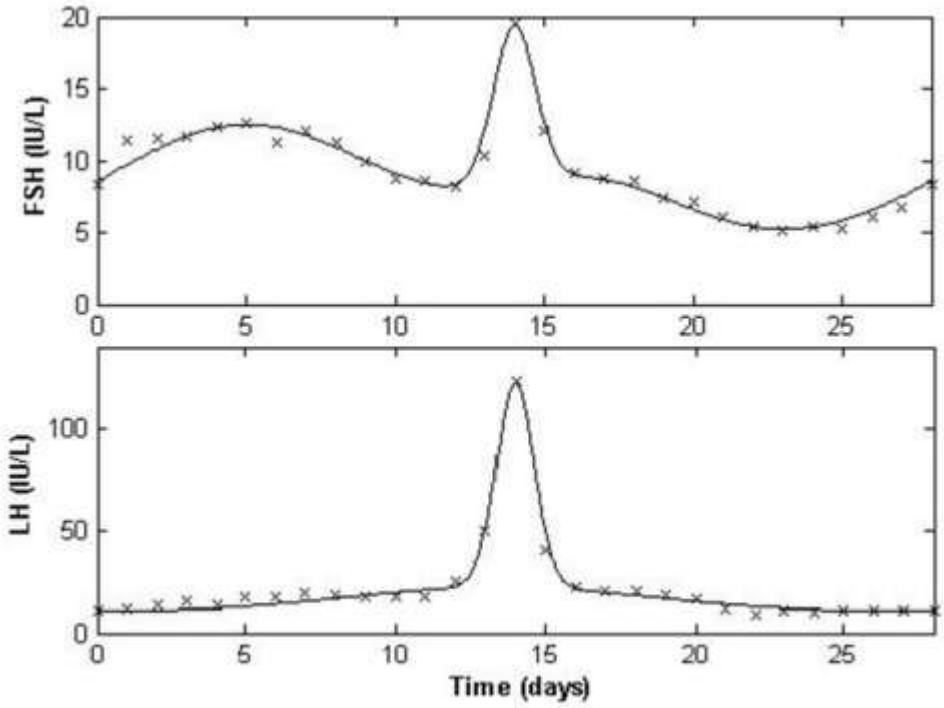

Figure 3.6 – Input functions for FSH and LH, compared to data

Tables 3.3 and 3.4 list the optimal parameter values for the ovarian model stages and the auxiliary equations, respectively. Figures 3.7, 3.8, and 3.9 display the relationships between the nine ovarian stages and the ovarian hormones E_2, P_4, and Ih; algebraically, these relationships are given by (3.6).

Table 3.3 – Ovarian system parameter values

Parameter	Value	Unit		Parameter	Value	Unit
b	0.120	$\frac{L}{IU}\cdot\frac{\mu g}{day}$		k_1	0.550	day^{-1}
c_1	0.174	$\frac{L}{IU}\cdot\frac{1}{day}$		k_2	0.690	day^{-1}
c_2	0.144	$\left(\frac{L}{IU}\right)^{\alpha}\cdot\frac{1}{day}$		k_3	0.689	day^{-1}
c_4	0.012	$\left(\frac{L}{IU}\right)^{\beta}\cdot\frac{1}{day}$		k_4	0.851	day^{-1}
c_5	0.0183	$\frac{L}{IU}\cdot\frac{1}{day}$		α	0.7736	(none)
c_8	1.266	$\left(\frac{L}{IU}\right)^{\gamma}\cdot\frac{1}{day}$		β	0.1566	(none)
d_1	0.672	day^{-1}		γ	0.0202	(none)
d_2	0.564	day^{-1}				

Table 3.4 – Auxiliary equation parameter values

Parameter	Value	Unit		Parameter	Value	Unit
e_0	55	pg/mL		p_2	$9.09\cdot10^{-4}$	kL^{-1}
e_1	$2.61\cdot10^{-3}$	L^{-1}		h_0	1	IU/mL
e_2	$4.37\cdot10^{-3}$	L^{-1}		h_1	$2.40\cdot10^{-4}$	IU/(µg·mL)
e_3	$6.60\cdot10^{-3}$	L^{-1}		h_2	$3.39\cdot10^{-4}$	IU/(µg·mL)
p_0	0.6	ng/mL		h_3	$1.77\cdot10^{-4}$	IU/(µg·mL)
p_1	$2.78\cdot10^{-4}$	kL^{-1}		h_4	$8.48\cdot10^{-5}$	IU/(µg·mL)

In Selgrade (2001), there is a condition given for a system of the form of (3.5) to have a unique, globally stable, periodic solution. The condition is that the integral with respect to time, for each diagonal entry, over one period of the forcing terms, must be negative. Because all coefficients (from Table 3.3) are positive and the forcing functions (3.12) are always positive, it is clear that the latter seven such integrals, constructed from (3.5), are negative. Using values from Table 3.3, numerical integration shows that the second is also negative, but the first is not, as shown in (3.13). The result is that the solution "blows up" when tracked over multiple periods. One way to counteract this, gaining stability, would be to reduce the growth coefficient c_1.

$$\int_0^{28} \left(c_1 \cdot FSH(t) - c_2 \cdot (LH(t))^{\alpha} \right) dt \approx 5.20 > 0 \qquad (3.13)$$

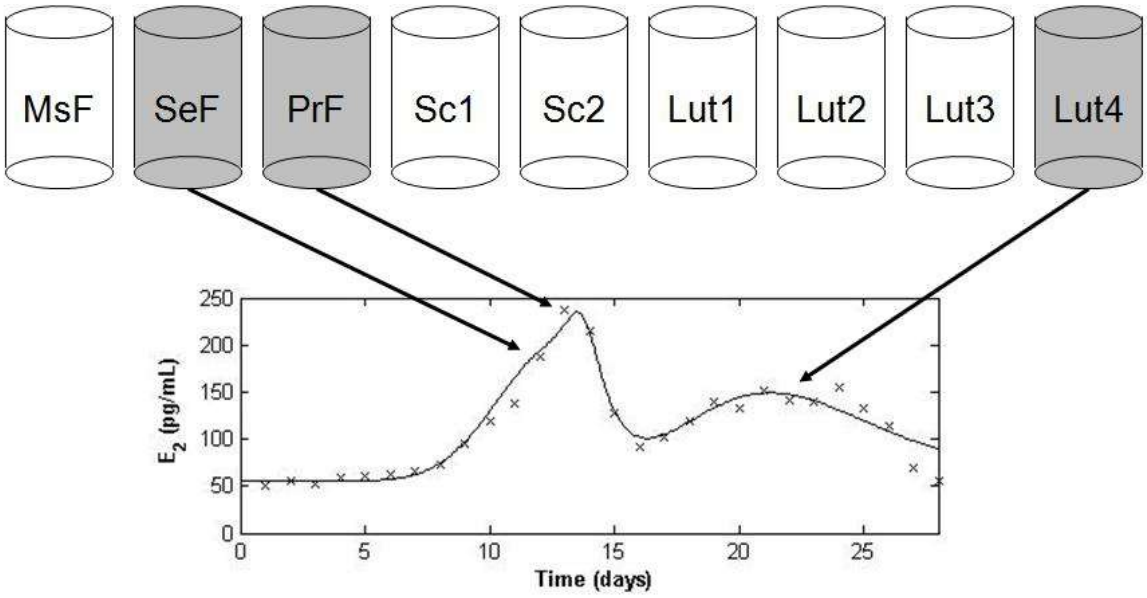

Figure 3.7 – Ovarian stages contributing to E_2

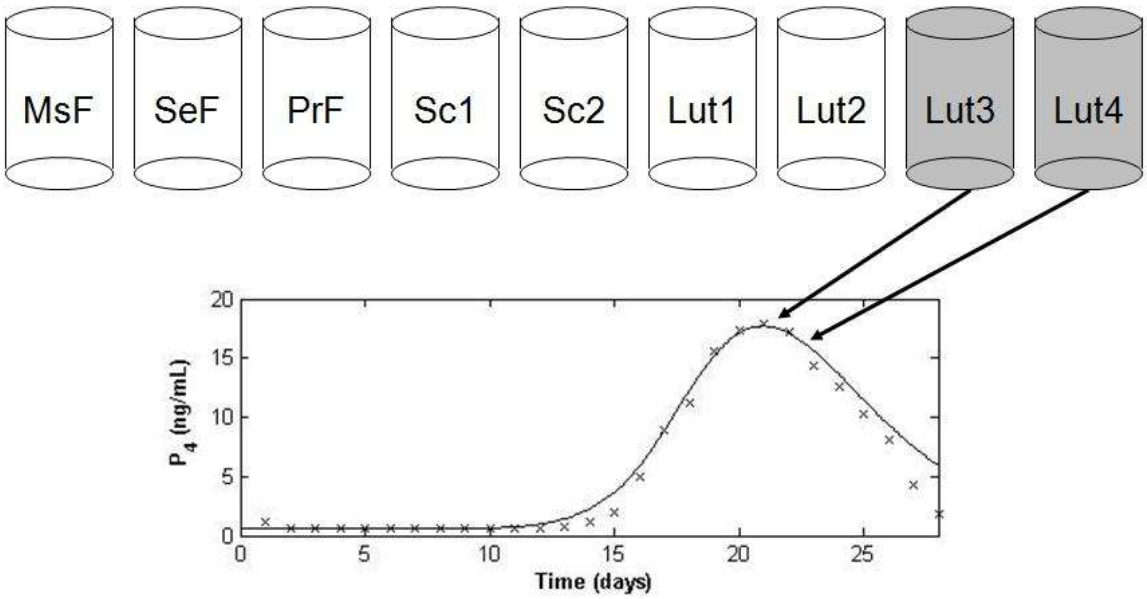

Figure 3.8 – Ovarian stages contributing to P_4

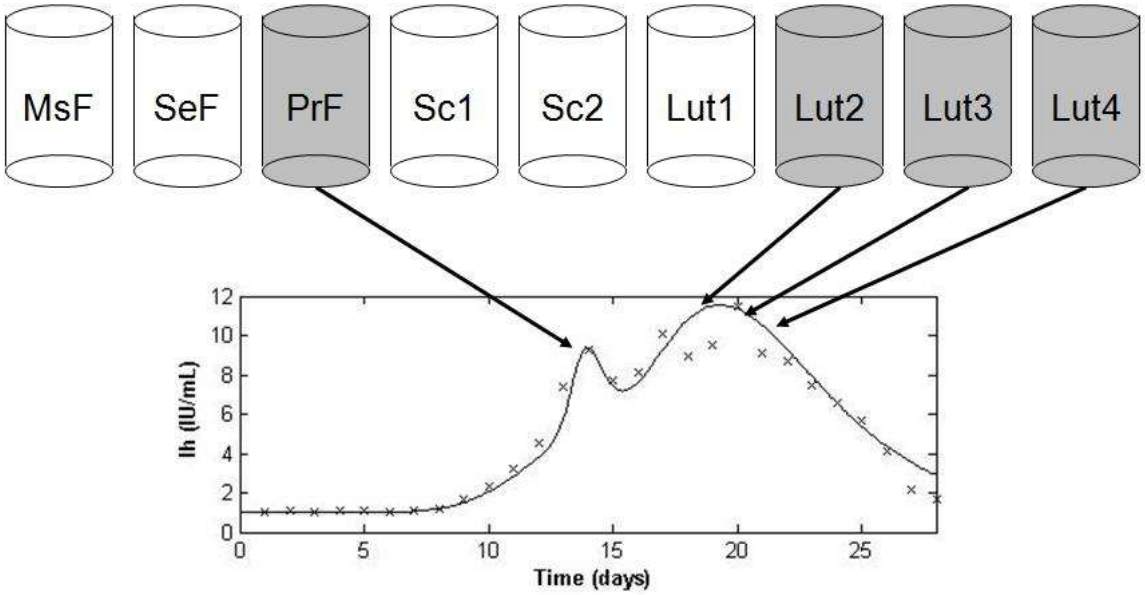

Figure 3.9 – Ovarian stages contributing to Ih

3.4 Fitting the Merged Model to the Welt Data

In the merged model, there are 46 parameters, but no input functions. We use the parameter values from the unmerged model as first estimates of the parameter values for the merged system. Because of the large number of parameters, the model fitting process is more difficult. The optimized parameter set is shown in Table 3.5; the units of these parameters are the same as those given in Tables 3.1-3.4.

For the stable unmerged models, the output had a period of exactly 28 days, matching the period of the input functions. Because we do not have the input functions in the merged model, the period of the system changes along with the parameters, but we want it to be as close to 28 days as possible. In numerical optimization, we found it helpful to analyze 84 days of model output, comparing it to three repetitions of our 28-day data set.

Table 3.5 – Merged model parameter values

Parameter	Value		Parameter	Value		Parameter	Value
$v_{0,LH}$	500		$c_{FSH,E}$	0.0018		α	0.79
$v_{1,LH}$	4500		d_{Ih}	2.0		β	0.16
Km_{LH}	180		a_{FSH}	8.21		γ	0.02
$Ki_{LH,P}$	12.2		b	0.05		e_0	40
k_{LH}	2.42		c_1	0.09		e_1	0.11
a	8		c_2	0.09		e_2	0.21
$c_{LH,P}$	0.26		c_4	0.13		e_3	0.45
$c_{LH,E}$	0.004		c_5	0.027		p_0	0
d_E	0.2		c_8	0.51		p_1	0.048
d_P	1.0		d_1	0.50		p_2	0.048
r_{LH}	14		d_2	0.56		h_0	0.4
v	2.5		k_1	0.55		h_1	0.009
v_{FSH}	375		k_2	0.69		h_2	0.029
$Ki_{FSH,Ih}$	3.5		k_3	0.85		h_3	0.018
k_{FSH}	1.90		k_4	0.85		h_4	0
$c_{FSH,P}$	12						

To eliminate problems due to initial conditions and/or phase shift, we simulate 150 days with the model, then find an LH surge in the middle of that 150 days and make that point to be the midpoint of our 84-day model output, matching up with the LH surge of the second period of the data. When we minimize the error over the entire 84-day

duration, we implicitly force the solution period to be approximately 28 days; if this is not the case, there will be large errors near the beginning and end of the 84 days. The parameter set presented in Table 3.5 leads to a model period of 28.02 days, except in the very rare circumstance that the initial conditions form an equilibrium for the system.

The output of the model, over 84 days, is shown in Figure 3.10 (the pituitary hormones LH and FSH) and Figure 3.11 (the ovarian hormones E_2, P_4, and Ih). It was our observation that the most difficult hormone profile to fit was that of FSH, particularly in early luteal phase. We were also unable to fit the E_2 profile well during the luteal phase.

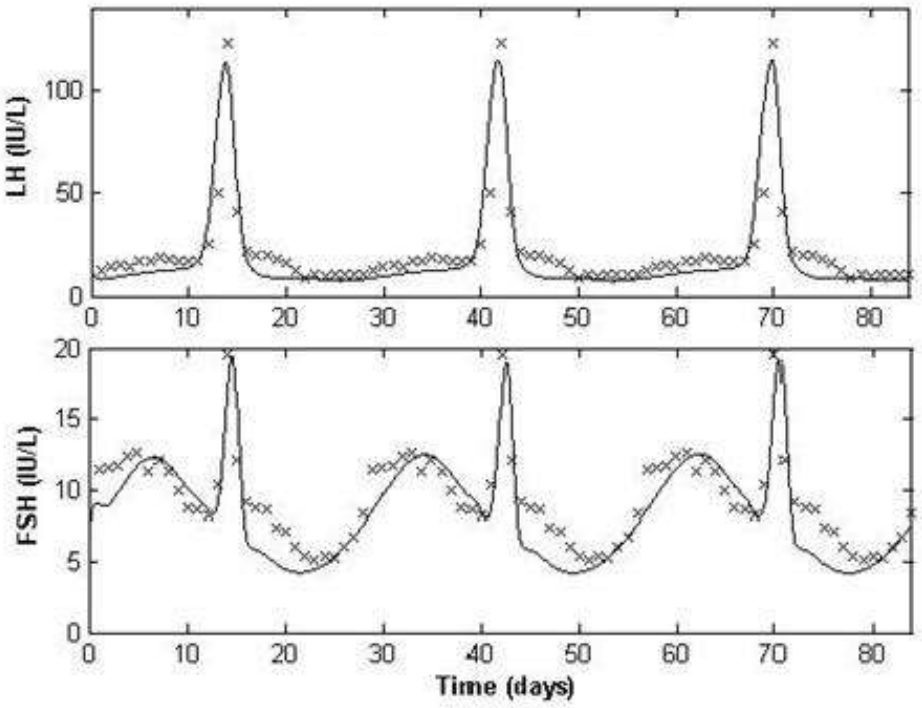

Figure 3.10 – Merged model output for the pituitary hormones

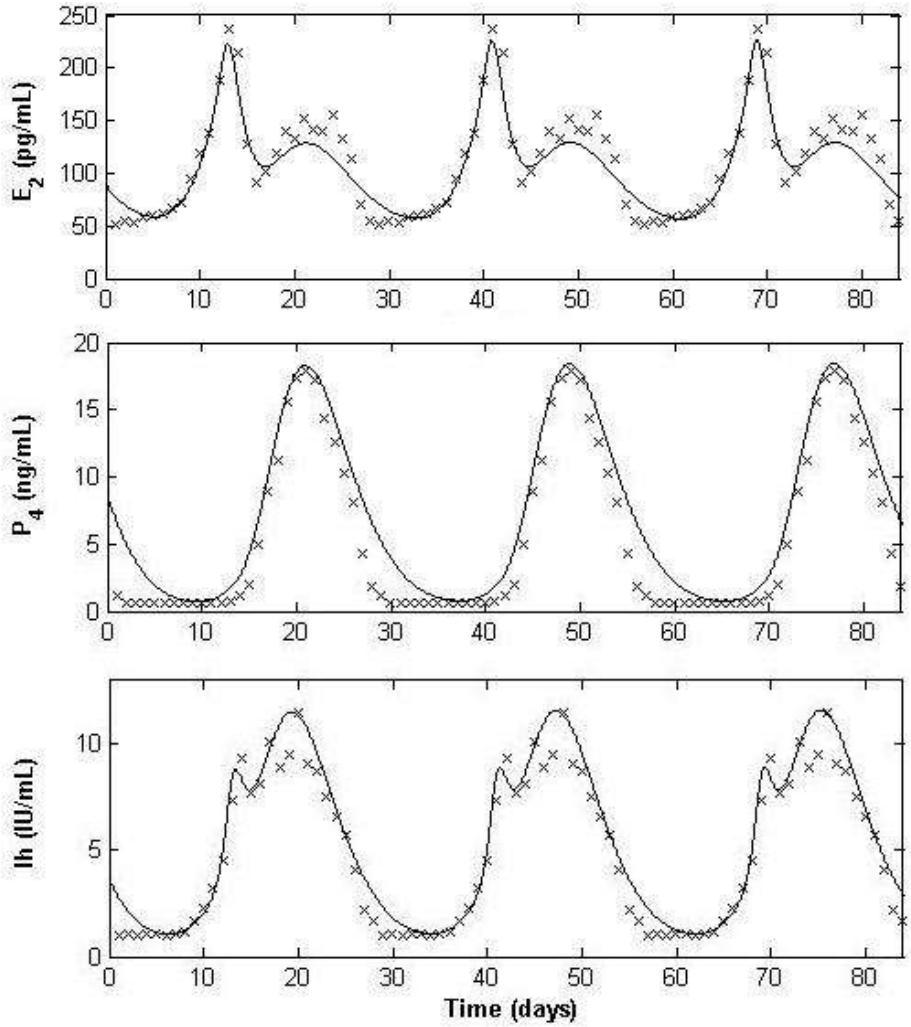

Figure 3.11 – Merged model output for the ovarian hormones

Chapter 4

Dynamics of the Five-Hormone Model

4.1 Equilibrium and Periodic Solutions

In studying the merged model, with the parameter set presented in Table 3.5, we are interested in both the periodic solutions and equilibrium solutions. We have already presented one periodic solution in Figures 3.10 and 3.11, with a period of 28.02 days, close to the assumed 28-day period of the data. We wish to ascertain whether there are other periodic solutions, and also whether there are equilibria. For each solution, determining the stability is also important, as unstable solutions are unlikely to be biologically relevant.

Given that our delay differential equation system (3.7) has dimension 13 and includes three delays, it is most practical to find and analyze periodic solutions numerically. Analytic stability results for systems of delay differential equations are difficult to obtain, because there are multiple Jacobian matrices involved. Using *dde23*, we can take the initial conditions which lead to a periodic or equilibrium solution, then perturb them slightly, and then obtain the solution over a relatively long period of time, perhaps even over several years. If the behavior of the perturbed system eventually mirrors that of the original solution, then we have a good idea that we have a stable

(periodic or equilibrium) solution. If it diverges from that solution, approaching a different equilibrium or periodic solution, then it is likely unstable. However, such divergence could also be caused by moving outside of the basin of attraction, so further investigation with smaller perturbations may be necessary to confirm the instability. In tracking equilibria and periodic solutions, stability, and bifurcations, we found the MATLAB package DDE-BIFTOOL (Engelborghs et al., 2002) (Engelborghs et al., 2001), which is freely available for scientific use, to be helpful.

The periodic solution discussed in section 3.4 is asymptotically stable, and has a very large domain of attraction, nearly to the point of global stability. In a 13-dimensional state space, we cannot guarantee that there are no other periodic solutions for this parameter set, but we were unable to find any others. In contrast, Clark et al. (2003) described two stable periodic solutions, after fitting this model to the McLachlan data (McLachlan et al., 1990).

Stability of equilibrium solutions can be easily determined analytically. Because of the constant nature of equilibria, delays are irrelevant, simplifying the delay differential equation system to a system of ordinary differential equations, with a single Jacobian matrix. As with an O.D.E. system, the eigenvalues of the Jacobian matrix determine the stability. If there are any eigenvalues with positive real part, then the equilibrium is unstable. If all of the eigenvalues have negative real part, then the equilibrium is asymptotically stable. For our parameter set, we found unstable

equilibria, but none that are stable. Table 4.1 gives the state variable values for an unstable equilibrium. Among the eigenvalues associated with this equilibrium are a complex conjugate pair with real part approximately 0.0237, indicating the instability.

Table 4.1 – A set of equilibrium conditions for the merged model

Variable	Value		Variable	Value
RP_{LH}	90.128		$Sc1$	128.29
LH	12.121		$Sc2$	114.55
RP_{FSH}	23.660		$Lut1$	116.63
FSH	7.0806		$Lut2$	92.965
MsF	40.501		$Lut3$	75.466
SeF	196.01		$Lut4$	75.466
PrF	119.65			

4.2 Bifurcations

Bifurcations occur when small changes to parameter values result in qualitative changes in solution behavior. These can include changes to the existence and/or stability of solutions. In varying single parameters from the values listed in Table 3.5, we found examples of Hopf and saddle-node bifurcations.

A Hopf bifurcation occurs when a complex conjugate pair of eigenvalues crosses the imaginary axis. Such a bifurcation is *supercritical* if, as the parameter passes the

bifurcation value, an equilibrium loses stability and a stable periodic solution is created. If the pair of eigenvalues have values $\pm bi,$ then the periodic solution will have a period of approximately $\frac{2\pi}{|b|}$ near the bifurcation point. We found multiple examples of supercritical Hopf bifurcations with this system. One such example occurs as the parameter α reaches a value of approximately 0.9124. This bifurcation is the reverse of the above description, in that an equilibrium gains stability and a periodic solution vanishes, as α increases (from its starting value of 0.79) beyond the bifurcation value. Figure 4.1 shows the maximal eigenvalue real part for the equilibrium solution. For $\alpha > 0.9124,$ all the eigenvalues have negative real part, so we have a stable equilibrium.

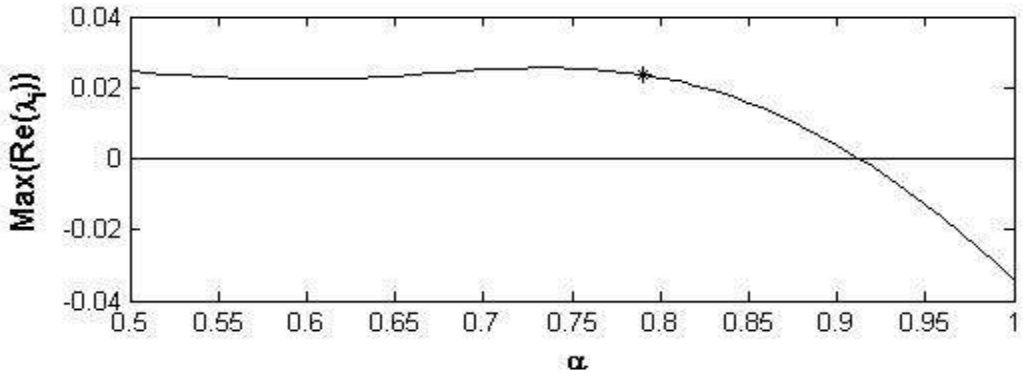

Figure 4.1 – Maximal eigenvalue real part for the equilibrium solution

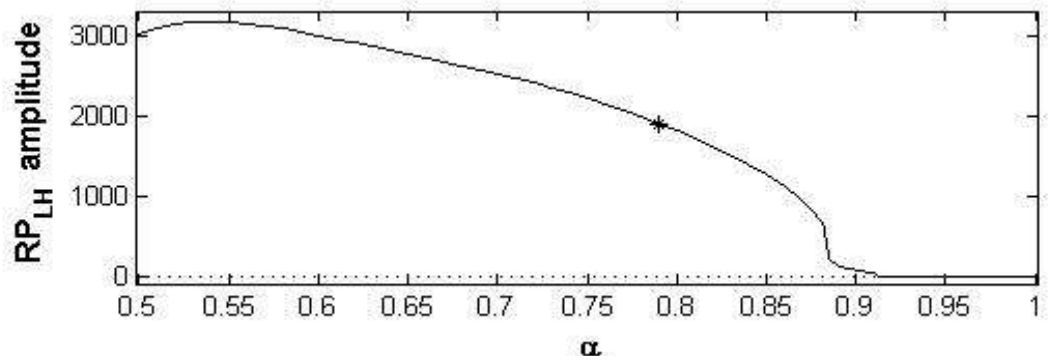

Figure 4.2 – Amplitude of the stable periodic solution versus α

For lower values (including the starred normal value 0.79 from Table 3.5), we have at least one eigenvalue with positive real part, so the equilibrium is unstable. Figure 4.2 shows the amplitude of the periodic solution, which decreases to zero as α approaches the bifurcation value. For $\alpha > 0.9124,$ the periodic solution does not exist.

The period of the periodic solution is displayed in Figure 4.3; our *dde23* solution indicates a period of 41.26 days as we approach the bifurcation. In Figure 4.4, the upper-rightmost eigenvalue is plotted, as α varies between 0.5 and 1. When the bifurcation value is reached, this eigenvalue crosses the imaginary axis from right to left, with an imaginary part of approximately $0.1524i$. By our formula $2\pi/b$, the periodic solution should, at the Hopf bifurcation point, have a period of 41.23 days, which is very close to what we found using the solver. There were also Hopf bifurcations found for several other parameters, including c_2, $v_{0,LH}$, Km_{LH}, v_{FSH}, e_1, and a, using DDE-BIFTOOL.

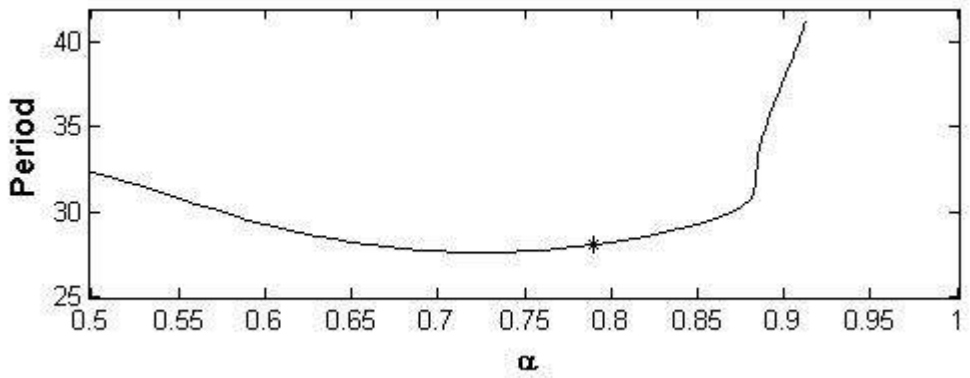

Figure 4.3 – Period (in days) of the stable periodic solution

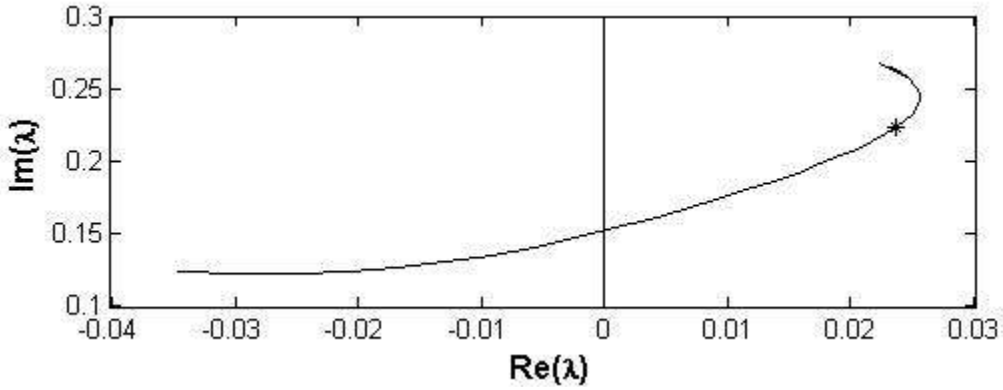

Figure 4.4 – Upper-rightmost eigenvalue, for $0.5 \le \alpha \le 1$

A saddle-node bifurcation, also known as a tangent bifurcation, occurs when two periodic solutions are suddenly created or destroyed, as a result of a small change in a parameter. We observed this phenomenon for only one parameter, Km_{LH}. As Km_{LH} varies from its starting value of 180, there are two saddle-node bifurcations and two Hopf bifurcations, leading to a variety of dynamical behavior. The Hopf bifurcations occur at Km_{LH} values of approximately 68.66 and 256.9, while the saddle-node bifurcations occur when Km_{LH} is roughly 246.1 or 308.2. Figure 4.5 shows existence of

equilibrium (amplitude zero) and periodic (nonzero amplitude) solutions, as Km_{LH} varies; solid lines indicate stable solutions, while dotted lines represent unstable ones. Figure 4.6 shows the variation in the period of non-equilibrium solutions as Km_{LH} varies.

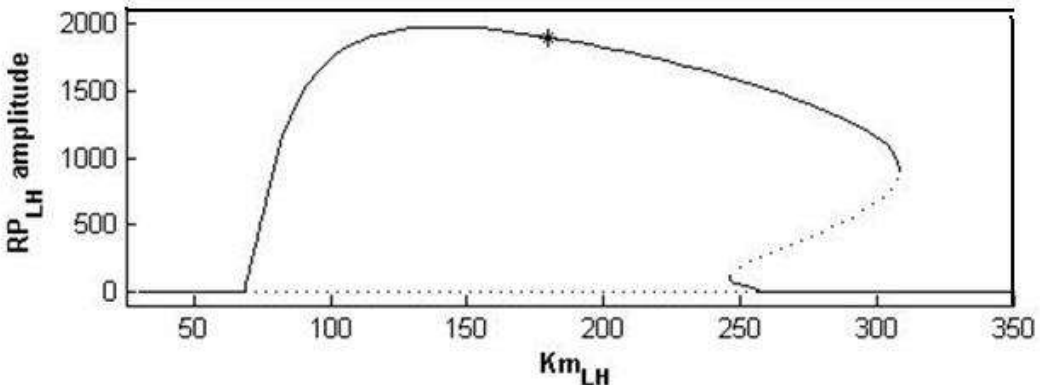

Figure 4.5 – Solutions and bifurcations of Km_{LH}

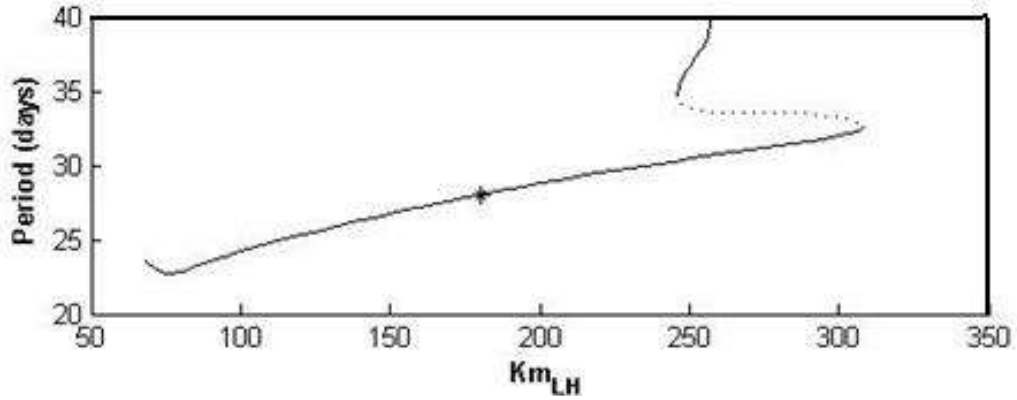

Figure 4.6 – Periods of periodic solutions, as Km_{LH} varies

For moderate values where $68.66 < Km_{LH} < 246.1$ (including the best-fit model value of 180), there is a stable periodic solution and an unstable equilibrium. As Km_{LH}

decreases, a Hopf bifurcation at 68.66 results in the loss of the periodic solution; at lower Km_{LH} values, there is only a stable equilibrium. At high Km_{LH} values, above 308.2, there is also only a stable equilibrium. The most interesting dynamical behavior occurs in between the two saddle-node bifurcation values. In the small range where $246.1 < Km_{LH} < 256.9,$ there are two stable periodic solutions, as well as an unstable periodic solution and an unstable equilibrium. Section 4.3 includes more discussion of the system dynamics in this range, using $Km_{LH} = 250.$ Finally, for $256.9 < Km_{LH} < 308.2,$ there is a stable periodic solution, an unstable periodic solution, and a stable equilibrium.

4.3 External Hormone Effects

In previous work fitting the same model to the McLachlan (1990) data, the existence of two stable periodic solutions is described by Harris (2001) and Clark et al. (2003). After fitting the model to the Welt data, our results were not the same; for the parameter set that best fits the data, there appears to be only one stable periodic solution. However, if we vary the parameter $Km_{LH},$ there is a small range for which two stable periodic solutions exist, as shown in Figure 4.5. We will further explore the dynamics of the system with $Km_{LH} = 250,$ as opposed to $Km_{LH} = 180$ originally, but all other parameters remaining as given in Table 3.5.

At this value of Km_{LH}, there is an unstable equilibrium, as well as three periodic solutions – two stable and one unstable. Plots of the circulating levels of E_2 associated with each of the three periodic solutions are shown in Figure 4.7. The solid lines indicate stable solutions, while the dotted line indicates the unstable one.

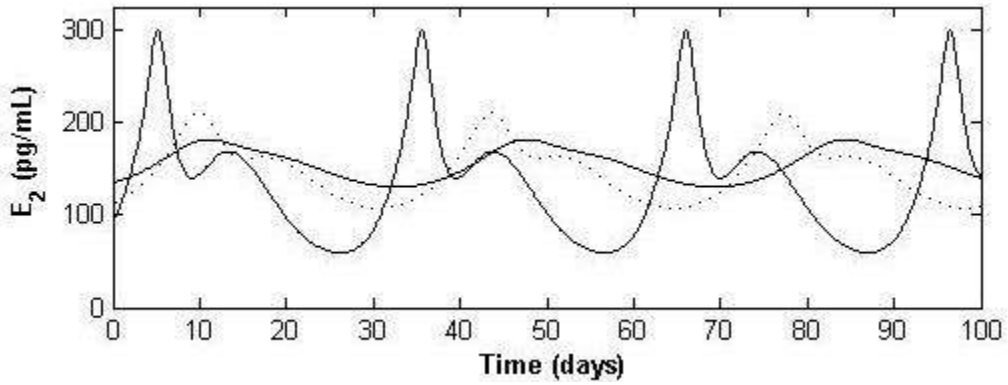

Figure 4.7 – E_2 levels for the three periodic solutions, at Km_{LH} = 250

Of these three solutions, the one with highest amplitude is the pseudo-normal solution, which is the continuation of the attracting solution associated with the standard parameters of Table 3.5. It has a period of approximately 30.4 days, which is within the range considered normal for a woman's menstrual cycle length. The hormone profiles are quite similar to those of the normal ($Km_{LH} = 180$) profiles, with an LH surge peaking at over 100 IU/L, about 20% below the average value from the Welt (1999) data, but still likely sufficient to lead to ovulation.

By comparison, the low-amplitude periodic solution has a period of 36.6 days, significantly longer than the 28-day average normal cycle. There is no LH surge, only a

slight mid-cycle rise; such a hormone profile is abnormal, and would not lead to ovulation. The LH levels over 100 days for the two stable cycles are shown in Figure 4.8, along with the data. The solid line indicates the pseudo-normal solution, and the dotted line the abnormal solution. The moderate-amplitude, unstable solution shown in Figure 4.7 is not biologically significant, because of its instability.

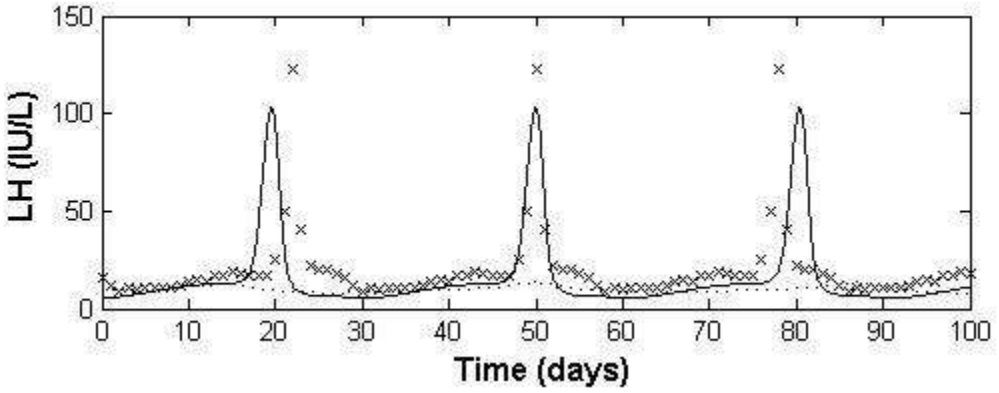

Figure 4.8 – LH levels for the two stable solutions at Km_{LH} = 250, with data

There are both similarities and differences between the pair of stable periodic solutions described here and those noted by Harris (2001) and Clark et al. (2003), beyond merely whether a parameter change is needed to observe them. Our predecessors' results showed a low-amplitude abnormal cycle with a decreased period (approximately 24 days), whereas we found an increased period (36.6 days) in the abnormal cycle. Both models indicate decreased levels of FSH in the abnormal cycle, but their model showed slightly higher non-surge LH levels, while ours did not. While it is difficult to quantify the size of basins of attraction for asymptotically stable periodic solutions in a 13-

dimensional space, the normal cycle appears to have a larger domain of attraction than the abnormal cycle, just as in (Harris, 2001) and (Clark et al., 2003).

Regarding the pseudo-normal and abnormal cycles, one question of interest is whether short-term external hormonal influences could toggle which hormonal profile a woman has, continuing even after cessation of the hormone exposure. That is, can short-term pharmaceutical intervention serve as a long-term solution for an abnormal menstrual cycle similar to the one described above? Also, could low-dose exposure to external hormones cause a normally cycling woman to begin having abnormal, anovulatory menstrual cycles? According to our model, the answer is "yes," in both cases.

In resolving the abnormal menstrual cycle, our model suggests that a short-term course of exogenous estradiol or progesterone could be effective in restoring a more normal cycle. First, we consider a five-day, follicular phase treatment with progesterone, as shown in Figure 4.9, sufficient to increase the bloodstream P_4 levels by 15 ng/mL. This is a high dose, which more than doubles the concentration of P_4, however, P_4 does not increase beyond the mid-luteal peak observed in a normal woman. The result of this one-time, five-day treatment is shown in Figure 4.10. The model shows that the subject's progesterone level (indicated with a solid line) slowly returns to a normal level over several cycles, while the control subject's P_4 levels (shown with a dotted line) remain in a low-amplitude cycle.

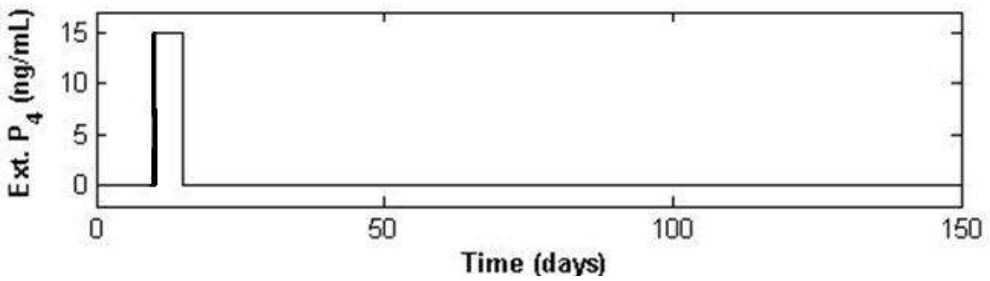

Figure 4.9 – External P_4 treatment dosage

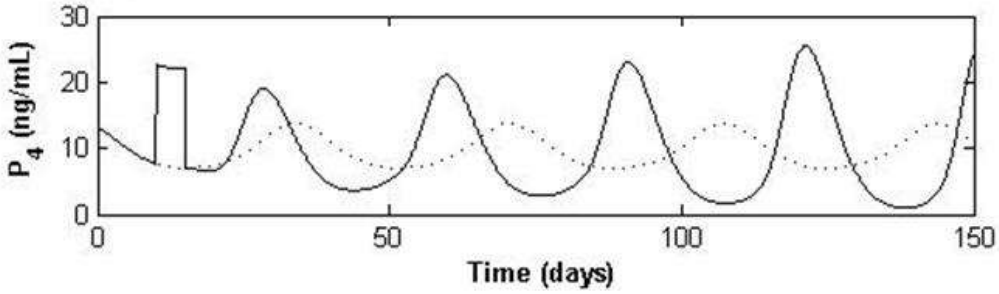

Figure 4.10 – Resulting bloodstream concentration of P_4

In considering potential treatment protocols using exogenous estradiol, we find that dosage is important. Figures 4.11 and 4.12 show the failure of a five-day, low dose course of E_2 (causing a 25 pg/mL bloodstream concentration increase) to restore a normal cycle. However, Figures 4.13 and 4.14 show that doubling the dosage over the same five days does cause the desired effect.

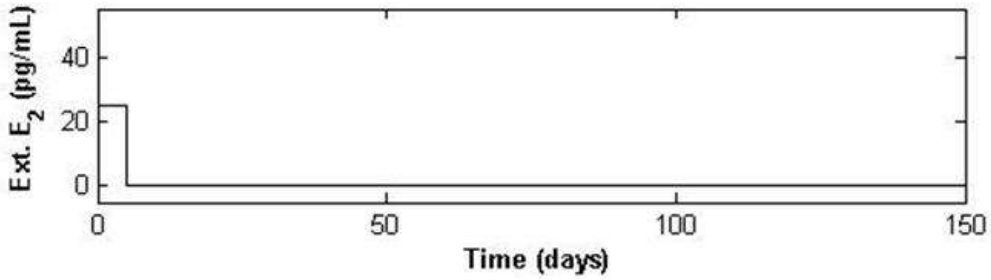

Figure 4.11 – External E_2 low-dose treatment dosage

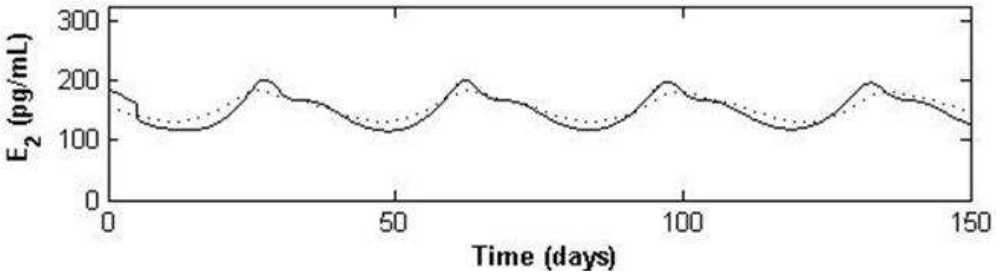

Figure 4.12 – Resulting bloodstream concentration of E_2

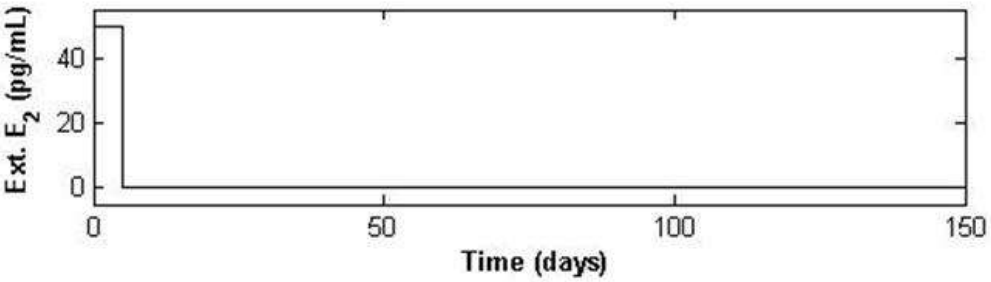

Figure 4.13 – External E_2 high-dose treatment dosage

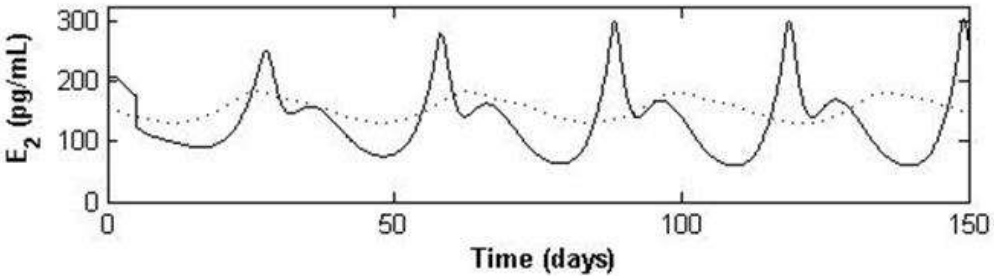

Figure 4.14 – Resulting bloodstream concentration of E_2

Given the apparently large basin of attraction for the pseudo-normal stable periodic solution, as compared to that of the abnormal periodic solution, there are likely a variety of other treatment protocols that would be effective as well, based on the model.

As discussed in Chapter 1, there is rising concern over the unintentional intake of endocrine hormones, particularly xenoestrogens, via food and drinking water. We sought to determine whether low-dose, longer-term exposure to ovarian hormones could take a woman from a normal cycle into an abnormal one, which would persist even after the hormone exposure ended. Our model showed that this is possible with a low-dose, 20-day exposure to exogenous inhibin, as shown in Figures 4.15 and 4.16. The amount of external hormones introduced was sufficient to cause a bloodstream rise of 2 IU/mL, sustained for the 20-day dosage period, which occurred during the follicular phase and early luteal phase. Following cessation of the external inhibin, the solid-line profile in Figure 4.16 shows the resulting low-amplitude cycle that is sustained indefinitely as a result. By comparison, the control subject, whose profile is shown with a dotted line, has a normal hormone profile throughout the 100 days.

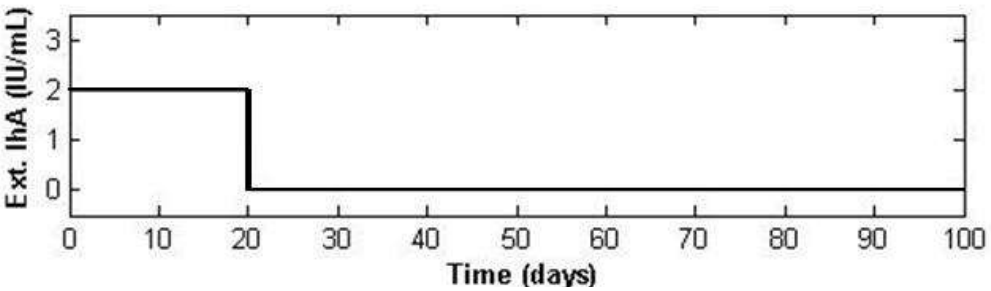

Figure 4.15 – External inhibin low-dose exposure level

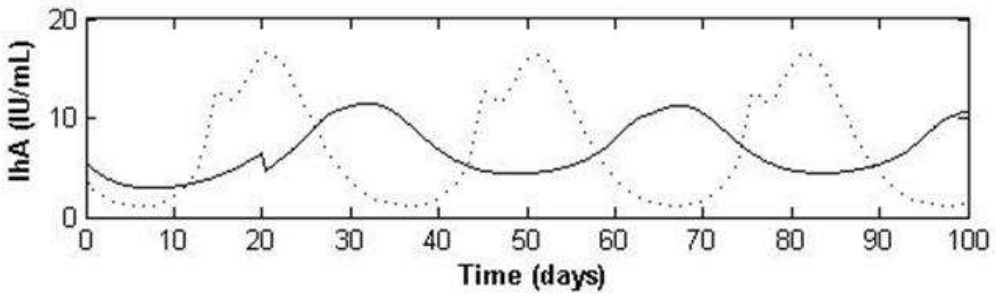

Figure 4.16 – Resulting bloodstream concentration of inhibin

When changing the dosage of exposure in the model simulations, we were surprised to find that 20-day exposure to a 50% higher dose of inhibin did not have the same effect. Instead, a resumption of a normal menstrual cycle occurred, but with a phase change, as the exogenous inhibin caused one extended cycle, roughly six weeks in duration. These results are shown in Figures 4.17 and 4.18. Although the recurrence of a normal menstrual cycle is likely related to the relatively small basin of attraction of attraction of the abnormal menstrual cycle, we have no physiological argument as to why a higher dose would not cause the same negative effect as a lower dose.

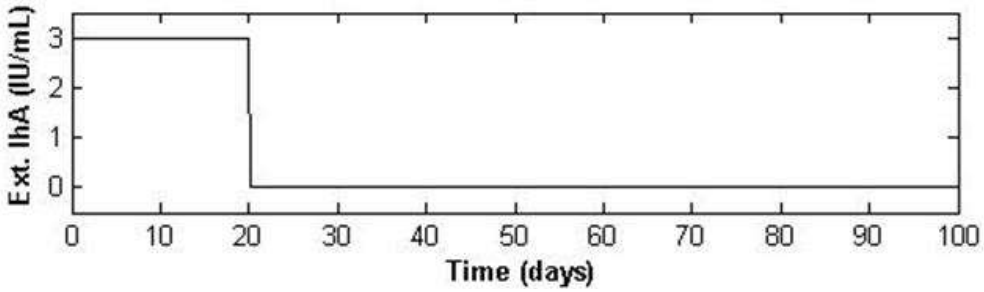

Figure 4.17 – External inhibin high-dose exposure level

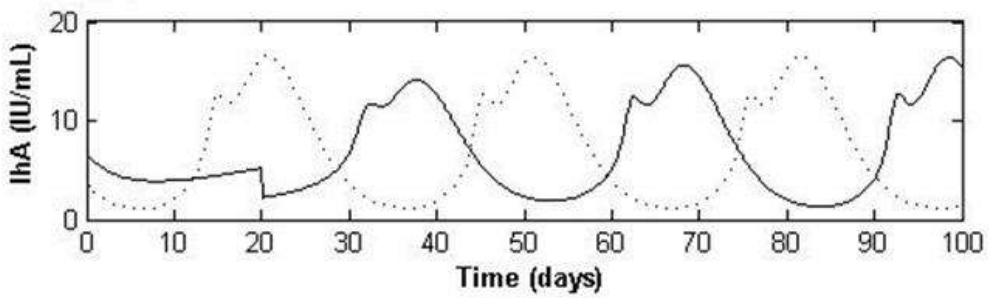

Figure 4.18 – Resulting bloodstream concentration of inhibin

Although our model showed that inhibin exposure could cause a change from normal to abnormal menstrual cycles, we did not find a parallel result for estradiol. This is significant because environmental exposure to xenoestrogens, not inhibin-like compounds, is the primary concern discussed in the medical literature. Also worth noting is that our model experiments with external inhibin are unlikely to be repeated in a clinical setting, given that attempting to cause abnormal menstrual cycles in healthy women is ethically dubious.

4.4 Sensitivity Analysis

In systems with large numbers of parameters, it is often desirable to identify those which have the greatest proportional effect on various aspects of the model. A non-dimensional sensitivity coefficient can be computed using (4.1).

$$S(p) = \frac{1}{\varepsilon}\left(\frac{X(p+\varepsilon p) - X(p)}{X(p)} \right) \tag{4.1}$$

In this equation, p represents the original value of a certain parameter, $X(p)$ is some output measurement when the parameter takes the value p, and ε is a small percentage by which we will perturb the parameter. Then $X(p+\varepsilon p)-X(p)$ is the change in X after augmenting the parameter, and $\frac{X(p+\varepsilon p)-X(p)}{X(p)}$ gives the relative change in X. Multiplying this quotient by $1/\varepsilon$ standardizes the results, allowing for comparison among different parameters, for varying values of ε. For example, if $\varepsilon = .005$ (i.e. a 0.5% perturbation of p) and the resulting relative change in X is 1.5%, the sensitivity coefficient would be 3, indicating that the magnitude of the effect was three times as great as the magnitude of the perturbation.

With the merged model, we performed a sensitivity analysis to determine which parameters have the greatest relative influence on various aspects of the system. Using $\varepsilon = .01$, a one-percent perturbation, we considered the effects on the peak values of each of the five hormones, as well as on the period length, for each of the parameters in the model, with the exception of the physiological constants. A table showing the full results of this sensitivity analysis is included as Appendix B.1.

In this model, the most sensitive parameter is α, the exponent on LH in the mass transfer between the first two ovarian stages. Not coincidentally, it was also one of the parameters for which we described a bifurcation in Section 4.2; the most sensitive parameters are a logical starting place when conducting bifurcation analysis. As α is

increased, the peak levels of all five hormones are significantly decreased, and the period is lengthened. The parameters c_2 (also involved in first-to-second-stage ovarian mass transfer) and $v_{0,LH}$ (the baseline LH production level) have similar effects, but to a lesser degree. Two other sensitive parameters, c_1 (an ovarian first-stage growth rate) and v_{FSH} (the baseline FSH production level) have the opposite effects of the above, increasing peak values for each of the five hormones, and decreasing cycle length. Some parameters are sensitive for some, but not all, of these measures. For example, increasing the Hill function threshold Km_{LH} causes a significant rise in the three ovarian hormones, but only a slight drop in the pituitary hormones. There are also some parameters which are not sensitive in any of the measures we are using.

Sensitivity analysis can also be helpful in fitting a model to data, because it can help identify the key parameters for which small changes have significant impacts on the output. This has the potential of greatly reducing the number of parameters being varied in an optimization routine, resulting in faster and perhaps better results.

Chapter 5

A New Multiple-Inhibin Model

5.1 A Revised Pituitary Model

One primary goal of the research leading to this dissertation was to expand the model to include both inhibins individually, instead of only total inhibin. Because circulating levels of each inhibin have a negative effect of FSH synthesis, we will change the FSH synthesis function from the one given in (3.4) to the following.

$$\text{FSH synthesis rate}\left(IhA, IhB\right) = \frac{v_{FSH}}{1 + \frac{IhA(t - d_{IhA})}{Ki_{FSH,IhA}} + \frac{IhB(t - d_{IhB})}{Ki_{FSH,IhB}}} \tag{5.1}$$

Having the negative feedback of *IhB* on FSH synthesis will allow us to reduce the unrealistic quadratic inhibition of E_2 on FSH release to a more realistic linear effect.

$$\text{FSH release rate}\left(E_2, P_4, RP_{FSH}\right) = k_{FSH} \cdot \frac{1 + c_{FSH,P} \cdot P_4(t)}{1 + c_{FSH,E} \cdot E_2(t)} \cdot RP_{FSH}(t) \tag{5.2}$$

The clearance term for FSH is unchanged. Making these two changes, the FSH system is now given by (5.3), instead of (3.10).

$$\begin{aligned}
\frac{d}{dt}RP_{FSH} &= \frac{v_{FSH}}{1+\dfrac{IhA(t-d_{IhA})}{Ki_{FSH,IhA}}+\dfrac{IhB(t-d_{IhB})}{Ki_{FSH,IhB}}} - k_{FSH}\cdot\frac{1+c_{FSH,P}\cdot P_4}{1+c_{FSH,E}\cdot E_2}\cdot RP_{FSH} \\
\frac{d}{dt}FSH &= \frac{1}{v}\cdot\frac{1+c_{FSH,P}\cdot P_4}{1+c_{FSH,E}\cdot E_2}\cdot RP_{FSH} - a_{FSH}\cdot FSH
\end{aligned} \tag{5.3}$$

The LH system is not directly affected by this change, and remains the same as in (3.8).

$$\begin{aligned}
\frac{d}{dt}RP_{LH} &= \frac{v_{0,LH}+v_{1,LH}\dfrac{\left(E_2(t-d_E)/Km_{LH}\right)^a}{1+\left(E_2(t-d_E)/Km_{LH}\right)^a}}{1+\dfrac{P_4(t-d_P)}{Ki_{LH,P}}} - k_{LH}\cdot\frac{1+c_{LH,P}\cdot P_4}{1+c_{LH,E}\cdot E_2}\cdot RP_{LH} \\
\frac{d}{dt}LH &= \frac{1}{v}\cdot k_{LH}\cdot\frac{1+c_{LH,P}\cdot P_4}{1+c_{LH,E}\cdot E_2}\cdot RP_{LH} - r_{LH}\cdot LH
\end{aligned} \tag{5.4}$$

5.2 An Expanded Ovarian Model

If we wish to represent inhibin B as a linear combination of ovarian stages, then the nine-stage ovarian model discussed in Chapter 3 is insufficient. This is because inhibin B has a peak during the mid-follicular phase, well before any of the other ovarian hormones peak, and several days before the peak of *MsF*, our first ovarian stage. To address this issue, we have increased the number of stages from nine to twelve, with two new stages added at the beginning, and one around the time of ovulation. The latter change is needed because inhibin B also has a mid-cycle peak, which occurs on a different day than any peaks of other ovarian hormones. Figure 5.1 is a schematic diagram for the new twelve-stage ovarian model. The associated equations are given by (5.5).

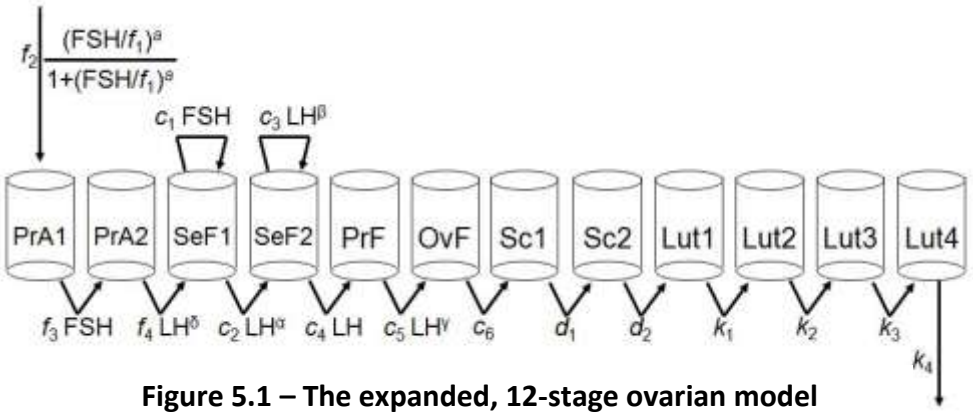

Figure 5.1 – The expanded, 12-stage ovarian model

$$\frac{d}{dt}PrA1 = f_2 \cdot \frac{\left(FSH/f_1\right)^b}{1+\left(FSH/f_1\right)^b} - f_3 \cdot FSH \cdot PrA1$$

$$\frac{d}{dt}PrA2 = f_3 \cdot FSH \cdot PrA1 - f_4 \cdot LH^{\delta} \cdot PrA2$$

$$\frac{d}{dt}SeF1 = f_4 \cdot LH^{\delta} \cdot PrA2 + \left(c_1 \cdot FSH - c_2 \cdot LH^{\alpha}\right) \cdot SeF1$$

$$\frac{d}{dt}SeF2 = c_2 \cdot LH^{\alpha} \cdot SeF1 + \left(c_3 \cdot LH^{\beta} - c_4 \cdot LH\right) \cdot SeF2$$

$$\frac{d}{dt}PrF = c_4 \cdot LH \cdot SeF2 - c_5 \cdot LH^{\gamma} \cdot PrF$$

$$\frac{d}{dt}OvF = c_5 \cdot LH^{\gamma} \cdot PrF - c_6 \cdot OvF$$

$$\frac{d}{dt}Sc1 = c_6 \cdot OvF - d_1 \cdot Sc1$$

$$\frac{d}{dt}Sc2 = d_1 \cdot Sc1 - d_2 \cdot Sc2$$

$$\frac{d}{dt}Lut1 = d_2 \cdot Sc2 - k_1 \cdot Lut1$$

$$\frac{d}{dt}Lut2 = k_1 \cdot Lut1 - k_2 \cdot Lut2 \qquad (5.5)$$

$$\frac{d}{dt}Lut3 = k_2 \cdot Lut2 - k_3 \cdot Lut3$$

$$\frac{d}{dt}Lut4 = k_3 \cdot Lut3 - k_4 \cdot Lut4$$

The input term for the first ovarian stage includes a Hill function. In contrast, the equivalent term in the nine-stage model was a constant multiplied by the bloodstream FSH level. The biological literature indicates that, at the luteal-follicular transition, there may be a critical FSH threshold for production of inhibin B (Welt et al., 1997). With this in mind, we have included this additional Hill function, with FSH as the catalyst. It is noteworthy that FSH does not lead directly to IhB production, but rather indirectly leads to it, by promoting follicular development, which leads to synthesis of inhibin B.

5.3 Changes to the Auxiliary Equations

The auxiliary equations given by (3.6) will remain largely intact, with only nomenclature changes. The old equation for total inhibin (*Ih*) now represents inhibin A (*IhA*); some of the ovarian stages have also been renamed. More significantly, we must add a fourth auxiliary equation, to model *IhB* in terms of the ovarian stages. The new auxiliary equations are given by (5.6).

$$\begin{aligned} E_2 &= e_0 + e_1 \cdot SeF2 + e_2 \cdot PrF + e_3 \cdot Lut4 \\ P_4 &= p_0 + p_1 \cdot Lut3 + p_2 \cdot Lut4 \\ IhA &= h_0 + h_1 \cdot PrF + h_2 \cdot Lut2 + h_3 \cdot Lut3 + h_4 \cdot Lut4 \\ IhB &= j_0 + j_1 \cdot PrA2 + j_2 \cdot PrF + j_3 \cdot OvF \end{aligned} \tag{5.6}$$

As with the others, the equation for inhibin B includes a constant baseline level. This equation also includes multiples of three ovarian stages. The broad peak of inhibin B during the follicular phase comes from the latter of the two new stages added at the beginning of the cycle. The other peak, around the time of ovulation, is obtained using two stages, the new ovulatory stage, and the stage immediately preceding it.

5.4 The New Merged Model

The addition of three new ovarian stages raises the dimension of the merged model by three. The 16-dimensional system is given by putting together the LH system (5.4), the FSH system (5.3), and the ovarian system (5.5). Along with this merged system, we have the four auxiliary equations given by (5.6), which model the ovarian hormones in terms of the sixteen state variables.

$$\frac{d}{dt}RP_{LH} = \frac{v_{0,LH} + v_{1,LH}\dfrac{\left(E_2(t-d_E)/Km_{LH}\right)^a}{1+\left(E_2(t-d_E)/Km_{LH}\right)^a}}{1+\dfrac{P_4(t-d_P)}{Ki_{LH,P}}} - k_{LH}\cdot\frac{1+c_{LH,P}\cdot P_4}{1+c_{LH,E}\cdot E_2}\cdot RP_{LH}$$

$$\frac{d}{dt}LH = \frac{1}{v}\cdot k_{LH}\cdot\frac{1+c_{LH,P}\cdot P_4}{1+c_{LH,E}\cdot E_2}\cdot RP_{LH} - r_{LH}\cdot LH$$

$$\frac{d}{dt}RP_{FSH} = \frac{v_{FSH}}{1+\dfrac{IhA(t-d_{IhA})}{Ki_{FSH,IhA}}+\dfrac{IhB(t-d_{IhB})}{Ki_{FSH,IhB}}} - k_{FSH}\cdot\frac{1+c_{FSH,P}\cdot P_4}{1+c_{FSH,E}\cdot E_2}\cdot RP_{FSH}$$

$$\frac{d}{dt}FSH = \frac{1}{v}\cdot\frac{1+c_{FSH,P}\cdot P_4}{1+c_{FSH,E}\cdot E_2}\cdot RP_{FSH} - a_{FSH}\cdot FSH$$

$$\frac{d}{dt}PrA1 = f_2\cdot\frac{\left(FSH/f_1\right)^b}{1+\left(FSH/f_1\right)^b} - f_3\cdot FSH\cdot PrA1$$

$$\frac{d}{dt}PrA2 = f_3\cdot FSH\cdot PrA1 - f_4\cdot LH^{\delta}\cdot PrA2$$

$$\frac{d}{dt}SeF1 = f_4\cdot LH^{\delta}\cdot PrA2 + \left(c_1\cdot FSH - c_2\cdot LH^{\alpha}\right)\cdot SeF1$$

$$\frac{d}{dt}SeF2 = c_2\cdot LH^{\alpha}\cdot SeF1 + \left(c_3\cdot LH^{\beta} - c_4\cdot LH\right)\cdot SeF2$$

$$\frac{d}{dt}PrF = c_4\cdot LH\cdot SeF2 - c_5\cdot LH^{\gamma}\cdot PrF$$

$$\frac{d}{dt}OvF = c_5\cdot LH^{\gamma}\cdot PrF - c_6\cdot OvF$$

$$\frac{d}{dt}Sc1 = c_6\cdot OvF - d_1\cdot Sc1$$

$$\frac{d}{dt}Sc2 = d_1\cdot Sc1 - d_2\cdot Sc2$$

$$\frac{d}{dt}Lut1 = d_2\cdot Sc2 - k_1\cdot Lut1$$

$$\frac{d}{dt}Lut2 = k_1\cdot Lut1 - k_2\cdot Lut2$$

$$\frac{d}{dt}Lut3 = k_2\cdot Lut2 - k_3\cdot Lut3 \qquad (5.7)$$

$$\frac{d}{dt}Lut4 = k_3\cdot Lut3 - k_4\cdot Lut4$$

5.5 Parameter Identification

In the early stages of expanding the model, it was unclear whether or not we could successfully decrease estradiol's inhibition of FSH synthesis from second-order to first-order, so we optimized the FSH system parameters for each of these cases. For quadratic inhibition, the system is given by (5.8). The optimized parameters and resulting FSH plot are shown in Table 5.1 and Figure 5.2, respectively.

$$\begin{aligned}\frac{d}{dt}RP_{FSH} &= \frac{v_{FSH}}{1+\dfrac{IhA(t-d_{IhA})}{Ki_{FSH,IhA}}+\dfrac{IhB(t-d_{IhB})}{Ki_{FSH,IhB}}} - k_{FSH}\cdot\frac{1+c_{FSH,P}\cdot P_4}{1+c_{FSH,E}\cdot E_2^2}\cdot RP_{FSH} \\ \frac{d}{dt}FSH &= \frac{1}{v}\cdot\frac{1+c_{FSH,P}\cdot P_4}{1+c_{FSH,E}\cdot E_2^2}\cdot RP_{FSH} - a_{FSH}\cdot FSH\end{aligned} \tag{5.8}$$

Table 5.1 – Optimized FSH parameters for quadratic E_2 inhibition

Parameter	Value	Unit		Parameter	Value	Unit
v_{FSH}	562	IU/day		$c_{FSH,E}$	$8.22\cdot10^{-4}$	mL^2/pg^2
$Ki_{FSH,IhA}$	2.74	IU/mL		d_{IhA}	2.5	day
$Ki_{FSH,IhB}$	143	IU/mL		d_{IhB}	1.4	day
k_{FSH}	2.00	day^{-1}		a_{FSH}	8.21	day^{-1}
$c_{FSH,P}$	19.0	mL/ng		v	2.5	L

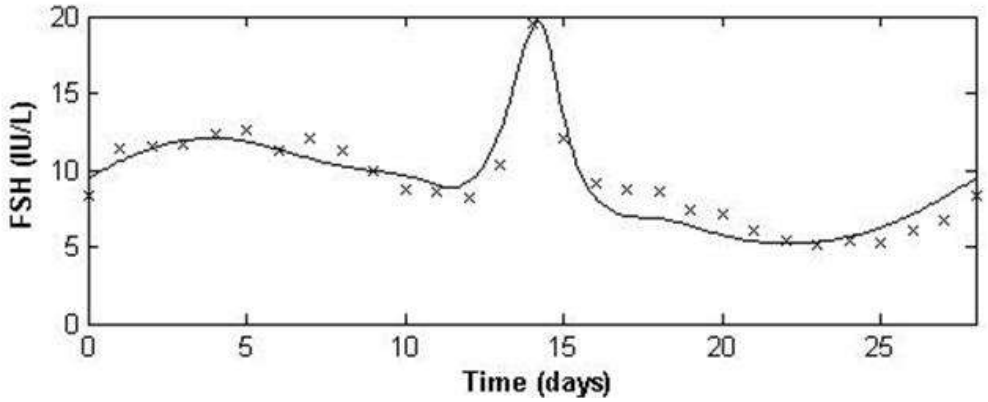

Figure 5.2 – FSH system plot for quadratic E_2 inhibition

For the more biologically realistic linear inhibition of FSH synthesis by estradiol, the FSH system was previously given by (5.3). Table 5.2 and Figure 5.3 show the parameter set and FSH plot using those parameters. Note that the units on $c_{FSH,E}$ are different than in the other parameter set. While the FSH model output is not as good with the reduced E_2 effect, there is hope that this will improve in the merged model. We did eventually use linear inhibition, rather than quadratic, in the merged model (5.7).

Table 5.2 – Optimized FSH parameters for linear E_2 inhibition

Parameter	Value	Unit		Parameter	Value	Unit
v_{FSH}	756	IU/day		$c_{FSH,E}$	0.350	mL/pg
$Ki_{FSH,IhA}$	2.00	IU/mL		d_{IhA}	2.5	Day
$Ki_{FSH,IhB}$	77.5	IU/mL		d_{IhB}	2.5	Day
k_{FSH}	2.00	day^{-1}		a_{FSH}	8.21	day^{-1}
$c_{FSH,P}$	38.0	mL/ng		v	2.5	L

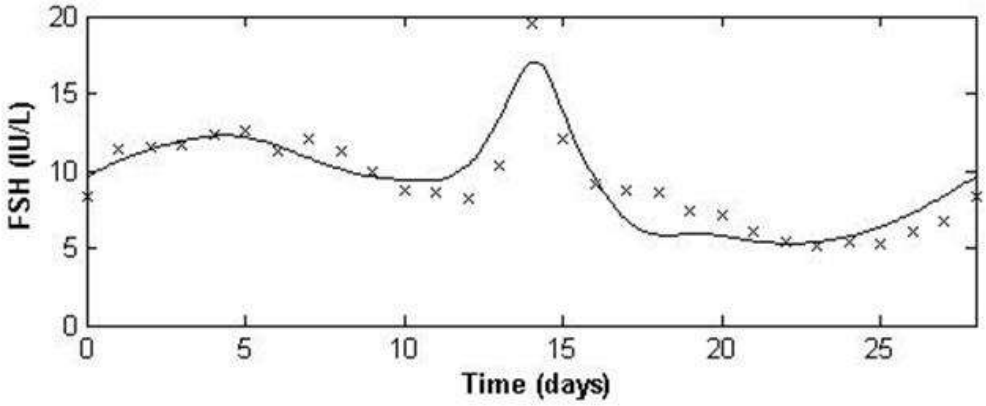

Figure 5.3 – FSH system plot for linear E_2 inhibition

There were no changes to the LH system, so all of those unmerged parameter values remain the same as in Chapter 3. For the twelve-compartment ovarian system, the optimized parameter values are listed in Table 5.3, followed by the auxiliary coefficient values, for (5.6), in Table 5.4.

Table 5.3 – Unmerged ovarian system parameter values

Parameter	Value	Unit		Parameter	Value	Unit
c_1	0.173	$\frac{L}{IU}\cdot\frac{1}{day}$		k_4	1.30	day^{-1}
c_2	0.144	$\left(\frac{L}{IU}\right)^{\alpha}\cdot\frac{1}{day}$		α	0.7736	(none)
c_3	0.0120	$\left(\frac{L}{IU}\right)^{\beta}\cdot\frac{1}{day}$		β	0.157	(none)
c_4	0.0115	$\frac{L}{IU}\cdot\frac{1}{day}$		γ	0.100	(none)
c_5	0.700	$\left(\frac{L}{IU}\right)^{\gamma}\cdot\frac{1}{day}$		δ	0.7736	(none)
c_6	2.00	day^{-1}		b	8	(none)
d_1	0.672	day^{-1}		f_1	11.0	IU/L
d_2	0.568	day^{-1}		f_2	1.50	µg/day
k_1	0.550	day^{-1}		f_3	0.500	$\frac{L}{IU}\cdot\frac{1}{day}$
k_2	1.30	day^{-1}		f_4	0.050	$\left(\frac{L}{IU}\right)^{\delta}\cdot\frac{1}{day}$
k_3	1.30	day^{-1}				

Table 5.4 – Auxiliary equation parameter values for the unmerged model

Parameter	Value	Unit		Parameter	Value	Unit
e_0	55	pg/mL		h_1	$4.7\cdot10^{-4}$	IU/(μg·mL)
e_1	$5.0\cdot10^{-3}$	L^{-1}		h_2	$2.3\cdot10^{-3}$	IU/(μg·mL)
e_2	$8.3\cdot10^{-3}$	L^{-1}		h_3	0	IU/(μg·mL)
e_3	0.019	L^{-1}		h_4	0	IU/(μg·mL)
p_0	0.6	ng/mL		j_0	30	pg/mL
p_1	0	kL^{-1}		j_1	55	L^{-1}
p_2	$4.2\cdot10^{-3}$	kL^{-1}		j_2	0	L^{-1}
h_0	1	IU/mL		j_3	0.013	L^{-1}

There are three parameters (h_3, h_4, and j_2) in Table 5.4 with value zero. If this remained true with the merged model, it would indicate unnecessary auxiliary equation terms, allowing for model simplification. Based on the values from Table 5.4, the plots of the four ovarian hormones, using the unmerged ovarian model, are given in Figures 5.4-5.7. As with the unmerged ovarian system for the five-hormone model discussed in section 3.3, the expanded ovarian system described here is unstable for the parameter values given in Tables 5.3 and 5.4. When tracked over multiple periods, the stage peaks increase with each period, tending toward infinity. As before, the best solution would be to reduce the value of c_1 sufficiently to gain stability, then to adjust other parameters accordingly to attain a good data fit. This issue may be one reason for the substantial changes in some parameter values between the unmerged and merged models.

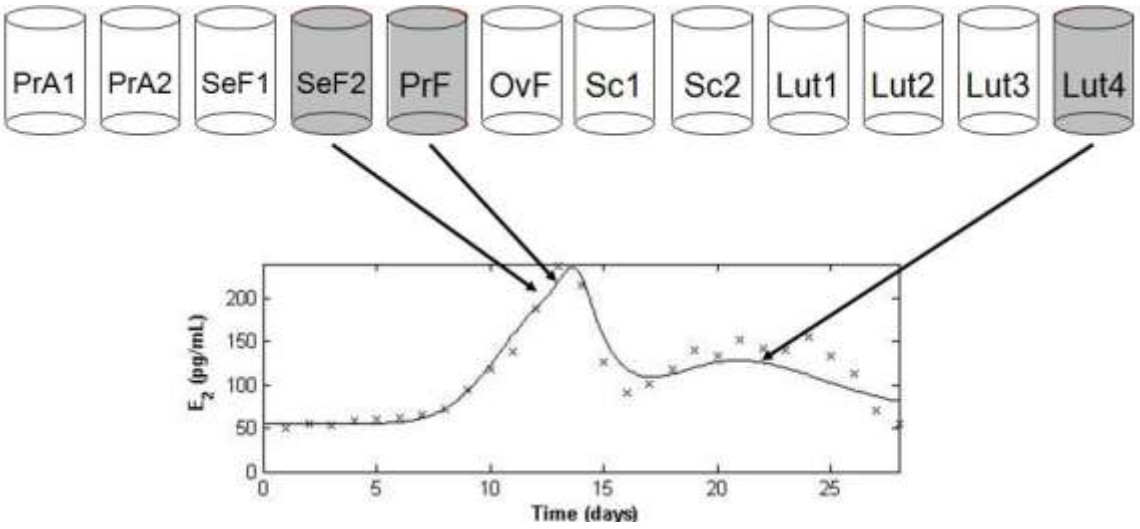

Figure 5.4 – E_2 model and data for the ovarian system

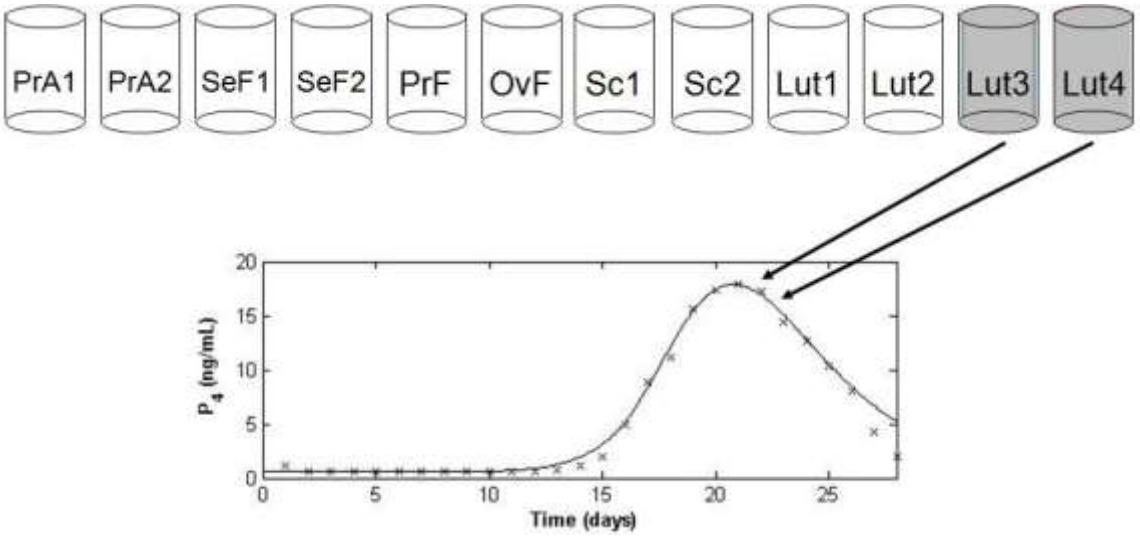

Figure 5.5 – P_4 model and data for the ovarian system

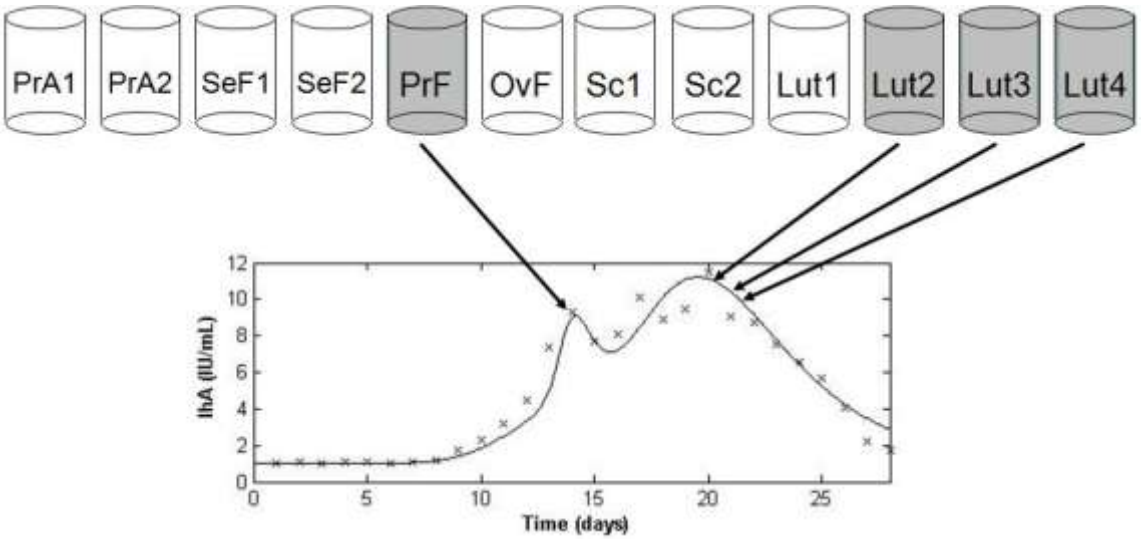

Figure 5.6 – Inhibin A model and data for the ovarian system

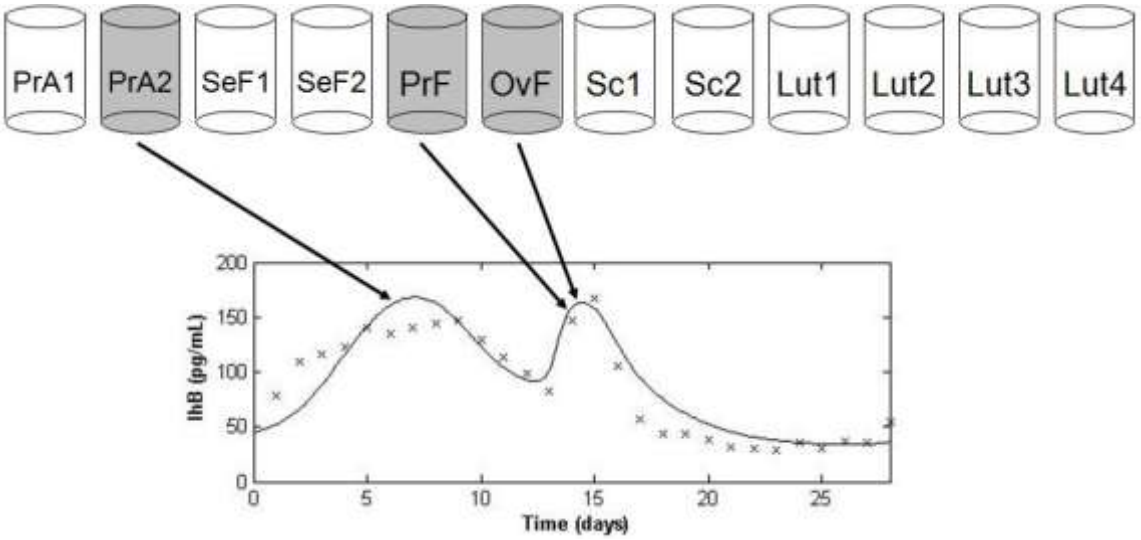

Figure 5.7 – Inhibin B model and data for the ovarian system

In the merged 16-dimensional system (5.7), together with the auxiliary equations (5.6), there are 58 parameters. Only three of these $(a_{FSH},\ r_{LH},\ \text{and}\ v)$ are biologically known constants. Using similar methods to those described in sections 3.3 and 3.4, we fit the model to the data, using the total scaled least-squares error in the six hormone profiles as our outcome measure. Given the high dimension of our parameter space, we make no claim to have globally optimized the parameter set. Table 5.5 gives our best-fit parameter set for the merged model; the units remain as given in Table 3.1 and Tables 5.2-5.4. Some of the auxiliary coefficients $(e_i\text{'s},\ p_i\text{'s},\ h_i\text{'s},\ \text{and}\ j_i\text{'s})$ are very small (on the order of 10^{-3} or 10^{-4}) but still significant, because the last ten of the twelve ovarian stages have peak values on the order of 10^3 or 10^4. The zero value for j_2 indicates that the contribution of PrF to IhB could be removed entirely.

With this parameter set, there is a stable periodic solution with a 27.99-day period, nearly matching the 28-day period assumed of the data. Figure 5.8 shows the model-predicted concentration for each of the six hormones, plotted over 84 days to show the periodic nature over multiple cycles. To reduce the short-term effect of varying initial conditions, the model was run for 150 days, with only an 84-day time toward the end of that duration being plotted. In making the plots, the model was centered to the LH surge of the middle period of the three periods shown.

Table 5.5 – Optimized parameter values for the merged model

Parameter	Value		Parameter	Value		Parameter	Value
α	0.8001		$c_{LH,E}$	c		p_0	0.6215
c_1	0.1900		k_{LH}	2.813		p_1	$2.92\cdot10^{-4}$
c_2	0.1818		v_{FSH}	756		p_2	$2.05\cdot10^{-3}$
c_3	0.0912		$Ki_{FSH,IhA}$	1.973		h_0	0.9
c_4	0.0245		$Ki_{FSH,IhB}$	107.3		h_1	$3.73\cdot10^{-4}$
c_5	0.4998		k_{FSH}	0.6010		h_2	$9.10\cdot10^{-4}$
c_6	0.9837		$c_{FSH,P}$	63.34		h_3	$4.15\cdot10^{-4}$
d_1	0.7145		$c_{FSH,E}$	0.3023		h_4	$2.43\cdot10^{-4}$
d_2	0.7485		d_{IhA}	2.5		j_0	29.78
k_1	0.6672		d_{IhB}	1.0		j_1	48.48
k_2	1.620		b	10		j_2	0
k_3	0.6050		f_1	10.86		j_3	$6.42\cdot10^{-3}$
k_4	1.014		f_2	2.994		δ	0.8825
β	0.2613		f_3	3.199		d_E	0.5086
γ	0.1285		f_4	0.0835		d_P	0.9156
$v_{0,LH}$	575.2		e_0	51.77		a	10
$v_{1,LH}$	3888		e_1	$5.10\cdot10^{-3}$		a_{FSH}	8.21
Km_{LH}	188.0		e_2	$5.54\cdot10^{-3}$		r_{LH}	14.0
$Ki_{LH,P}$	12.36		e_3	0.0155		v	2.50
$c_{LH,P}$	0.0150						

As with fitting the previous five-hormone model, the greatest difficulty is with the FSH profile, particularly in the early luteal phase. Of more importance physiologically is the discrepancy between the model and the FSH data in the late follicular phase. It is our hope that superior optimization techniques may yet produce an improved fit with this model. If this still fails, then changes to the FSH equations would be necessary.

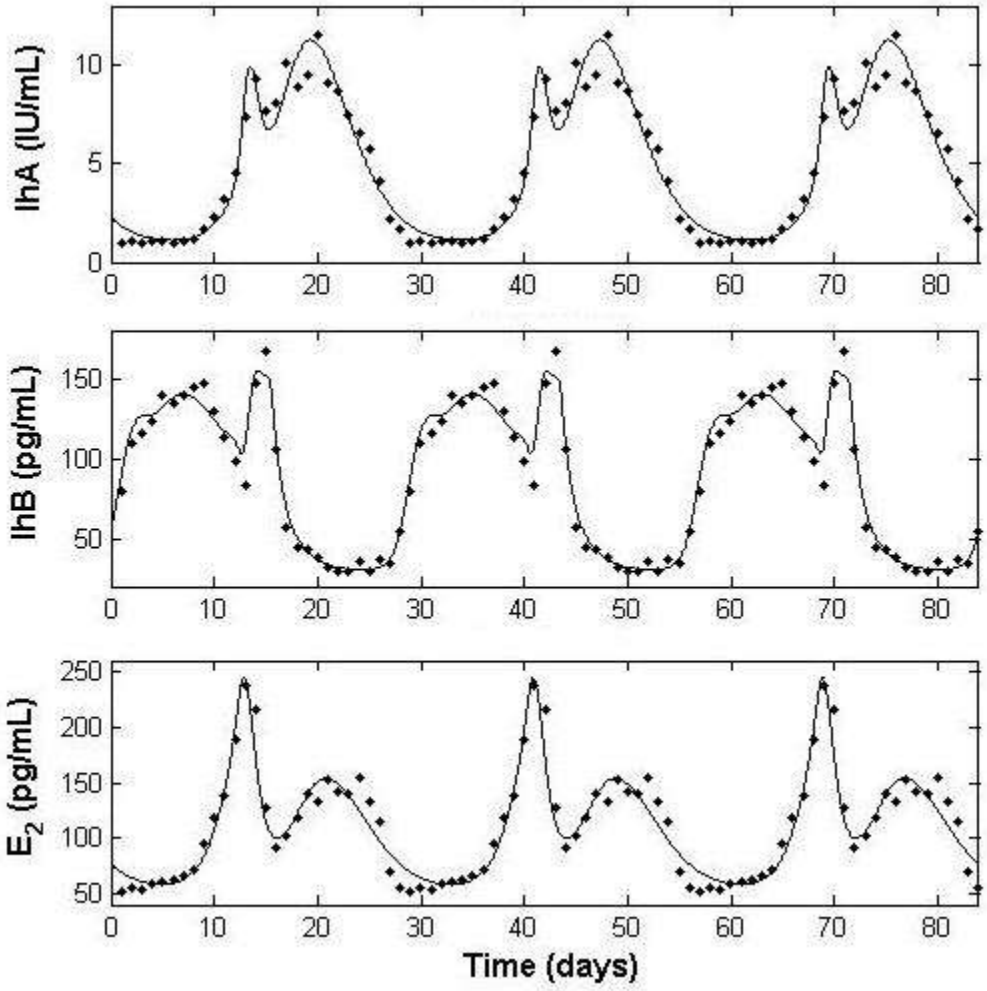

Figure 5.8 – Model-predicted InA, InB, and E_2 plots for the merged system

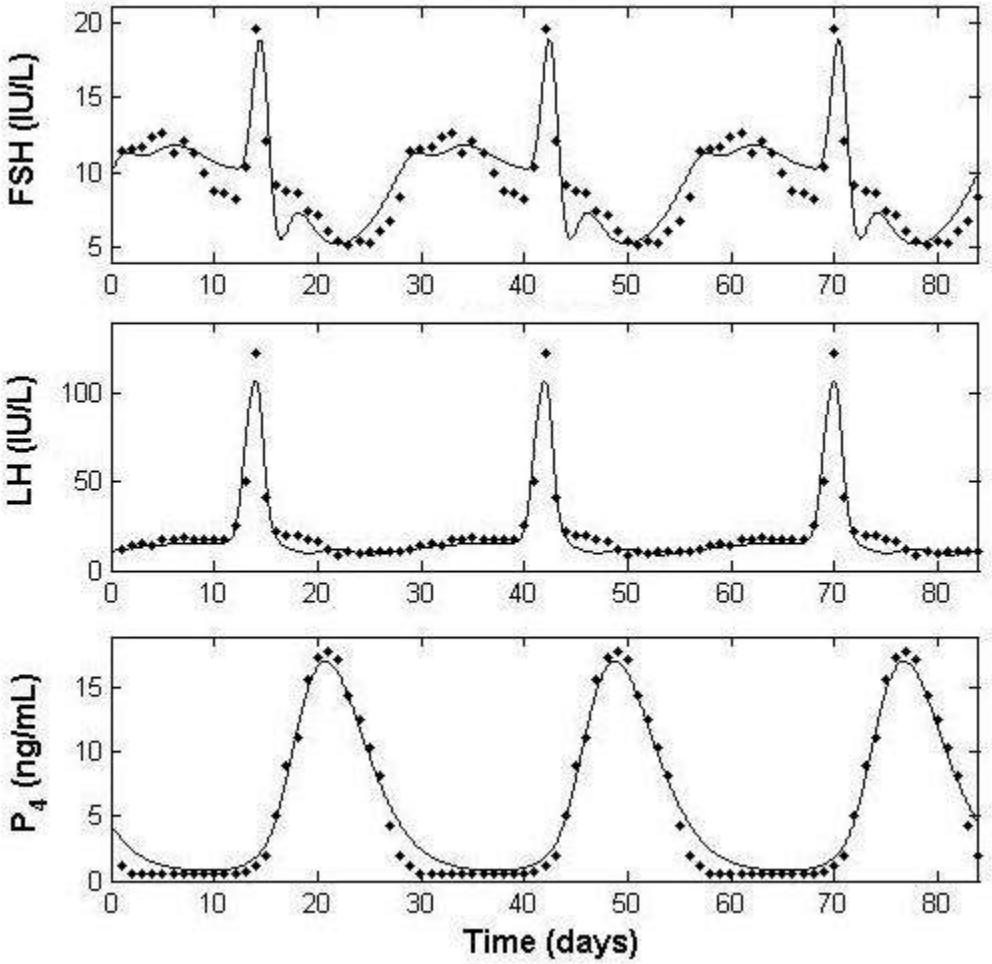

Figure 5.9 – Model-predicted FSH, LH, and P_4 plots for the merged system

Chapter 6

Dynamics of the Six-Hormone Model

6.1 Equilibrium and Periodic Solutions

For the parameter values given in Table 5.5, the system (5.7) has a locally asymptotically stable periodic solution, shown in Figure 5.8. This solution has a 27.99 day period. There is also an unstable equilibrium solution at the point given in Table 6.1. Additionally, under unusual initial conditions, LH, FSH, and the first three ovarian stages can tend toward zero, while the latter nine ovarian stages undergo unchecked exponential growth. Clearly, hormone concentrations that tend toward infinity are not biologically realistic, but neither are the initial conditions required to cause this phenomenon in the model (for example, a reserve pool FSH level seven times higher than the typical maximum predicted by the model).

6.2 Bifurcations

After fitting the five-hormone model in Chapter 4, we discussed the presence of Hopf bifurcations for multiple parameters, as well as saddle-node bifurcations for one parameter. In varying single parameters of the six-hormone model from the values given in Table 5.5, we again find Hopf bifurcations for several parameters, including Km_{LH}, α, c_1, c_2, $v_{0,LH}$, and v_{FSH}. We also find an example of a period-doubling

Table 6.1 – Unstable equilibrium conditions

Parameter	Value		Parameter	Value		Parameter	Value
RP_{LH}	225.99		*SeF1*	761.44		*Sc2*	3249.7
LH	14.800		*SeF2*	6710.8		*Lut1*	3645.8
RP_{FSH}	29.118		*PrF*	3442.7		*Lut2*	1501.4
FSH	8.2626		*OvF*	2472.8		*Lut3*	4020.9
PrA1	0.0069		*Sc1*	3404.4		*Lut4*	2399.7
PrA2	0.2024						

bifurcation, for $c_2 \approx 0.048$; the associated alternate-month cycles are shown in Figure 6.1. For one parameter, we observe a small interval (roughly $0.448 < \alpha < 0.466$) with two stable periodic solutions; this may be due to two saddle-node bifurcations relatively close together. The profiles of these two solutions are shown in Figure 6.2. However, neither the simultaneous stable periodic solutions nor the alternate-month profile have physiological significance, as the ovarian hormone concentrations involved are an order of magnitude higher than those observed in normal women, even while pituitary hormone concentrations remain at reasonable levels. As α increases, approaching 0.913, the amplitude of the stable periodic solution decreases to zero, as shown in Figure 6.4; at values above 0.913, the amplitude is zero, indicating that the periodic solution has been replaced by a stable equilibrium. The α region with two stable periodic solutions corresponds to the overlap seen in Figures 6.4 and 6.5.

In Chapter 4, we found that, for the five-hormone model, there were two saddle-node bifurcations for Km_{LH}. This led to a small range of Km_{LH} values at which there were two stable periodic solutions. Figure 6.6 is the bifurcation diagram comparable to Figure 4.5; for the six-hormone model, we see that there is no reasonable Km_{LH} value with a saddle-node bifurcation or multiple stable periodic solutions.

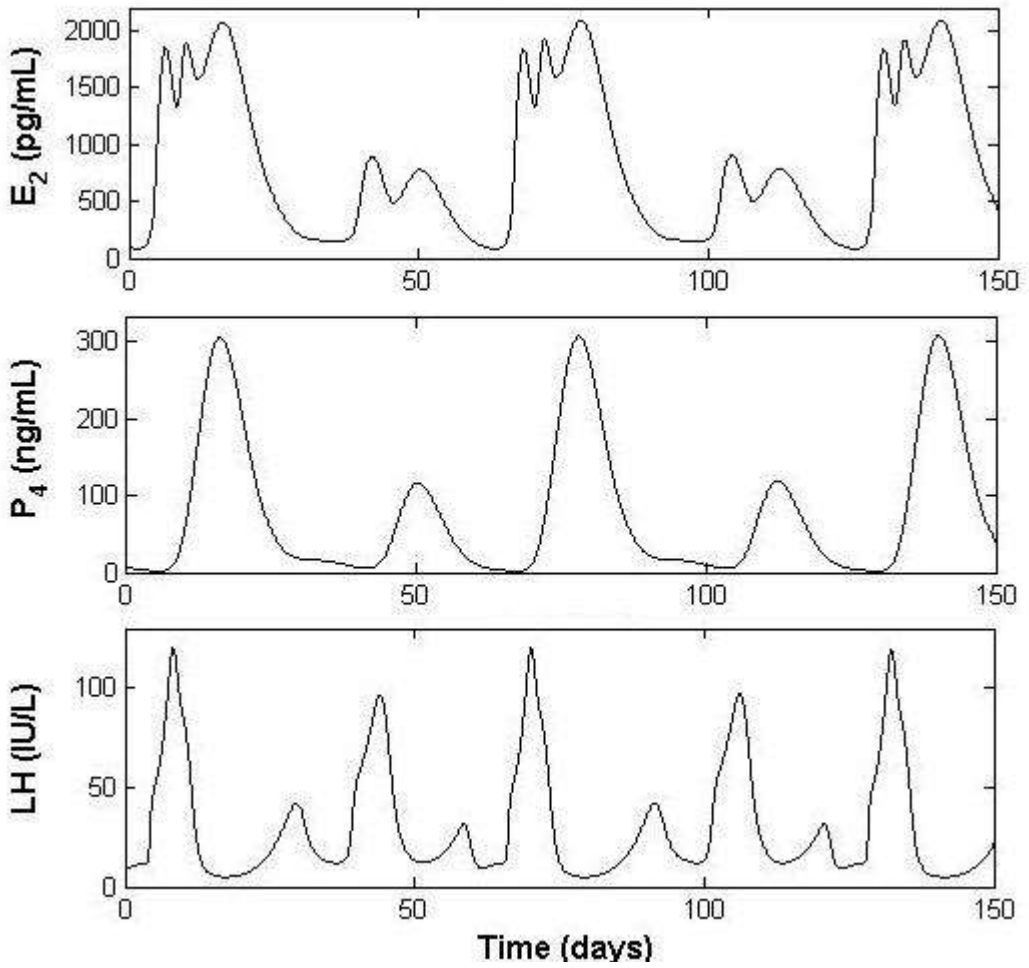

Figure 6.1 – Alternate-month hormone profiles for c_2 = 0.045

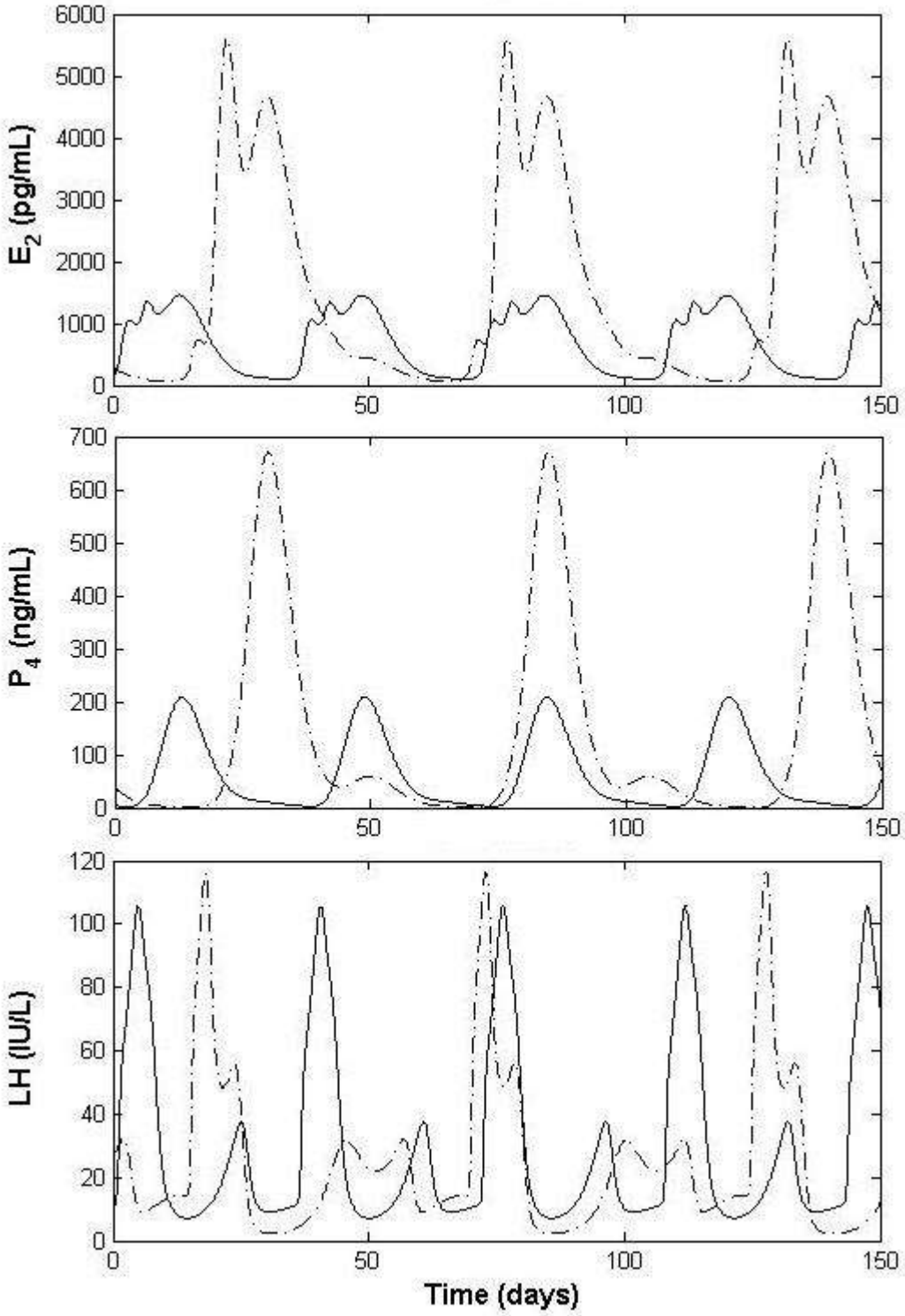

Figure 6.2 – Profiles of the two periodic solutions at α = 0.45

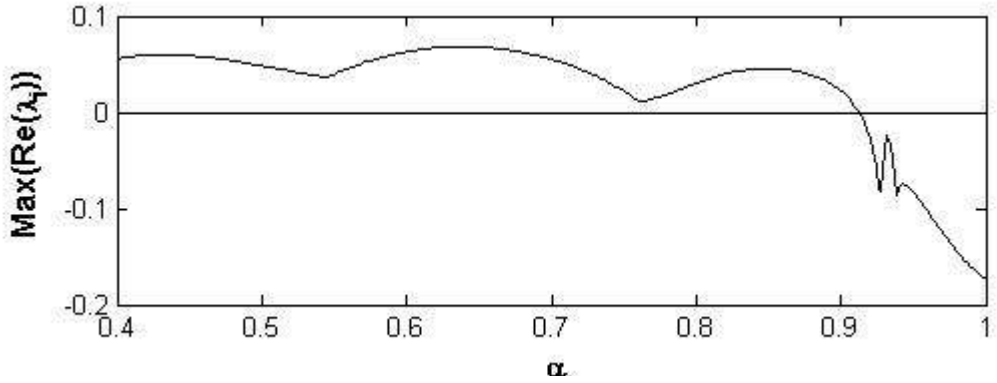

Figure 6.3 – Maximal eigenvalue real part for the equilibrium solution

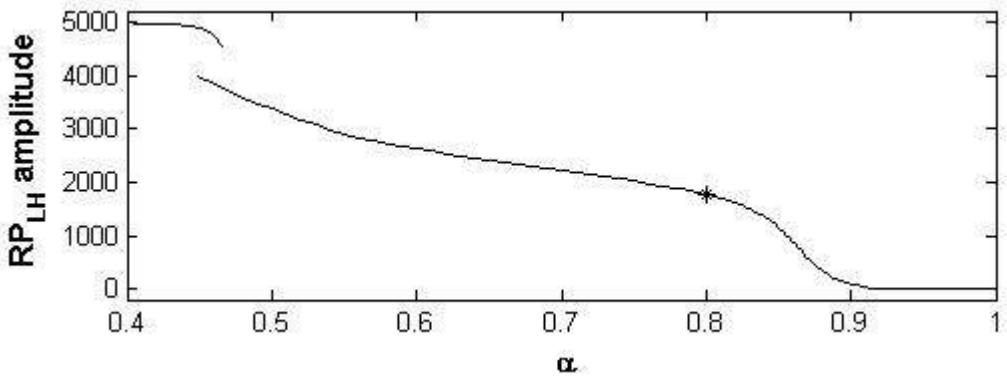

Figure 6.4 – Amplitude of the stable periodic solution versus α

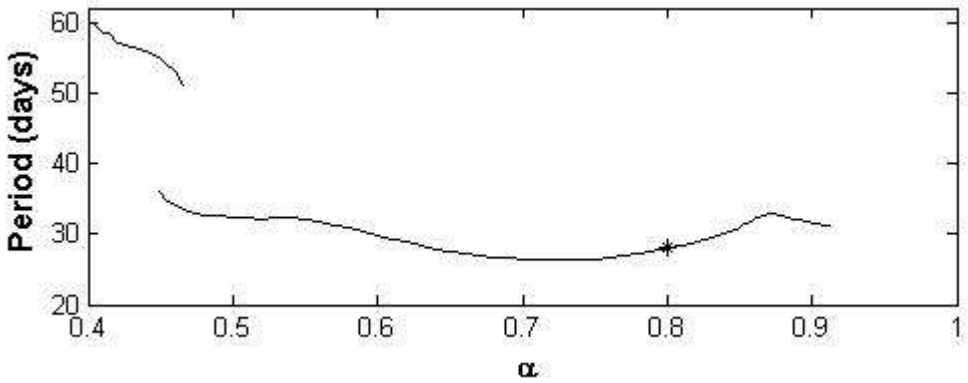

Figure 6.5 – Period (in days) of the stable periodic solution

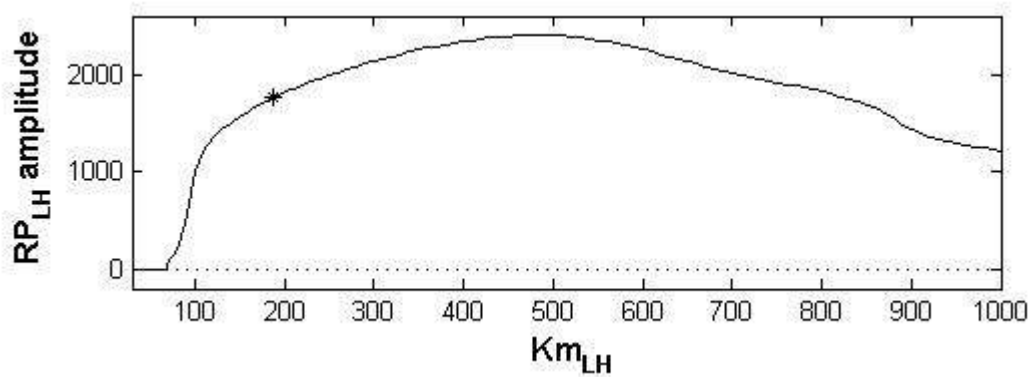

Figure 6.6 – Periodic and equilibrium solutions of Km_{LH}

6.3 Sensitivity Analysis

With the six-hormone model, we conducted a more extensive sensitivity analysis than the one discussed in Chapter 4 for the five-hormone model. By identifying the various peaks and valleys for each hormone across one cycle, we were able to determine sensitivity coefficients for each of these features, for each parameter, with the exception of the biological constants. The computation, as before, is done using (4.1). Appendix B.2 is an extensive table of sensitivity coefficients. On the whole, the most sensitive coefficients appear to be (in descending order) α, c_1, c_2, Km_{LH}, v_{FSH}, $v_{0,LH}$, e_1, and f_1. The parameter α controls the strength of LH's promotion of mass transfer between two consecutive follicular ovarian stages. Similarly, c_1 and c_2 are also involved in early-stage ovarian processes, the former with exponential follicular growth, and the latter with mass transfer between the same pair of stages as with α. Km_{LH} and f_1 are threshold

values for the two Hill functions in the system. Finally, v_{FSH} and $v_{0,LH}$ are the baseline production levels of FSH and LH, respectively.

6.4 External Hormone Effects

In section 4.3, we discussed the effects of external hormones on the menstrual cycle, using the five-hormone model with the Welt data (Welt et al., 1999). In particular, for a parameter set with two stable periodic solutions, we looked at hormone treatment or exposure amounts which could lead to a long-lasting qualitative change in the menstrual cycle. For the six-hormone model, we found no bifurcations that lead to multiple physiologically relevant stable periodic solutions, so we cannot repeat that kind of analysis. However, we will discuss the effects of sustained external hormones (as with oral contraception or post-menopausal hormone replacement therapy) on the menstrual cycle.

We begin by considering various doses of E_2, administered continuously throughout the cycle. Figure 6.7 shows the effects, over 100 days, of a low dose of E_2, which raises the circulating E_2 level by 25 pg/mL. In each plot, the solid line indicates the predicted hormone concentrations with the external hormones being administered, while the broken line is the control, with no external hormones. The five-hormone model found this dose to be insufficient to resolve an abnormal menstrual cycle. Figure 6.7 shows that the 25 pg/mL dose of E_2 causes only a minimal decrease in the amplitude

of the LH surge, so this dose is likely insufficient for contraception. It is noteworthy that we observe a reduction in the cycle length, from 28 days to roughly 26.5 days, even at this low dose of estradiol.

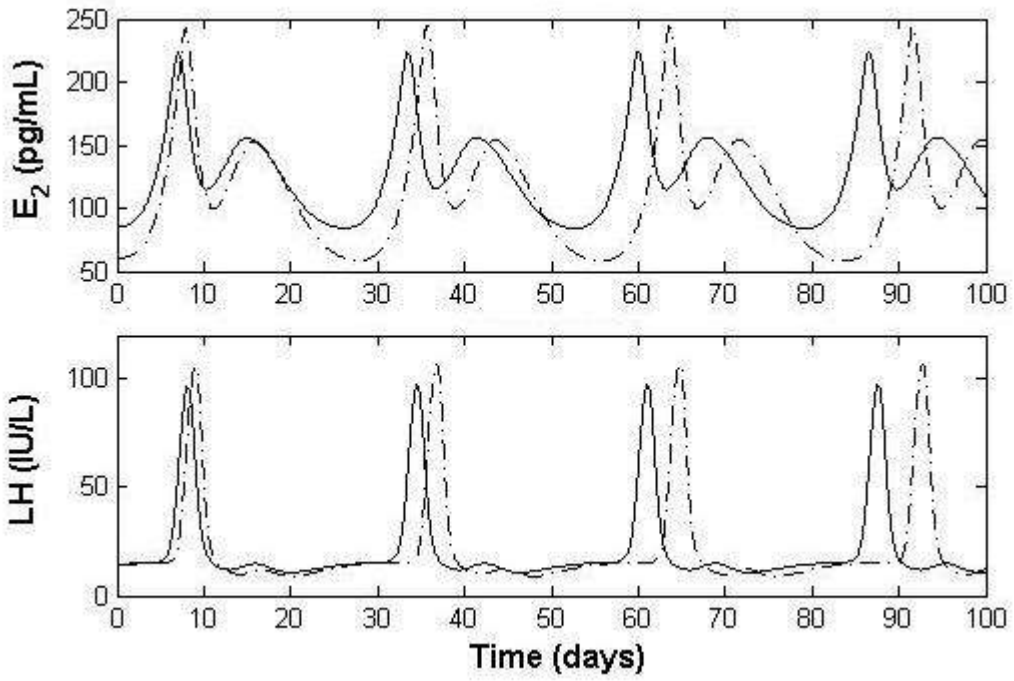

Figure 6.7 – Hormone levels with and without a 25 pg/mL dose of E_2

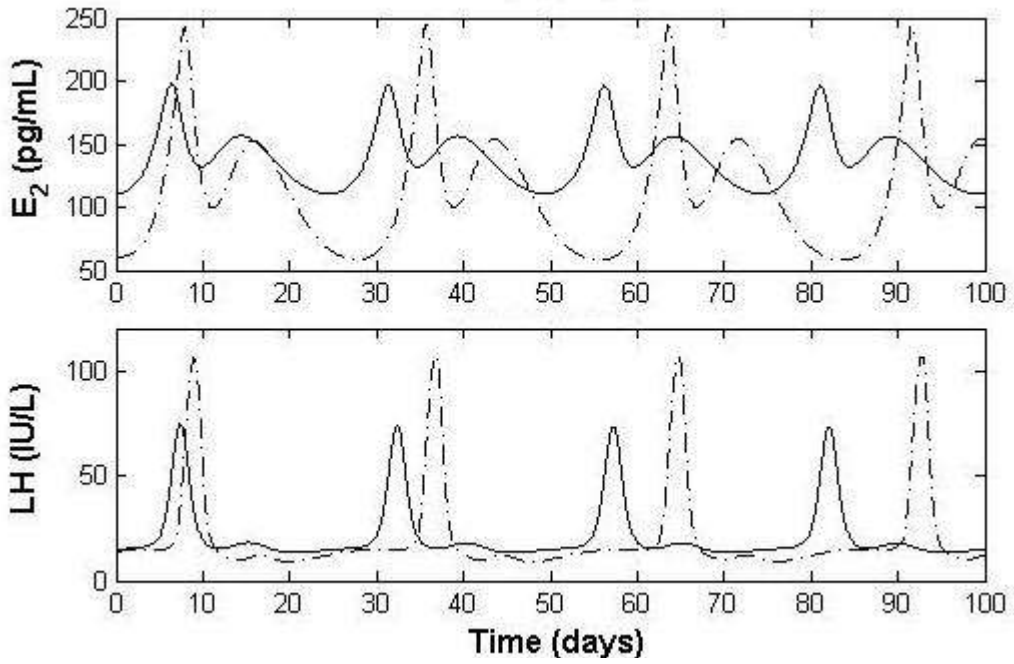

Figure 6.8 – Hormone levels with and without a 50 pg/mL dose of E_2

When the external E_2 dose is doubled to 50 pg/mL, as shown in Figure 6.8, the decrease in the LH peak amplitude becomes substantial, 27% lower than the control case. This decrease might be sufficient to suppress ovulation, but that is unclear. Also, the cycle length is further shortened, to less than 25 days.

A higher E_2 dose of 75 pg/mL results in a 58% decrease in the LH peak, making ovulation highly unlikely; the associated E_2 and LH levels are shown in Figure 6.9. As the E_2 dose is increased to even higher levels, the amplitudes of hormone concentration fluctuations decrease to zero, causing a pharmaceutically-induced equilibrium, shown in Figure 6.10.

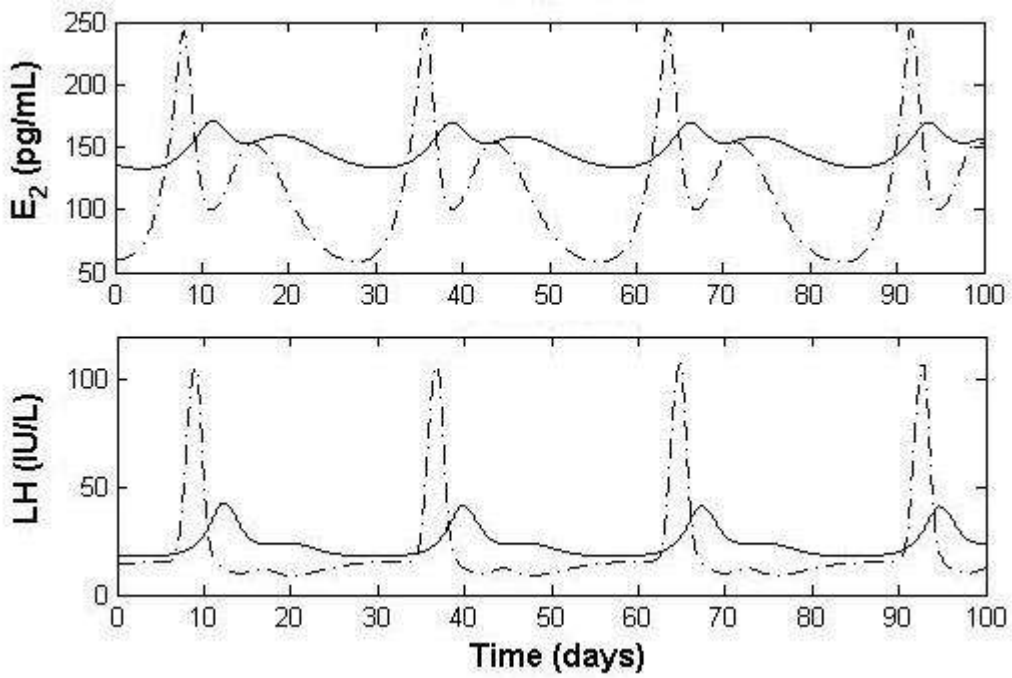

Figure 6.9 – Hormone levels with and without a 75 pg/mL dose of E_2

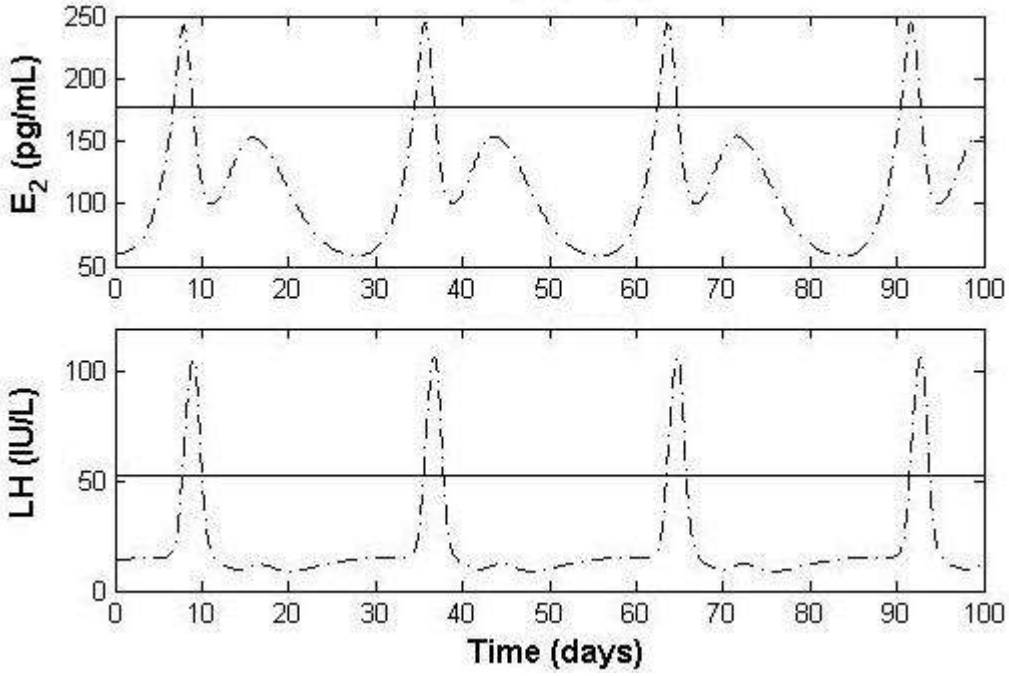

Figure 6.10 – Hormone levels with and without a 125 pg/mL dose of E_2

We also explore the use of exogenous progesterone. Many oral contraceptives include progestin, a synthetic compound that acts similarly to P_4. With a 2 ng/mL effective dose of P_4 administered continuously, the model shows a substantial increase in peak levels of all four ovarian hormones. This likely occurs because the higher progesterone levels reduce the storage of FSH, leading to higher FSH concentrations through most of the cycle, but a smaller mid-cycle FSH surge. The higher bloodstream levels of FSH lead to increased ovarian activity. The corresponding effect on LH is much smaller, because of the crucial role of estradiol in LH regulation.

Figure 6.11 shows the resulting concentrations of E_2, P_4, and LH. In each of these three plots, the solid line indicates the hormone profile with the external P_4, while the broken line models a control subject. It is noteworthy that there is no significant reduction in the amplitude of the LH surge associated with this treatment.

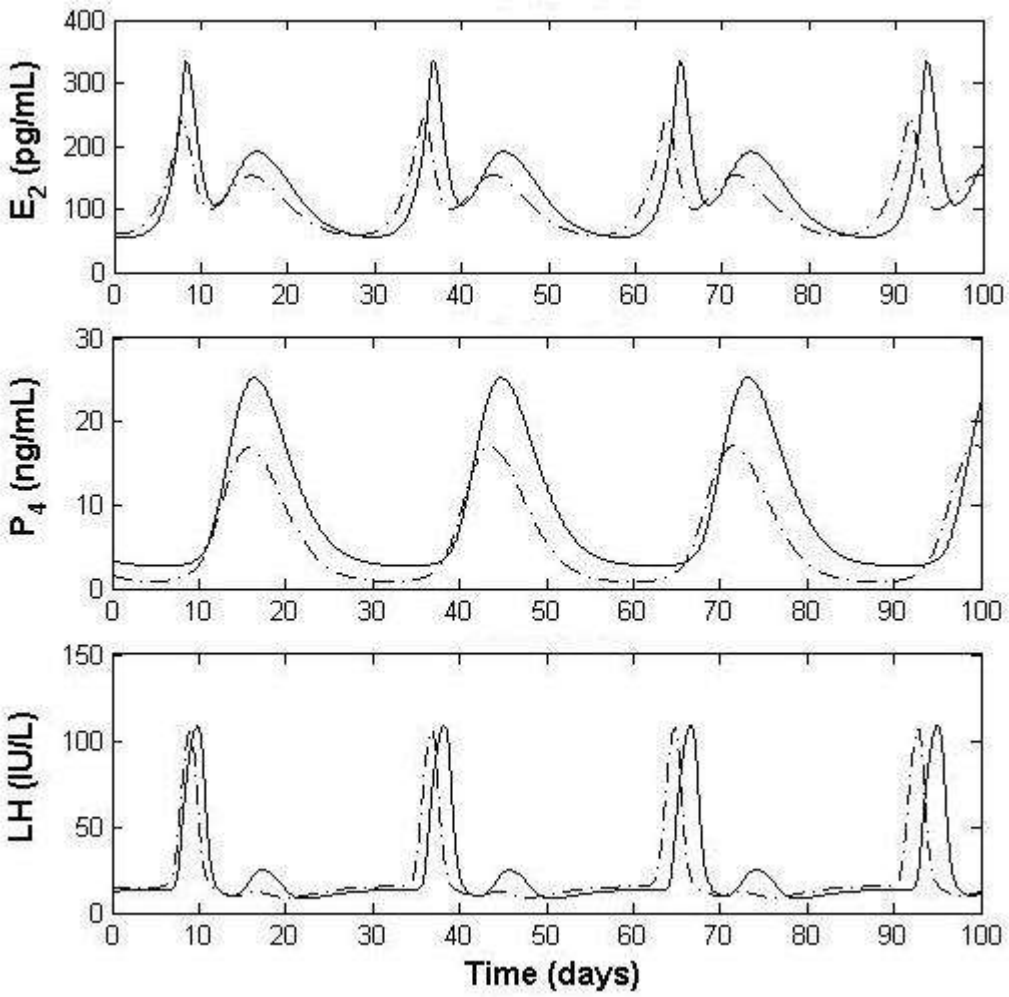

Figure 6.11 – Hormone levels with and without a 2 ng/mL dose of P_4

With an increased dosage of P_4, the model shows the same results: markedly higher levels of all four ovarian hormones and a substantial drop in mid-cycle peak FSH levels, but only a small decrease in the mid-cycle LH peak. Additionally, the luteal phase secondary peak of LH seen in Figure 6.11 becomes more prominent with a higher dosage; it is likely associated with the increased luteal phase peak in E_2.

Standard oral contraceptive therapies can consist of estrogen only, progestin only (the “minipill”), or a combination of estrogen and progestin (Speroff et al., 1999). While any of these can prevent conception, through multiple physiological mechanisms, a low-amplitude peak of LH at mid-cycle is the endocrinological marker of anovulation. The clinical benefit of prescribing a pill containing both estrogen and progestin together is that a reduced dose of each can be used. Our model seems to perform appropriately regarding external E_2, but not for P_4, indicating a need for future model refinement.

Chapter 7

The Aging Process: Progression Toward Menopause

7.1 Hormonal Changes in Advance of Menopause

As discussed in section 2.3, there are measurable age-related changes in hormone levels well before menopause. While menopause occurs on average at around age 50, these changes begin around the mid-thirties; they are largely caused by a decreasing number of ovarian follicles (Welt et al., 1999). There is a notable early-follicular-phase increase in FSH among women over 35, caused primarily by a simultaneous decrease in inhibin B produced by the ovaries. It is also possible that late-luteal decreases in inhibin A may contribute to this effect (Muttukrishna et al., 2000). Closer to menopause, there is an increase in the mid-cycle peak value of LH.

The data set that we are using (Welt et al., 1999) included 44 normally-cycling women, 23 under age 35, and 21 between the ages of 35 and 46. The older women have a decreased level of inhibin B throughout the cycle, as compared to the younger women. They also have noticeably lower inhibin A levels throughout the luteal phase, but this did not rise to the level of statistical significance, because of a high variance among the older women; however, longitudinal studies following individual women show a clear decrease in inhibin A over time. The Welt data sets show a significant increase in estradiol during

the late follicular phase; however, the authors note that other studies have mixed results regarding whether estradiol levels increase, decrease, or remain relatively constant as women approach menopause.

7.2 Parallel Parameter Sets

To fit the data for older women, we wish to change a small number of parameters from the values given in Table 5.5, which related to younger women. As a group, these changes are intended to represent the effects of aging. The parameters to differ include e_1 and e_2 (auxiliary coefficients for the late-follicular rise in E_2), h_0, h_1, h_2, h_3, and h_4 (auxiliary coefficients for inhibin A), j_0, j_1, j_2, and j_3 (auxiliary coefficients for inhibin B), and α (an early-stage ovarian system parameter, indirectly related to the late-follicular rise in E_2.) The 12 parameters which were allowed to vary are shown in Table 7.1, while the other 46 parameters are unchanged from the values given in Table 5.5. Figures 7.1 and 7.2 show the resulting hormone profiles.

Table 7.1 – Free parameters in the parallel parameter sets

Parameter	Younger	Older		Parameter	Younger	Older
α	0.8001	0.8467		j_0	29.78	18.32
h_0	0.90	0.90		j_1	48.48	34.30
h_1	$3.73\cdot10^{-4}$	$2.86\cdot10^{-4}$		j_2	0	0
h_2	$9.10\cdot10^{-4}$	$4.16\cdot10^{-4}$		j_3	$6.42\cdot10^{-3}$	$3.41\cdot10^{-3}$
h_3	$4.15\cdot10^{-4}$	$3.80\cdot10^{-4}$		e_1	$5.10\cdot10^{-3}$	$3.81\cdot10^{-3}$
h_4	$2.43\cdot10^{-4}$	$2.35\cdot10^{-4}$		e_2	$5.54\cdot10^{-3}$	$6.85\cdot10^{-3}$

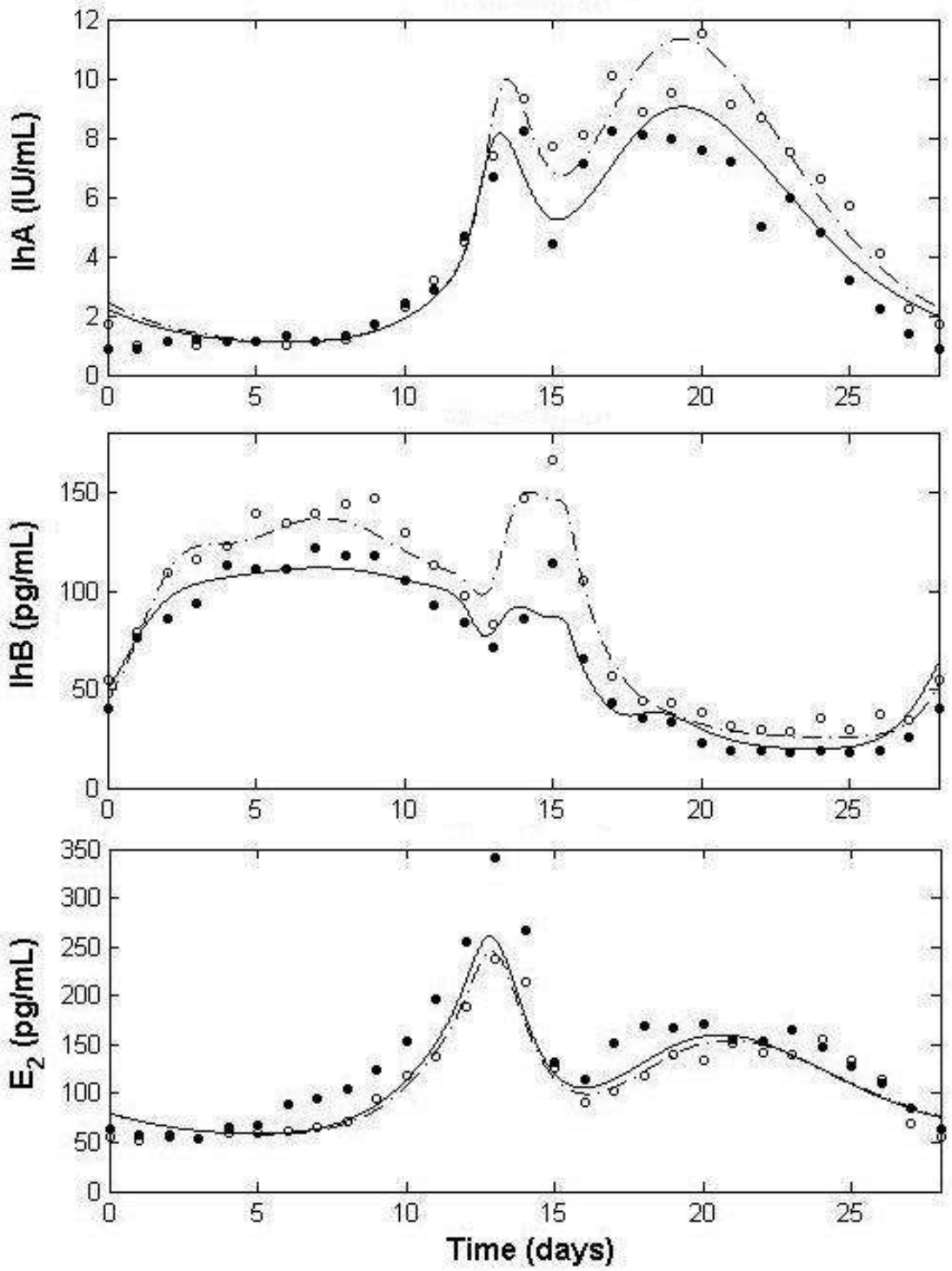

Figure 7.1 – IhA, IhB, E_2 plots for younger (o,…) and older (•,–) women

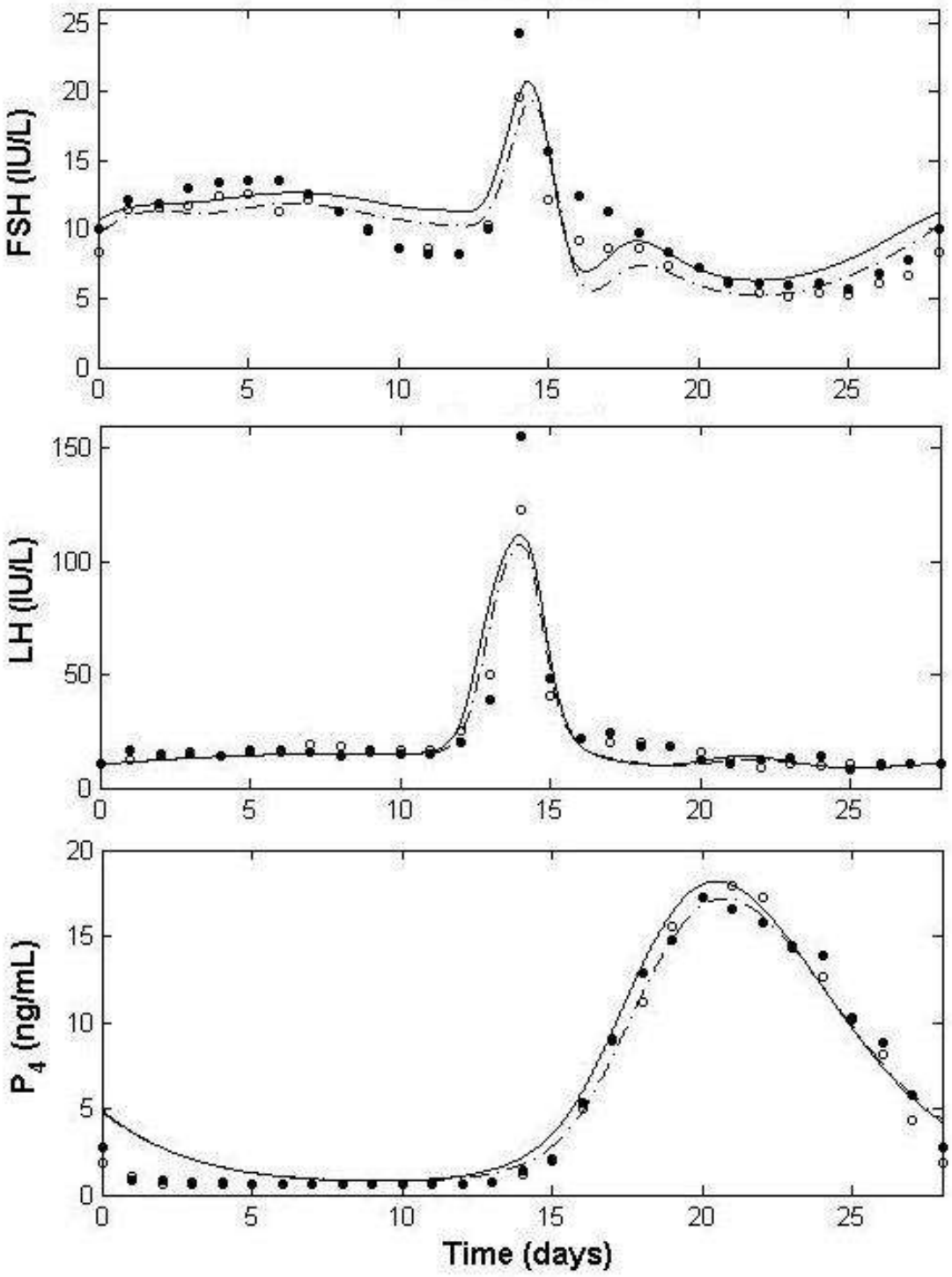

Figure 7.2 – FSH, LH, P_4 plots for younger (o,…) and older (•,–) women

In Figures 7.1 and 7.2, the open circles represent the data points for the younger women and the filled circles represent the data points for the older women. The broken lines represent the model output for the younger women, and the solid lines represent the model output for the older women. As direct effects of changing the auxiliary coefficients for both inhibins, the older women have much lower peak levels of inhibin, which keeps with the data. As a result, the older women have slightly higher levels of FSH in the early follicular phase, but not as much higher as in the data; this is a concern that should be addressed in future versions of this model. Also, the LH surge is only marginally higher for the older women, whereas the change in peak height should be more substantial. Of less concern is failing to keep pace with the earlier rise in E_2, as other published studies show mixed results regarding the relative estradiol levels of peri-menopausal women.

Chapter 8

Summary and Future Work

Because of the availability of daily normal hormone concentrations in women for two forms of inhibin, we have expanded a compartment model from five hormones to six. We have fit both the five-hormone and six-hormone models to the multiple-inhibin data (Welt et al., 1999). For each model, we discussed the existence and stability of equilibrium and periodic solutions, analyzed bifurcations, and determined sensitive parameters. Following this, we modeled the effects of exogenous hormones, because they can have significant effects on the menstrual cycle. This has significance related to oral contraception, treatment of abnormal menstrual cycles, and post-menopausal hormone replacement therapy. Finally, we discussed the effects of age-related changes in reproductive hormone production that occur in the years leading up to menopause.

Expanding this model from five hormones to six, including both inhibins, is an important step. However, the fit obtained is not ideal, particularly for FSH during the early luteal phase. Implementation of improved global optimization routines, such as a pattern search algorithm, may lead to identification of a parameter set that better fits the model to the data.

At that time, attempts should be made to reduce the values of the Hill function exponents a and b. In previous versions of this model, a took the value 8, indicating a steep increase in the production of LH when the circulating E_2 level surpasses a critical threshold concentration. A Hill function exponent of 8 is high, but justifiable in this case; however, the current parameter set in the six-hormone model has this exponent at 10, which may be too large. Additionally, the parameter set also has a value of 10 for b, which is more difficult to justify; while there may be a critical level of FSH needed for significant early-follicular synthesis of inhibin B, the steepness of the effect is probably not sufficient to warrant the large exponent.

Along with the re-fitting, it is now clear that there are aspects of the model itself which should be changed to improve the biological realism. Both the current and previous models include a Hill function in the LH synthesis term, to model the regulatory effects of estradiol on LH. As discussed in section 2.2, E_2 inhibits LH at low levels, and promotes it at higher levels. It is possible that this estradiol effect may occur at the level of LH release, rather than LH synthesis, as shown in the current model.

In section 6.4, we found that the six-hormone model responds appropriately to external doses of estrogen, but not to external progesterone. Accurately fitting progesterone along with the rest of the model also was problematic when dealing with the data set for older women; this suggests the model may require progesterone-related

adjustments. Given that the late-luteal stage linear combinations make sense, the FSH and LH release terms, and their coefficients, should be examined.

In Chapter 7, we have only begun to scratch the surface of age-related changes. There are other data sets in the physiological literature that separately give day-by-day hormone values for women from multiple age groups. Eventually, the processes surrounding puberty and menopause could be considered in detail, leading to a single model that incorporates the full reproductive life cycle, from pre-adolescent girls to post-menopausal women. Such a model would likely replace some of the currently constant parameters with time-dependent functions.

Finally, a deterministic model is of limited value, because of the substantive differences among healthy women of the same age. Peak and baseline hormone levels, as well as menstrual cycle period lengths, have significant variations within published data sets. Even if we could create a "perfect" model which replicates the average hormone profile very well, is true to the known biology in the way it is structured, and responds appropriately to a variety of external hormone challenges, such a model would still be missing both variation among individuals and "random" fluctuation over time. For this reason, a stochastic model would be superior by allowing for study of individual differences, for example, the likelihood of a particular treatment regimen resolving an abnormal menstrual cycle (as in section 4.3). However, development of a stochastic model requires access to longitudinal data sets for individual women (rather than the

aggregated data that is readily available) as well as the expertise of a statistical collaborator. Nonetheless, this seems to be a logical eventual direction for this line of research.

List of References

http://www.vivo.colostate.edu/hbooks/pathphys/endocrine/basics/steroidogenesis.html. Steroid biosynthesis chart, R. A. Bowen, Colorado State University.

D. T. Baird, The Ovary, Ch. 5 in Hormonal Control of Reproduction, C.R. Austin, R.V. Short, eds., Cambridge, London, 1984, pp. 91-114.

A. C. Bauer-Dantoin, J. Weiss, and J. L. Jameson, Roles of estrogen, progesterone, and gonadotropin-releasing hormone (GnRH) in the control of pituitary GnRH receptor gene expression at the time of the preovulatory gonadotropin surges, Endocrinology, 136 (1995), pp. 1014-1019.

V. Beral, E. Banks, G. Reeves, D. Bull, Breast cancer and hormone-replacement therapy in the Million Women Study, Lancet, 362 (2003), pp.419-427.

L. H. Clark, P. M. Schlosser, J.F. Selgrade, Multiple stable periodic solutions in a model for hormonal control of the menstrual cycle, Bull Mathematical Biol, 65 (2003), pp. 157-173.

D. L. Davis, H. L. Bradlow, M .Wolff, T. Woodruff, D. G. Hoel, and H. Anton-Culver, Medical hypothesis: xenoestrogens as preventable causes of breast cancer, Environ Health Perspect 101 (1993), pp. 372-377.

J. H. Dorrington and D. T. Armstrong, Follicle-stimulating hormone stimulates estradiol-17-β synthesis in cultured Sertoli cells, Proc Nat Acad Sci USA, 72 (1975), pp.2677-2681.

K. Engelborghs, T. Luzyanina, and D. Roose, Numerical bifurcation analysis of delay differential equations using DDE-BIFTOOL, ACM Trans. Math. Softw, 28 (2002), pp. 1-21.

K. Engelborghs, T. Luzyanina, G. Samaey, DDE-BIFTOOL v. 2.00: a Matlab package for bifurcation analysis of delay differential equations, Technical Report TW-330, Department of Computer Science, K.U.Leuven, Leuven, Belgium, 2001.

N. P. Groome, P. J. Illingworth, M. O'Brien, R. Pai, F. E. Rodger, J. P. Mather, and A. S. McNeilly, Measurement of dimeric inhibin B throughout the human menstrual cycle, J Clin Endocrinol Metab, 81 (1996), pp. 1401-1405.

M. E. Hadley, Endocrinology, Simon & Schuster Co., Englewood Cliffs, 3rd rd., 1992.

L. A. Harris, Differential equation Models for the hormonal regulation of the menstrual cycle, PhD thesis, North Carolina State University, Raleigh, NC, 2001, web site http://www.lib.ncsu.edu/theses/available/etd-04222002-153727/unrestricted/etd.pdf

S. M. McKinlay, D. J. Brambilla, J. G. Posner, The normal menopause transition, American Journal of Human Biology, 4 (1992), pp. 37-46.

R. I. McLachlan, N. L. Cohen, K. D. Dahl, W. J. Bremner, and M. R. Soules, Serum inhbin levels during the periovulatory interval in normal women: relationships with sex steroid and gonadotropin levels, Clinical Endocrinology, 32 (1990), pp. 39-48.

S. Muttukrishna, T. Child, G. M. Lockwood, N. P. Groome, D. H. Barlow, and W. L. Ledger, Serum concentrations of dimeric inhibins, activin A, gonadotropins, and ovarian steroids during the menstrual cycle in older women, Human Reproduction, 15 (2000), pp. 549-556.

K. Oktay, H. Newton, J. Mullan, and R. G. Gosden, Development of human primordial follicles to antral stages in SCID/hpg mice stimulated with follicle stimulating hormone, Human Reproduction, 13 (1998), pp. 1133-1138.

T. D. Pache, J. W. Wladimiroff, F. H. de Jong, W. C. Hop, and B. C. J. M. Fauser, Growth patterns of nondominant ovarian follicles during the normal menstrual cycle, Fertil Steril, 54 (1990), 638-642.

C. J. Pauerstein, C. A. Eddy, H. D. Croxatto, R. Hess, T. M. Siler-Khodr, and H. B. Croxatto, Temporal relationships of estrogen, progesterone, and luteinizing hormone levels to ovulation in women and infrahuman primates, Am J Obstet Gynecol, 130 (1978), pp. 876-886.

L. Plouffe and S. N. Luxenburg, Biological modeling on a microcomputer using standard spreadsheet and equation solver programs: The hypothalamic-pituitary-ovarian axis as an example, Computers and Biomedical Research, 25 (1992), pp. 117-130.

G. Rannevik, S. Jeppsson, O. Johnell, B. Bjerre, Y. Laurell-Borulf, and A. Svanberg, A longitudinal study of the perimenopausal transition: altered profiles of steroid and pituitary hormones, SHBG, and bone mineral density, Maturitas, 21 (1995), pp. 103-113.

I. Reinecke and P. Deuflhard, A complex mathematical model of the human menstrual cycle, Journal of Theoretical Biology, 247 (2007), pp. 303-330.

R. A. Rudel, S. J. Melly, P. W. Geno, G. Sun, and J. G. Brody, Identification of alkylphenols and other estrogenic phenolic compounds in wastewater, septage, and groundwater on Cape Cod, Massachusetts, Environ Sci Technol 32 (1998), pp. 861-869.

P. M. Schlosser and J. F. Selgrade, A model of gonadotropin regulation during the menstrual cycle in women: qualitative features, Environ Health Perspect, 108 (2000), pp. 873-881.

J. F. Selgrade, Modeling Hormonal Control of the Menstrual Cycle, Comments Theor Biol, 6 (2001), pp. 79-101.

J. F. Selgrade and P. M. Schlosser, A model for the production of ovarian hormones during the menstrual cycle, Fields Institute Communications, 21 (1999), pp. 429-446.

L. Speroff, R. H. Glass, and N. G. Kase, Clinical Gynecologic Endocrinology and Infertility, Lippincott Williams & Wilkins, 6th ed., 1999.

A. E. Treloar, R. E. Boynton, G. B. Borghild, B. W. Brown, Variation of the human menstrual cycle through reproductive life, Int J Fertil, 12 (1967), pp. 77-126.

R. F. Vollman, The Menstrual Cycle, in Major Problems in Obstetrics and Gynecology, E. Friedman, ed., W. B. Saunders Co., Philadelphia, 1977.

C. K. Welt, K. A. Martin, A. E. Taylor, G. M. Lambert-Messerlian, W. F. Crowley, Jr., J. A. Smith, D. A. Schoenfield, and J. E. Hall, Frequency modulation of follicle-stimulating hormone (FSH) during the luteal-follicular transition: Evidence for FSH control of inhibin B in normal women. J Clin Endocrinol Metab 82 (1997), pp. 2645-2652.

C. K. Welt, D. J. McNicholl, A. E. Taylor, and J. E. Hall, Female reproductive aging Is marked by decreased secretion of dimeric inhibin, J Clin Endocrinol Metab, 84 (1999), pp. 105-111.

S. S. C. Yen, The Human Menstrual Cycle: Neuroendocrine Regulation, Ch. 7 in Reproductive Endocrinology: Physiology, Pathophysiology, and Clinical Management, S. S. C. Yen, R. B. Jaffe, and R. L. Barbieri, eds., W. B. Saunders Co., 4th ed., 1999.

J. R. Young and R. B. Jaffe, Strength-duration characteristics of estrogen effects on gonadotropin response to gonadotropin-releasing hormone in women, J Clin Endocrinol Metab, 42 (1976), pp. 432-442.

A. J. Zeleznik and C. R. Pohl, Control of Follicular Development, Corpus Luteum Function, the Maternal Recognition of Pregnancy, and the Neuroendocrine Regulation of the Menstrual Cycle in Higher Primates, Ch. 45 in Knobil and Neill's Physiology of Reproduction, J. D. Neill, ed, Elsevier, 3rd ed., 2006, pp. 2449-2510.

Appendices

Appendix A

Tables of Data

A.1 McLachlan Data

This table is copied from Harris (2001), who estimated numerical data based on graphs in McLachlan, et al. (1990) using the software program *DataThief*.

Table A.1 – McLachlan data for normal hormone levels

Day	E_2	P_4	Ih	LH	FSH
	ng/L	nmol/L	U/L	µg/L	µg/L
0	56.387	1.2	297.9	25.34	142.5
1	49.168	0.4	284.1	28.74	158.3
2	51.3653	1.2	313.8	29.36	175.1
3	53.5627	1.113	308.7	33.71	168
4	55.76	1.2	299.3	34.29	179.1
5	61.494	0.8	298.7	36.78	180.6
6	67.228	0.933	302.2	37.35	177.3
7	72.962	0.8	301.5	38.88	177
8	78.696	0.533	339.8	38.52	166.1
9	92.67	0.533	352	35.28	153.4
10	104.3	0.667	329.7	38.71	144.4
11	143.04	0.533	346.3	34.54	134.5
12	181.75	0.667	388.8	37.02	118.9
13	231.05	0.933	461.7	56.62	116.6
14	296.92	1.33	625.4	142.9	155.3
15	248.43	2.933	745.8	369.2	325.4

Table A.1 (continued)

Day	E_2	P_4	Ih	LH	FSH
	ng/L	nmol/L	U/L	µg/L	µg/L
16	123.4	6	636.9	124	210.7
17	93.76	12.667	584.2	44.63	138.9
18	114.82	25.067	778.3	41.39	127.1
19	133.5	37.067	993.9	34.32	118.2
20	149.85	42.667	1279	29.18	107.3
21	155.57	51.867	1486	21.18	101.2
22	174.28	53.2	1632	17.95	86.53
23	178.83	49.867	1597	16.64	81.36
24	162.19	40	1440	13.38	75.29
25	149.06	33.3333	1154	12.02	76.79
26	130.04	22.667	919.5	13.54	82.1
27	112.23	14.667	711.1	16.02	91.23
28	92.044	11.733	675.8	16.56	100.4
29	75.373	7.33	532.2	24.72	121.9
30	66.983	4.667	423.4	28.2	133.9

A.2 Groome Data

These values were estimated from plots in Groome, et al. (1996) using *DigitizeIt*.

Table A.2 – Groome data for normal hormone levels

	pmol/L	nmol/L	pg/mL	U/L	U/L	pg/mL
1	363	10.5	1.4	3.01	2.67	8.05
2	312	9.34	7.32	3.25	2.92	26.9
3	286	1.23	6.41	3.95	4.46	36.3
4	159	2.37	4.98	4.15	5.93	52.6
5	204	0.285	5.19	3.48	6.37	57.7
6	351	0.353	5.81	4.18	6.88	72.3
7	312	0.865	7.25	3.82	5.92	71.4
8	313	0.427	7.77	4.67	5.91	88.5
9	390	0.115	6.44	4.41	4.63	80.9
10	370	0.437	7.88	4.91	4.63	75.7
11	428	0.442	9.32	4.9	4.37	74.9
12	569	0.384	12.6	4.59	3.92	67.2
13	1100	0.389	15.1	5.24	3.6	46.7
14	1160	0.33	21.1	9.17	4.36	56.1
15	1150	0.97	33.2	34.7	11.7	63
16	736	2.75	23.7	19.8	9.03	135
17	442	7.58	32	7.23	6.08	63.9
18	480	16.5	38.1	7.23	5.82	32.2
19	506	22.5	46.7	6.01	4.03	32.2
20	628	33.1	44.4	5.34	4.41	19.4
21	621	43.3	59.3	3.67	3.77	20.3
22	692	36.2	59.7	3.36	3.06	20.3
23	705	36.5	40.2	5.57	2.74	17.8
24	686	40.3	53.5	2.64	1.97	16.9
25	788	33.4	38.8	2.38	2.09	15.2
26	565	20.1	20.2	2.57	1.96	15.2
27	558	12.9	20.3	2.77	2.34	6.7
28	424	7.83	12	5.18	3.75	6.71
29	303	4.47	5.02	n/a	n/a	6.72

A.3 Welt Data

These values were estimated from plots in Welt, et al. (1999) using *DigitizeIt*.

Table A.3 – Welt data for normal hormone levels in younger (ages 20-34) women

Day	E_2	P_4	IHA	LH	FSH	IHB
	pg/mL	ng/mL	IU/mL	IU/L	IU/L	pg/mL
1	51	1.1	1.0	12	11.4	79
2	55	0.6	1.1	14	11.6	109
3	53	0.6	1.0	15	11.7	116
4	59	0.6	1.1	14	12.4	123
5	60	0.6	1.1	17	12.6	140
6	62	0.6	1.0	17	11.3	135
7	66	0.6	1.1	19	12.1	140
8	72	0.6	1.2	18	11.3	144
9	95	0.6	1.7	17	10.0	147
10	119	0.6	2.3	17	8.7	130
11	138	0.6	3.2	17	8.6	113
12	188	0.6	4.5	25	8.2	98
13	237	0.7	7.4	50	10.4	83
14	215	1.2	9.3	123	19.6	147
15	127	2.0	7.7	41	12.1	167
16	91	5.0	8.1	22	9.2	106
17	102	8.9	10.1	20	8.7	57
18	119	11.2	8.9	20	8.6	44
19	140	15.6	9.5	18	7.4	43
20	133	17.3	11.5	16	7.2	38
21	152	17.9	9.1	12	6.1	32
22	142	17.2	8.7	9	5.4	30
23	140	14.4	7.5	11	5.2	29
24	155	12.6	6.6	10	5.4	36
25	133	10.3	5.7	11	5.3	30
26	114	8.1	4.1	11	6.1	37
27	70	4.3	2.2	11	6.7	35
28	55	1.9	1.7	11	8.3	55

Table A.4 – Welt data for normal hormone levels in older (ages 35-46) women

Day	E_2	P_4	IHA	LH	FSH	IHB
	pg/mL	ng/mL	IU/mL	IU/L	IU/L	pg/mL
1	58	0.8	0.9	17	12.2	76
2	57	0.8	1.1	15	11.9	86
3	53	0.7	1.2	16	13.0	94
4	65	0.7	1.1	14	13.4	113
5	68	0.6	1.1	16	13.5	111
6	88	0.6	1.3	16	13.6	111
7	94	0.6	1.1	16	12.6	122
8	104	0.6	1.3	14	11.3	118
9	124	0.6	1.7	16	9.9	118
10	153	0.6	2.4	15	8.6	106
11	196	0.7	2.9	15	8.2	93
12	256	0.6	4.7	20	8.2	84
13	341	0.7	6.7	39	10.0	72
14	267	1.4	8.2	155	24.2	86
15	132	2.1	4.4	48	15.7	114
16	114	5.3	7.1	22	12.5	66
17	152	9.0	8.2	24	11.3	43
18	169	12.9	8.1	18	9.7	36
19	168	14.8	8.0	18	8.3	34
20	172	17.3	7.6	12	7.2	23
21	155	16.6	7.2	11	6.2	19
22	154	15.8	5.0	12	6.1	19
23	165	14.3	6.0	13	6.0	18
24	148	13.9	4.8	14	6.1	19
25	128	10.2	3.2	8	5.7	18
26	111	8.8	2.2	10	6.8	19
27	86	5.8	1.4	11	7.8	26
28	64	2.7	0.9	11	10.1	40

Appendix B

Sensitivity Coefficients

B.1 Five-Hormone Model

Computed using formula (4.1) with $\varepsilon = 0.01$, these sensitivity coefficients are referenced in section 4.4. Those with an absolute value of at least 0.25 are marked in **bold**.

Table B.1 – Sensitivity coefficients for the five-hormone model

Parameter	E_2 peak	P_4 peak	Ih peak	LH peak	FSH peak	Period
$v_{0,LH}$	**-0.65**	**-0.44**	**-0.42**	**-0.79**	**-1.38**	**0.25**
$v_{1,LH}$	-0.10	-0.20	-0.20	**0.74**	0.21	-0.04
Km_{LH}	**0.90**	**1.18**	**1.14**	-0.18	**-0.35**	**0.29**
$Ki_{LH,P}$	-0.03	-0.01	-0.01	0.08	-0.01	0.14
k_{LH}	-0.06	-0.10	-0.10	-0.06	-0.10	-0.04
a	**0.36**	**0.32**	**0.30**	**0.65**	0.16	0.04
$c_{LH,P}$	-0.01	-0.03	-0.03	0.04	-0.04	0.00
$c_{LH,E}$	0.03	0.06	0.05	0.06	0.05	0.04
d_E	0.04	0.06	0.06	0.09	0.02	0.04
d_P	-0.01	-0.01	-0.01	0.03	0.04	0.00
v_{FSH}	**0.74**	**0.51**	**0.49**	**1.04**	**2.50**	**-0.68**
$Ki_{FSH,Ih}$	0.16	0.10	0.09	0.22	**0.63**	**-0.29**
k_{FSH}	0.18	0.16	0.16	**0.27**	0.05	0.04
$c_{FSH,P}$	0.17	0.15	0.15	**0.25**	0.05	0.04
$c_{FSH,E}$	-0.19	-0.17	-0.16	**-0.28**	-0.05	0.00
d_{Ih}	0.10	0.11	0.10	0.14	**0.42**	0.14

Table B.1 (continued)

Parameter	E_2 peak	P_4 peak	Ih peak	LH peak	FSH peak	Period
b	0.00	-0.01	-0.01	-0.01	-0.10	-0.04
c_1	**0.74**	**0.52**	**0.50**	**1.06**	**1.59**	**-0.61**
c_2	**-0.83**	**-0.78**	**-0.75**	**-1.16**	**-1.20**	**0.29**
c_4	0.04	0.03	0.03	0.02	-0.10	0.00
c_5	-0.10	-0.04	-0.04	-0.14	-0.20	-0.04
c_8	0.03	**0.53**	**0.44**	0.01	**0.28**	0.00
d_1	0.07	0.24	**0.26**	0.11	0.12	-0.04
d_2	0.06	0.21	0.23	0.10	0.09	0.00
k_1	0.07	0.21	0.24	0.11	0.10	-0.04
k_2	0.07	0.15	**-0.46**	0.11	0.09	-0.18
k_3	-0.05	**-0.47**	**-0.29**	-0.04	0.03	-0.04
k_4	-0.04	**-0.43**	0.00	-0.07	-0.24	0.00
α	**-1.78**	**-1.82**	**-1.76**	**-2.52**	**-2.21**	**0.43**
β	0.04	0.04	0.03	0.04	-0.01	0.00
γ	-0.01	0.03	0.03	-0.01	0.02	0.00
e_0	**-0.34**	**-0.37**	**-0.35**	-0.18	-0.03	-0.04
e_1	**-0.46**	**-0.53**	**-0.51**	**-0.45**	-0.16	-0.18
e_2	**-0.42**	**-0.53**	**-0.52**	**0.32**	**0.26**	-0.14
e_3	-0.04	-0.03	-0.03	0.02	0.18	0.11
p_0	0.00	0.00	0.00	0.00	0.00	0.00
p_1	0.11	0.09	0.08	0.13	0.01	-0.04
p_2	0.08	0.05	0.05	0.09	0.02	-0.07
h_0	-0.07	-0.05	-0.04	-0.08	-0.22	0.07
h_1	-0.08	-0.07	-0.07	-0.10	**-0.34**	0.00
h_2	-0.02	0.01	0.01	-0.01	-0.06	0.18
h_3	0.00	0.01	0.01	0.00	-0.04	0.11
h_4	0.00	0.01	0.01	0.00	-0.04	0.11

B.2 New Model

Computed using formula (4.1) with $\varepsilon = 0.01,$ these sensitivity coefficients are referenced in section 6.3. They are taken using the parameter values from Table 5.5. Those with an absolute value of at least 0.25 are marked in **bold**. This analysis has more depth than that of section B.1, as we consider not only the highest peak for each hormone, but also secondary peaks, as well as the valleys. The three biological constants $(a_{FSH}, r_{LH}, \text{ and } v)$ are not included, since their values are fixed.

The following is the key to the peak and valley codes at the top of the table:

- E_2vf – Early follicular (main) valley of estradiol
- E_2pm – Mid-cycle (main) peak of estradiol
- E_2vf – Early luteal (secondary) valley of estradiol
- E_2pl – Mid-follicular (secondary) peak of estradiol
- P_4v – Valley of progesterone
- P_4p – Peak of progesterone
- IHAv – Valley of inhibin A
- IHAp – Peak of inhibin A
- LHb – Baseline (valley) of luteinizing hormone
- LHp – Peak of luteinizing hormone

- LHpl – Luteal secondary (undesirable) peak of luteinizing hormone
- FSHpf – Follicular peak of follicle-stimulating hormone
- FSHvf – Late-follicular valley of follicle-stimulating hormone
- FSHpm – Mid-cycle peak of follicle-stimulating hormone
- FSHvl – Luteal valley of follicle-stimulating hormone
- IHBpf – Follicular peak of inhibin B
- IHBvf – Follicular valley of inhibin B
- IHBpm – Mid-cycle peak of inhibin B
- IHBvl – Luteal valley of inhibin B
- Per – Period

Table B.2 – Sensitivity coefficients for the six-hormone model

	E_2vf	E_2pm	E_2vl	E_2pl	P_4v	P_4p	IHAv	IHAp
α	-0.06	**-2.37**	0.02	**-1.77**	**0.89**	**-2.75**	**0.26**	**-2.59**
c_1	**0.42**	**0.87**	-0.21	**0.51**	**0.42**	**0.80**	**0.63**	**0.76**
c_2	-0.11	**-1.03**	0.04	**-0.73**	**0.30**	**-1.13**	0.02	**-1.07**
c_3	-0.01	0.03	0.03	0.05	0.09	0.07	0.02	0.07
c_4	-0.12	-0.02	-0.02	0.05	**-0.43**	0.13	**-0.25**	0.12
c_5	-0.06	0.02	**-0.26**	0.21	-0.03	**0.33**	-0.12	**0.27**
c_6	-0.08	0.07	0.11	0.10	-0.15	0.15	-0.15	0.16
d_1	-0.14	0.08	0.13	0.15	**-0.27**	0.22	**-0.26**	0.23
d_2	-0.13	0.08	0.12	0.14	**-0.25**	0.20	**-0.25**	0.21
k_1	-0.15	0.09	0.13	0.16	**-0.30**	0.24	**-0.29**	**0.25**
k_2	0.05	0.03	0.07	0.04	0.09	0.06	0.05	**-0.30**
k_3	-0.06	0.05	0.13	0.15	-0.19	0.03	-0.18	-0.22
k_4	0.14	-0.09	-0.15	**-0.64**	**0.30**	**-0.78**	**0.39**	-0.18
β	-0.03	0.05	0.05	0.08	0.00	0.11	-0.04	0.10
γ	-0.01	-0.02	-0.15	0.09	0.04	0.13	-0.01	0.11
$v_{0,LH}$	-0.22	**-0.60**	0.15	**-0.28**	-0.10	**-0.44**	-0.20	**-0.42**
$v_{1,LH}$	0.00	-0.13	-0.21	-0.14	-0.12	-0.18	-0.05	-0.18
Km_{LH}	-0.14	**1.16**	**0.72**	**0.98**	-0.07	**1.43**	-0.13	**1.36**
$Ki_{LH,P}$	-0.17	-0.02	-0.01	-0.01	-0.20	-0.01	-0.19	-0.01
$c_{LH,P}$	0.00	0.00	0.00	0.00	0.01	0.00	0.01	0.00
$c_{LH,E}$	-0.06	0.06	0.01	0.05	-0.13	0.08	-0.11	0.07
k_{LH}	0.14	-0.13	-0.03	-0.11	**0.32**	-0.17	**0.26**	-0.16
v_{FSH}	**0.56**	**0.30**	-0.11	0.16	**0.84**	**0.26**	**0.91**	**0.24**
$Ki_{FSH,IhA}$	**0.38**	0.05	-0.02	0.03	**0.63**	0.04	**0.63**	0.04
$Ki_{FSH,IhB}$	0.07	0.13	-0.06	0.07	0.07	0.11	0.10	0.10
k_{FSH}	-0.10	0.14	-0.01	0.08	-0.22	0.13	-0.18	0.13
$c_{FSH,P}$	-0.10	0.14	-0.01	0.08	-0.22	0.13	-0.18	0.13
$c_{FSH,E}$	0.10	-0.14	0.01	-0.09	0.23	-0.14	0.19	-0.13

Table B.2 (continued)

	E_2vf	E_2pm	E_2vl	E_2pl	P_4v	P_4p	IHAv	IHAp
d_{IhA}	-0.09	0.10	0.02	0.07	-0.18	0.11	-0.17	0.10
d_{IhB}	0.02	-0.03	0.00	-0.02	0.04	-0.03	0.04	-0.03
b	-0.03	**0.30**	0.04	0.19	-0.11	**0.30**	-0.07	**0.28**
f_1	-0.14	**0.59**	-0.10	**0.36**	**-0.44**	**0.56**	**-0.28**	**0.53**
f_2	0.01	-0.09	0.05	-0.04	0.05	-0.07	0.02	-0.06
f_3	0.00	0.00	0.00	0.00	0.00	0.00	0.00	0.00
f_4	-0.01	0.12	-0.04	0.07	-0.05	0.11	-0.02	0.10
e_0	**0.91**	-0.16	**0.31**	0.04	0.03	**-0.44**	0.04	**-0.42**
e_1	**0.49**	**-0.33**	**-0.28**	**-0.56**	**0.96**	**-0.85**	**0.83**	**-0.80**
e_2	0.08	0.16	0.02	-0.20	0.03	**-0.27**	0.08	**-0.27**
e_3	**-0.26**	0.05	**0.24**	**0.68**	**-0.55**	0.04	**-0.48**	0.04
p_0	0.00	0.05	-0.02	0.02	**0.76**	0.06	-0.01	0.03
p_1	0.01	0.03	0.01	0.02	0.05	0.22	0.01	0.03
p_2	0.08	0.06	0.01	0.05	**0.31**	**0.84**	0.13	0.06
h_0	-0.04	-0.06	0.02	-0.04	-0.05	-0.06	**0.74**	0.03
h_1	-0.03	-0.04	-0.01	-0.03	-0.05	-0.05	0.01	-0.03
h_2	-0.10	0.02	0.00	0.01	-0.17	0.02	-0.14	**0.39**
h_3	-0.13	0.02	0.00	0.02	-0.23	0.02	-0.16	**0.43**
h_4	-0.05	0.01	0.00	0.01	-0.09	0.01	-0.05	0.13
j_0	-0.03	-0.04	0.01	-0.02	-0.03	-0.03	-0.04	-0.03
j_1	-0.03	-0.08	0.05	-0.04	-0.03	-0.06	-0.05	-0.06
j_2	0.00	0.00	0.00	0.00	0.00	0.00	0.00	0.00
j_3	-0.01	-0.02	0.00	-0.01	-0.01	-0.02	-0.01	-0.02
δ	-0.03	**0.31**	-0.10	0.17	-0.15	**0.26**	-0.07	**0.25**
d_E	-0.18	0.21	0.06	0.17	**-0.29**	**0.27**	**-0.24**	**0.25**
d_P	0.00	0.00	-0.01	0.00	-0.01	0.00	0.00	0.00
a	-0.03	0.02	0.02	0.02	-0.06	0.03	-0.06	0.03

Table B.2 (continued)

	LHb	LHp	LHpl	FSHpf	FSHvf	FSHpm	FSHvl
α	-0.23	**-2.62**	**2.84**	0.17	**1.63**	**-3.75**	**2.13**
c_1	-0.19	**0.92**	**-1.47**	**-0.30**	**-1.00**	**1.97**	**-0.61**
c_2	-0.06	**-1.09**	**1.38**	0.11	**0.76**	**-1.69**	**0.87**
c_3	0.03	0.03	-0.10	0.02	-0.03	-0.03	-0.06
c_4	0.03	-0.03	0.16	0.02	0.10	-0.06	-0.09
c_5	0.09	0.01	-0.19	0.04	0.05	0.16	-0.21
c_6	0.07	0.06	-0.04	0.04	0.04	0.07	-0.10
d_1	0.12	0.07	-0.10	0.07	0.04	0.04	-0.18
d_2	0.12	0.06	-0.03	0.06	0.04	0.04	-0.20
k_1	0.13	0.07	-0.10	0.07	0.04	0.05	-0.18
k_2	0.00	0.02	-0.16	-0.02	0.02	0.00	0.24
k_3	0.13	0.04	**-0.47**	0.03	0.03	0.04	0.17
k_4	**-0.33**	-0.07	**1.17**	-0.07	-0.03	-0.08	0.14
β	0.04	0.05	-0.08	0.02	-0.03	-0.01	-0.08
γ	0.03	-0.02	-0.16	0.01	0.02	0.08	-0.10
$v_{0,LH}$	**0.99**	**-0.49**	**2.38**	0.23	**0.65**	**-1.17**	**0.33**
$v_{1,LH}$	-0.01	**0.73**	-0.05	-0.01	0.02	0.13	0.13
Km_{LH}	**-0.27**	0.08	**2.26**	0.07	-0.03	-0.12	**-1.08**
$Ki_{LH,P}$	**0.34**	0.06	**-0.42**	0.06	0.04	-0.04	0.00
$c_{LH,P}$	-0.01	0.00	0.00	0.00	0.00	0.00	-0.02
$c_{LH,E}$	0.04	0.06	-0.05	0.02	-0.01	0.04	-0.06
k_{LH}	-0.09	-0.03	0.13	-0.05	0.00	-0.06	0.12
v_{FSH}	**-0.27**	**0.33**	**-1.25**	0.12	-0.03	**1.44**	**0.82**
$Ki_{FSH,IhA}$	-0.17	0.05	**-0.75**	-0.10	0.03	**0.37**	**0.77**
$Ki_{FSH,IhB}$	-0.05	0.15	-0.17	0.13	-0.04	**0.58**	-0.03
k_{FSH}	0.05	0.14	0.03	0.07	-0.01	-0.16	-0.09
$c_{FSH,P}$	0.05	0.14	0.03	0.07	-0.01	-0.15	-0.09
$c_{FSH,E}$	-0.07	-0.14	-0.05	-0.07	0.01	0.15	0.11

Table B.2 (continued)

	LHb	LHp	LHpl	FSHpf	FSHvf	FSHpm	FSHvl
d_{IhA}	0.07	0.09	0.08	0.04	0.06	**0.35**	-0.07
d_{IhB}	-0.02	-0.03	0.07	0.03	0.02	0.00	0.03
b	-0.12	**0.42**	**0.79**	0.01	-0.03	0.10	-0.23
f_1	0.08	**0.61**	**-0.25**	**0.58**	0.03	**1.56**	**-0.42**
f_2	0.02	-0.11	0.07	-0.12	0.04	**-0.37**	0.05
f_3	0.00	0.00	-0.02	0.00	0.00	0.00	0.00
f_4	0.00	0.14	0.01	0.13	-0.04	**0.41**	-0.07
e_0	0.13	-0.12	**-0.84**	-0.03	0.04	0.03	**0.35**
e_1	**-0.41**	**-0.30**	**0.24**	-0.21	-0.01	0.02	**0.63**
e_2	-0.11	0.16	**0.28**	-0.04	-0.02	0.10	0.22
e_3	**0.59**	0.06	**-1.77**	0.11	0.01	0.10	-0.05
p_0	-0.04	0.02	0.05	0.03	-0.11	-0.13	-0.02
p_1	-0.05	0.02	0.13	0.00	0.02	0.00	-0.02
p_2	-0.22	0.03	**0.50**	-0.05	0.04	-0.02	-0.06
h_0	0.02	-0.07	0.08	-0.05	0.00	-0.23	-0.02
h_1	0.00	-0.03	0.15	0.01	-0.04	-0.19	0.02
h_2	0.04	0.01	0.15	0.05	0.00	0.01	**-0.34**
h_3	0.02	0.02	**-0.61**	0.06	0.00	0.02	**-0.34**
h_4	0.02	0.01	0.17	0.02	0.00	0.01	-0.08
j_0	0.02	-0.04	0.13	-0.03	0.00	-0.14	-0.02
j_1	0.03	-0.10	0.09	-0.10	0.04	**-0.36**	0.05
j_2	0.00	0.00	0.00	0.00	0.00	0.00	-0.02
j_3	0.00	-0.02	0.11	0.00	-0.01	-0.09	0.00
δ	0.00	**0.34**	-0.01	**0.31**	-0.11	**1.02**	-0.23
d_E	0.13	0.21	-0.07	0.05	0.01	0.05	-0.19
d_P	-0.02	0.02	-0.01	0.00	0.00	0.01	0.01
a	0.02	0.01	0.10	0.02	0.04	-0.03	-0.01

Table B.2 (continued)

	IHBpf	IHBvf	IHBpm	IHBvl	Per
α	**0.47**	**3.04**	**-1.88**	**0.39**	**1.14**
c_1	**-0.63**	**-1.96**	**0.64**	-0.10	**-1.18**
c_2	**0.26**	**1.42**	**-0.80**	0.16	**0.61**
c_3	0.03	-0.05	0.04	0.00	0.04
c_4	0.03	**0.43**	0.12	-0.05	0.04
c_5	0.08	**0.33**	**0.36**	-0.03	0.04
c_6	0.06	-0.12	**-0.39**	-0.04	0.04
d_1	0.12	0.09	0.06	-0.02	0.07
d_2	0.11	0.09	0.06	-0.02	0.07
k_1	0.13	0.10	0.06	-0.02	0.07
k_2	-0.04	0.04	0.02	0.03	-0.07
k_3	0.06	0.06	0.03	0.02	-0.07
k_4	-0.15	-0.08	-0.06	0.05	**-0.32**
β	0.05	-0.03	0.06	-0.01	0.07
γ	0.02	0.14	0.19	-0.01	0.00
$v_{0,LH}$	-0.11	**1.17**	**-0.40**	0.03	**0.57**
$v_{1,LH}$	-0.03	-0.05	-0.15	0.00	-0.11
Km_{LH}	0.12	**0.47**	**0.90**	-0.09	**0.43**
$Ki_{LH,P}$	0.07	0.08	-0.02	-0.01	0.21
$c_{LH,P}$	0.00	0.00	0.00	0.00	-0.04
$c_{LH,E}$	0.04	0.02	0.04	-0.01	0.07
k_{LH}	-0.10	-0.06	-0.09	0.03	-0.14
v_{FSH}	**0.50**	-0.04	0.24	0.10	**-1.00**
$Ki_{FSH,IhA}$	-0.12	0.03	0.04	0.10	**-0.54**
$Ki_{FSH,IhB}$	**0.36**	-0.05	0.10	-0.01	-0.21
k_{FSH}	0.15	0.04	0.10	-0.02	0.07
$c_{FSH,P}$	0.15	0.04	0.10	-0.02	0.07
$c_{FSH,E}$	-0.15	-0.04	-0.10	0.02	-0.11

Table B.2 (continued)

	IHBpf	IHBvf	IHBpm	IHBvl	Per
d_{IhA}	0.04	0.13	0.08	-0.02	0.14
d_{IhB}	0.04	0.02	-0.02	0.00	-0.04
b	0.01	0.00	0.19	-0.03	0.04
f_1	**-1.12**	**-1.88**	**0.42**	-0.19	-0.18
f_2	**0.46**	**0.41**	0.12	0.02	0.11
f_3	0.00	0.00	0.00	0.00	0.00
f_4	**-0.43**	**-0.55**	-0.09	-0.04	-0.07
e_0	-0.07	-0.09	**-0.28**	0.03	-0.11
e_1	**-0.38**	**-0.34**	**-0.51**	0.12	**-0.64**
e_2	-0.09	-0.14	-0.22	0.01	-0.14
e_3	0.21	0.04	0.03	-0.04	**0.39**
p_0	0.11	-0.16	0.03	0.00	-0.04
p_1	0.00	0.03	0.02	0.00	-0.04
p_2	-0.07	0.07	0.05	0.00	-0.11
h_0	-0.12	0.00	-0.05	0.00	0.11
h_1	0.02	-0.06	-0.03	0.00	0.04
h_2	0.08	0.01	0.01	-0.03	0.11
h_3	0.10	0.02	0.02	-0.04	-0.04
h_4	0.03	0.01	0.01	-0.01	0.07
j_0	0.14	**0.29**	0.17	**0.97**	0.07
j_1	**0.49**	**0.41**	0.12	0.02	0.14
j_2	0.00	0.00	0.00	0.00	0.00
j_3	0.01	**0.35**	**0.61**	0.01	0.04
δ	**-1.02**	**-1.59**	**-0.50**	-0.10	-0.18
d_E	0.09	0.12	0.14	-0.05	0.21
d_P	0.00	0.00	0.00	0.00	0.00
a	0.18	-0.01	0.03	-0.08	0.07

Appendix C

MATLAB Codes for the Five-Hormone Model

C.1 merge.m

```
%Input: None
%Output: Plots of model-predicted hormone concentrations and the data
clear;
close all;

load('welt_data'); %A .mat file with 84-length vectors with the data
t_data=[1:84];

global t_0; global t_f; global dt;
t_0=0; %Starting day
t_f=84; %Ending day (84 days = 3 cycles)
dt=0.01; %Output mesh size 0.01 days
n=round(1/dt); %100 output points per day

%Constants
global V; V=2.5; %Volume of dispensation (Liters)
global a_FSH; a_FSH=8.21; %Clearance rate of FSH (/day)
global r_LH; r_LH=14; %Clearance rate of LH (/day)
global a; a=8; %Hill function exponent in LH synthesis term

Q=zeros(42,1);
Q(1:11)=[0.79 0.05 0.09 0.09 0.027 0.51 0.5 0.56 0.55 0.69 0.85];
Q(12:22)=[0.85 0.13 0.16 0.02 500 4500 180 12.2 0.26 0.0040 2.42];
Q(23:27)=[375 1.90 0.0018 3.5 12];
Q(28:39)=[40 0.11 0.21 0.45 0 0.048 0.048 0.4 0.009 0.029 0.018 0];
Q(40:42)=[0.2 1 2];

%Normal initial conditions for normal parameter set
%RP_LH, LH, RP_FSH, FSH, MsF, SeF, PrF, Sc1, Sc2, Lut1, Lut2, Lut3, Lut4
IC=[74 12 12 6.7 5.25 9.25 3.5 3 15 44 63 76 105];

%Unstable equilibrium for normal parameter set
 %IC=[90.128 12.121 23.66 7.0806 40.501 196.01 119.65 128.29 114.55 ...
 %116.63 92.965 75.466 75.466];

%The following are not the standard values
 %Q(18)=250; %Set Km_LH = 250 to get two stable periodic solutions
```

```
%Abnormal stable cycle at Km_LH = 250
 %IC=[55.527 8.7125 25.049 5.4591 42.85 414.66 183.16 195.09 ...
 %    174.19 177.35 141.37 114.76 114.76];

%Equilibrium initial conditions
 %IC=[63.689 9.5973 24.337 5.8964 45.143 334.72 162.55 173.47 ...
 %    154.88 157.7 125.7 102.04 102.04];

%Randomized initial conditions
 %IC=IC.*(0.95+rand(1,13)./10);
 %IC=IC.*(2*rand(1,13));
 %IC=IC.*2.^(-0.05+0.10*rand(1,13));

t=[t_0:dt:t_f]';
sol=dde23('mergede',Q(40:42)',IC',[t_0, t_f],[],Q);
OV_out=deval(sol,t)';

RP_LH_model=OV_out(:,1);
LHmodel=OV_out(:,2);
FSHmodel=OV_out(:,4);
SeF=OV_out(:,6);
PrF=OV_out(:,7);
Lut2=OV_out(:,11);
Lut3=OV_out(:,12);
Lut4=OV_out(:,13);

for i=1:length(t)
    E2model(i)=Q(28)+Q(29)*SeF(i)+Q(30)*PrF(i)+Q(31)*Lut4(i);
    P4model(i)=Q(32)+Q(33)*Lut3(i)+Q(34)*Lut4(i);
    IHAmodel(i)=Q(35)+Q(36)*PrF(i)+Q(37)*Lut2(i)+Q(38)*Lut3(i) ...
        +Q(39)*Lut4(i);
end;

en=1+(t_f-t_0)*n;
[junk,P4pk1]=max(P4model(en-60*n:en-30*n));
P4peak=t_0+dt*(P4pk1-1);
[junk,P4peak2]=max(P4model(en-60*n-1+P4pk1+5*n:en-60*n-1+P4pk1+30*n));
P4per=(P4peak2+5*n-1)*dt %Period using P4

%Amplitude using RP_LH
RP_LH_amp=max(RP_LH_model(en-60*n:en))-min(RP_LH_model(en-60*n:en))

t_p=min(t_f,84);

figure(1);
plot(t_data(1:t_p),E2data(1:t_p),'kx',t,E2model,'-k');
title('\fontsize{14} \bf E_2 Model');
legend('Data','Model');
axis([0 84 0 250]);
xlabel('\fontsize{10} \bf Time (days)');
ylabel('\fontsize{10} \bf E_2 (pg/mL)');
```

```
figure(2);
plot(t_data(1:t_p),P4data(1:t_p),'kx',t,P4model,'-k');
title('\fontsize{14} \bf P_4 Model');
legend('Data','Model');
axis([0 84 0 20]);
xlabel('\fontsize{10} \bf Time (days)');
ylabel('\fontsize{10} \bf P_4 (ng/mL)');

figure(3);
plot(t_data(1:t_p),IHAdata(1:t_p),'kx',t,IHAmodel,'-k');
title('\fontsize{14} \bf IhA Model');
legend('Data','Model');
axis([0 84 0 13]);
xlabel('\fontsize{10} \bf Time (days)');
ylabel('\fontsize{10} \bf Ih (IU/mL)');

figure(4);
plot(t_data(1:t_p),LHdata(1:t_p),'kx',t,LHmodel,'k-');
title('\fontsize{14} \bf LH Model');
legend('Data','Model');
axis([0 84 0 140]);
xlabel('\fontsize{10} \bf Time (days)');
ylabel('\fontsize{10} \bf LH (IU/L)');

figure(5);
plot(t_data(1:t_p),FSHdata(1:t_p),'kx',t,FSHmodel,'-k');
title('\fontsize{14} \bf FSH Model');
legend('Data','Model');
axis([0 84 0 20]);
xlabel('\fontsize{10} \bf Time (days)');
ylabel('\fontsize{10} \bf FSH (IU/L)');
hold on;
```

C.2 merge_compare.m

```
%Compares model output from two parameter sets
%Input: None
%Output: Plots (centered to the LH surge) for two parameter sets
%        plus period length and total error for each
clear;
close all;
load('welt_data');
t_data=day;

global t_0; global t_f; global dt;
t_0=0;
t_f=150;
dt=0.01;
n=round(1/dt);

%Constants
global V; V=2.5;
global a_FSH; a_FSH=8.21;
global r_LH; r_LH=14;
global a; a=8;

Q=zeros(42,1);
Q(1:11)=[0.79 0.05 0.09 0.09 0.13 0.027 0.51 0.5 0.56 0.55 0.69];
Q(12:22)=[0.85 0.85 0.16 0.02 500 4500 180 12.2 0.26 0.0040 2.42];
Q(23:27)=[375 1.90 0.0018 3.5 12];
Q(28:39)=[40 0.11 0.21 0.45 0 0.048 0.048 0.4 0.009 0.029 0.018 0];
Q(40:42)=[0.2 1 2];

%Normal initial conditions for normal parameter set
%RP_LH, LH, RP_FSH, FSH, MsF, SeF, PrF, Sc1, Sc2, Lut1, Lut2, Lut3, Lut4
IC=[74 12 12 6.7 5.25 9.25 3.5 3 15 44 63 76 105];

t=[t_0:dt:t_f]';
sol=dde23('mergede',Q(40:42),IC',[t_0, t_f],[],Q);
OV_out=deval(sol,t)';

RP_LH_model=OV_out(:,1);
LHmodel=OV_out(:,2);
FSHmodel=OV_out(:,4);
SeF=OV_out(:,6);
PrF=OV_out(:,7);
Lut2=OV_out(:,11);
Lut3=OV_out(:,12);
Lut4=OV_out(:,13);

for i=1:length(t)
    E2model(i)=Q(28)+Q(29)*SeF(i)+Q(30)*PrF(i)+Q(31)*Lut4(i);
    P4model(i)=Q(32)+Q(33)*Lut3(i)+Q(34)*Lut4(i);
```

```
    IHAmodel(i)=Q(35)+Q(36)*PrF(i)+Q(37)*Lut2(i)+Q(38)*Lut3(i) ...
        +Q(39)*Lut4(i);
end;

terr=err_lsq(Q,IC,welt_data) %Error computation

en=1+(t_f-t_0)*n;
[junk,P4pk1]=max(P4model(en-60*n:en-30*n));
P4peak=t_0+dt*(P4pk1-1);
[junk,P4peak2]=max(P4model(en-60*n-1+P4pk1+5*n:en-60*n-1+P4pk1+30*n));
P4per=(P4peak2+5*n-1)*dt %Period, looking at P4 peaks

RP_LH_amp=max(RP_LH_model(en-60*n:en))-min(RP_LH_model(en-60*n:en));

[junk,pk]=max(OV_out(en-60*n:en,:));
allpk=t_0+dt*(pk-1);

%Put any changes to the parameter set Q here
%Q(18)=250; %An example of such a change

sol=dde23('mergede',Q(40:42),IC',[t_0, t_f],[],Q);
OV_out=deval(sol,t)';

RP_LH_rep=OV_out(:,1);
LH_rep=OV_out(:,2);
FSH_rep=OV_out(:,4);
SeF_rep=OV_out(:,6);
PrF_rep=OV_out(:,7);
Lut2_rep=OV_out(:,11);
Lut3_rep=OV_out(:,12);
Lut4_rep=OV_out(:,13);

for i=1:length(t)
    E2_rep(i)=Q(28)+Q(29)*SeF_rep(i)+Q(30)*PrF_rep(i)+Q(31)*Lut4_rep(i);
    P4_rep(i)=Q(32)+Q(33)*Lut3_rep(i)+Q(34)*Lut4_rep(i);
    IHA_rep(i)=Q(35)+Q(36)*PrF_rep(i)+Q(37)*Lut2_rep(i)...
        +Q(38)*Lut3_rep(i)+Q(39)*Lut4_rep(i);
end;
terr_rep=err_lsq(Q,IC,welt_data)

en=1+(t_f-t_0)*n;
[junk,P4pk1]=max(P4model(en-60*n:en-30*n));
P4peak=t_0+dt*(P4pk1-1);
[junk,P4peak2]=max(P4model(en-60*n-1+P4pk1+5*n:en-60*n-1+P4pk1+30*n));
P4per_rep=(P4peak2+5*n-1)*dt

RP_LH_amp=max(RP_LH_rep(en-60*n:en))-min(RP_LH_rep(en-60*n:en));

[junk,pk]=max(OV_out(en-60*n:en,:));
allpk=t_0+dt*(pk-1);

%Center both model outputs for 150-day plot
[junk,tc]=max(LHmodel(n*(t_f-72):n*(t_f-42)));
tc=tc+n*(t_f-72)-1;
```

```
[junk,tcrep]=max(LH_rep(n*(t_f-72):n*(t_f-42)));
tcrep=tcrep+n*(t_f-72)-1;
txa=tc-42*n;
txb=tc+42*n;
txc=tcrep-42*n;
txd=tcrep+42*n;

t_p=min(t_f,84);

figure(1);
plot(t_data(1:t_p),E2data(1:t_p),'.',[0:dt:84],E2model(txa:txb), ...
    '-.r',[0:dt:84],E2_rep(txc:txd),'-k');
title('\fontsize{14} \bf E_2 Model');
legend('Data','Model');
axis([0 84 0 240]);
xlabel('\fontsize{10} \bf Time (days)');
ylabel('\fontsize{10} \bf E_2 (pg/L)');

figure(2);
plot(t_data(1:t_p),P4data(1:t_p),'.',[0:dt:84],P4model(txa:txb), ...
    '-.r',[0:dt:84],P4_rep(txc:txd),'-k');
title('\fontsize{14} \bf P_4 Model');
legend('Data','Model');
axis([0 84 0 20]);
xlabel('\fontsize{10} \bf Time (days)');
ylabel('\fontsize{10} \bf P_4 (ng/L)');

figure(3);
plot(t_data(1:t_p),IHAdata(1:t_p),'.',[0:dt:84],IHAmodel(txa:txb), ...
    '-.r',[0:dt:84],IHA_rep(txc:txd),'-k');
title('\fontsize{14} \bf IhA Model');
legend('Data','Model');
axis([0 84 0 12]);
xlabel('\fontsize{10} \bf Time (days)');
ylabel('\fontsize{10} \bf IhA (IU/mL)');

figure(4);
plot(t_data(1:t_p),LHdata(1:t_p),'.',[0:dt:84],LHmodel(txa:txb), ...
    '-.r',[0:dt:84],LH_rep(txc:txd),'-k');
title('\fontsize{14} \bf LH Model');
legend('Data','Model');
axis([0 84 0 140]);
xlabel('\fontsize{10} \bf Time (days)');
ylabel('\fontsize{10} \bf LH (IU/L)');

figure(5);
plot(t_data(1:t_p),FSHdata(1:t_p),'.',[0:dt:84],FSHmodel(txa:txb), ...
    '-.r',[0:dt:84],FSH_rep(txc:txd),'-k');
title('\fontsize{14} \bf FSH Model');
legend('Data','Model');
axis([0 84 0 20]);
xlabel('\fontsize{10} \bf Time (days)');
ylabel('\fontsize{10} \bf FSH (IU/L)');
```

C.3 external.m

```
clear;
close all;
%Plots model predictions with and without exogenous hormones
load('welt_data');
t_data=day;

global t_0; global t_f; global dt;
t_0=0;
t_f=250;
dt=0.1;
n=round(1/dt);

for i=length(E2data)+1:t_f %Expand 28 days to more
    E2data(i)=E2data(i-28);
    P4data(i)=P4data(i-28);
    IHAdata(i)=IHAdata(i-28);
    IHBdata(i)=IHBdata(i-28);
    LHdata(i)=LHdata(i-28);
    FSHdata(i)=FSHdata(i-28);
end;

%Constants
global V; V=2.5;
global a_FSH; a_FSH=8.21;
global r_LH; r_LH=14;
global a; a=8;

%Current value
Q=zeros(42,1);
Q(1:11)=[0.79 0.05 0.09 0.09 0.13 0.027 0.51 0.5 0.56 0.55 0.69];
Q(12:22)=[0.85 0.85 0.16 0.02 500 4500 180 12.2 0.26 0.0040 2.42];
Q(23:27)=[375 1.90 0.0018 3.5 12];
Q(28:39)=[40 0.11 0.21 0.45 0 0.048 0.048 0.4 0.009 0.029 0.018 0];
Q(40:42)=[0.2 1 2];

%Make any parameter changes here, if so desired
Q(18)=250; % Km_LH=250 gives two stable periodic solutions

%External introduction of hormones
startE2=0.001; %Day number to start E2 dose
endE2=150.001; %Day number to end E2 dose
doseE2=50; %Dosage amount (bloodstream concentration increase)
startP4=10.001;
endP4=15.001;
doseP4=0;
startIHA=0.001;
endIHA=20.001;
doseIHA=0;
```

```
Q(43:51)=[startE2 endE2 doseE2 startP4 endP4 doseP4 startIHA ...
          endIHA doseIHA]';

%Pseudo-normal cycle initial conditions (KmLH=250)
IC1=[74 12 12 6.7 5.25 9.25 3.5 3.0 15 44 63 76 105];

%Abormal cycle initial conditions (KmLH=250)
IC3=[44.222 8.3202  15.507  4.9731  19.656  265.47  123.42  152.34 ...
     157.28  183 158.78  135.68  140.09];

t=[t_0:dt:t_f]';

%Simulation WITH external hormones (experimental subject)
%Change IC1' to IC3' to start from abormal cycle
sol=dde23('mergede3',[d_E d_P d_IHA],IC1',[t_0, t_f],[],Q);
OV_out=deval(sol,t)';
RP_LH_model=OV_out(:,1);
LHmodel=OV_out(:,2);
FSHmodel=OV_out(:,4);
SeF=OV_out(:,6);
PrF=OV_out(:,7);
Lut2=OV_out(:,11);
Lut3=OV_out(:,12);
Lut4=OV_out(:,13);
for i=1:length(t)
    E2model(i)=e0+e1*SeF(i)+e2*PrF(i)+e3*Lut4(i) ...
        +doseE2*(heaviside(t(i)-startE2)-heaviside(t(i)-endE2));
    P4model(i)=p0+p1*Lut3(i)+p2*Lut4(i) ...
        +doseP4*(heaviside(t(i)-startP4)-heaviside(t(i)-endP4));
    IHAmodel(i)=h0+h1*PrF(i)+h2*Lut2(i)+h3*Lut3(i)+h4*Lut4(i) ...
        +doseIHA*(heaviside(t(i)-startIHA)-heaviside(t(i)-endIHA));
end;

%Simulation WITHOUT external hormones (control subject)
%Change IC1' to IC3' to start from abnormal cycle
doseE2=0; doseP4=0; doseIHA=0; Q(45)=0; Q(48)=0; Q(51)=0;
sol=dde23('mergede3',[d_E d_P d_IHA],IC1',[t_0, t_f],[],Q);
OV_out=deval(sol,t)';
RP_LH_model=OV_out(:,1);
LHmodel2=OV_out(:,2);
FSHmodel2=OV_out(:,4);
SeF=OV_out(:,6);
PrF=OV_out(:,7);
Lut2=OV_out(:,11);
Lut3=OV_out(:,12);
Lut4=OV_out(:,13);
for i=1:length(t)
    E2model2(i)=e0+e1*SeF(i)+e2*PrF(i)+e3*Lut4(i) ...
        +doseE2*(heaviside(t(i)-startE2)-heaviside(t(i)-endE2));
    P4model2(i)=p0+p1*Lut3(i)+p2*Lut4(i) ...
        +doseP4*(heaviside(t(i)-startP4)-heaviside(t(i)-endP4));
```

```
    IHAmodel2(i)=h0+h1*PrF(i)+h2*Lut2(i)+h3*Lut3(i)+h4*Lut4(i) ...
        +doseIHA*(heaviside(t(i)-startIHA)-heaviside(t(i)-endIHA));
end;

%Plots of data
t_p=min(t_f,84);
figure(1);
plot(t_data(1:t_p),E2data(1:t_p),'k.',t,E2model,'k-',t,E2model2,'k:');
%plot(t,E2model,'k-',t,E2model2,'k:');
title('\fontsize{14} \bf E_2 Model');
legend('Data','Model');
xlabel('\fontsize{10} \bf Time (days)');
ylabel('\fontsize{10} \bf E_2 (pg/mL)');

figure(2);
plot(t_data(1:t_p),P4data(1:t_p),'k.',t,P4model,'k-',t,P4model2,'k:');
%plot(t,P4model,'k-',t,P4model2,'k:');
title('\fontsize{14} \bf P_4 Model');
legend('Data','Model');
xlabel('\fontsize{10} \bf Time (days)');
ylabel('\fontsize{10} \bf P_4 (ng/mL)');

figure(3);
plot(t_data(1:t_p),IHAdata(1:t_p),'k.',t,IHAmodel,'k',t,IHAmodel2,'k:');
%plot(t,IHAmodel,'k-',t,IHAmodel2,'k:');
title('\fontsize{14} \bf IhA Model');
legend('Data','Model');
xlabel('\fontsize{10} \bf Time (days)');
ylabel('\fontsize{10} \bf IhA (IU/mL)');

figure(4);
plot(t_data(1:t_p),LHdata(1:t_p),'.',t,LHmodel,'-',t,LHmodel2,':');
title('\fontsize{14} \bf LH Model');
legend('Data','Model');
xlabel('\fontsize{12} \bf Time (days)');
ylabel('\fontsize{12} \bf LH (IU/L)');

figure(5);
plot(t_data(1:t_p),FSHdata(1:t_p),'.',t,FSHmodel,'-',t,FSHmodel2,':');
title('\fontsize{14} \bf FSH Model');
legend('Data','Model');
xlabel('\fontsize{12} \bf Time (days)');
ylabel('\fontsize{12} \bf FSH (IU/L)');
```

C.4 mergede.m

```
%Right-hand side of merged system, without external hormones
%This function is called by dde23, the delay equation solver
function d_merge=mergede(t,data_in,Z,Q);
%Input: t = time (days)
%       data_in = current values for the 13 state variables
%       Z is a 13 x 3 matrix giving the 13 state variable values
%           at each of three past times, associated with the delays
%       Q is the parameter set

global V;
global a;
global r_LH;
global a_FSH;

alpha=Q(1); b=Q(2); c1=Q(3); c2=Q(4); c5=Q(5);
c8=Q(6); d1=Q(7); d2=Q(8); k1=Q(9); k2=Q(10);
k3=Q(11); k4=Q(12); c4=Q(13); beta=Q(14); gamma=Q(15);
v_0_LH=Q(16);  v_1_LH=Q(17); Km_LH=Q(18); Ki_LH_P=Q(19); c_LH_P=Q(20);
c_LH_E=Q(21); k_LH=Q(22); v_FSH_A=Q(23); k_FSH=Q(24); c_FSH_E=Q(25);
Ki_FSH_IHA=Q(26); c_FSH_P=Q(27); e0=Q(28); e1=Q(29); e2=Q(30);
e3=Q(31); p0=Q(32); p1=Q(33); p2=Q(34); h0=Q(35); h1=Q(36);
h2=Q(37); h3=Q(38); h4=Q(39); d_E=Q(40); d_P=Q(41); d_IHA=Q(42);

RP_LH=data_in(1);
LH=data_in(2);
RP_FSH=data_in(3);
FSH=data_in(4);
MsF=data_in(5);
SeF=data_in(6);
PrF=data_in(7);
Sc1=data_in(8);
Sc2=data_in(9);
Lut1=data_in(10);
Lut2=data_in(11);
Lut3=data_in(12);
Lut4=data_in(13);

E2=e0+e1*SeF+e2*PrF+e3*Lut4;
P4=p0+p1*Lut3+p2*Lut4;
IHA=h0+h1*PrF+h2*Lut2+h3*Lut3+h4*Lut4;

E2old=e0+e1*Z(6,1)+e2*Z(7,1)+e3*Z(13,1); %index 1 = 1st delay, d_E2
P4old=p0+p1*Z(12,2)+p2*Z(13,2); %index 2 = 2nd delay, d_P4
IHAold=h0+h1*Z(7,3)+h2*Z(11,3)+h3*Z(12,3)+h4*Z(13,3); %index 3 = d_IhA
```

```
syn_LH=(v_0_LH + v_1_LH*(E2old/Km_LH)^a/(1+(E2old/Km_LH)^a))/ ...
    (1+P4old/Ki_LH_P);
rel_LH=k_LH*(1+c_LH_P*P4)*RP_LH/(1+c_LH_E*E2);
d_RP_LH=syn_LH - rel_LH;
d_LH=rel_LH/V - r_LH*LH;
d_RP_FSH=(v_FSH_A/(1+IHAold/Ki_FSH_IHA))...
    -(k_FSH*(1+c_FSH_P*P4)*RP_FSH)/(1+c_FSH_E*E2^2);
d_FSH=1/V*(k_FSH*(1+c_FSH_P*P4)*RP_FSH)/(1+c_FSH_E*E2^2)...
    -a_FSH*FSH;
d_MsF=b*FSH+(c1*FSH-c2*LH^alpha)*MsF;
d_SeF=c2*LH^alpha*MsF+(c4*LH^beta-c5*LH)*SeF;
d_PrF=c5*LH*SeF-c8*LH^gamma*PrF;
d_Sc1=c8*LH^gamma*PrF-d1*Sc1;
d_Sc2=d1*Sc1-d2*Sc2;
d_Lut1=d2*Sc2-k1*Lut1;
d_Lut2=k1*Lut1-k2*Lut2;
d_Lut3=k2*Lut2-k3*Lut3;
d_Lut4=k3*Lut3-k4*Lut4;

d_merge=[d_RP_LH d_LH d_RP_FSH d_FSH d_MsF d_SeF d_PrF d_Sc1 ...
    d_Sc2 d_Lut1 d_Lut2 d_Lut3 d_Lut4]';
```

C.5 mergede3.m

```
%Equivalent to mergede.m, but called by external.m, to model
%    the effects of exogenous hormones
function d_merge=mergede3(t,data_in,Z,Q);

global V;
global a;
global r_LH;
global a_FSH;

alpha=Q(1); b=Q(2); c1=Q(3); c2=Q(4); c5=Q(5);
c8=Q(6); d1=Q(7); d2=Q(8); k1=Q(9); k2=Q(10);
k3=Q(11); k4=Q(12); c4=Q(13); beta=Q(14); gamma=Q(15);
v_0_LH=Q(16); v_1_LH=Q(17); Km_LH=Q(18); Ki_LH_P=Q(19); c_LH_P=Q(20);
c_LH_E=Q(21); k_LH=Q(22); v_FSH_A=Q(23); k_FSH=Q(24); c_FSH_E=Q(25);
Ki_FSH_IHA=Q(26); c_FSH_P=Q(27); e0=Q(28); e1=Q(29); e2=Q(30);
e3=Q(31); p0=Q(32); p1=Q(33); p2=Q(34); h0=Q(35); h1=Q(36);
h2=Q(37); h3=Q(38); h4=Q(39); d_E=Q(40); d_P=Q(41); d_IHA=Q(42);
startE2=Q(43); endE2=Q(44); doseE2=Q(45);
startP4=Q(46); endP4=Q(47); doseP4=Q(48);
startIHA=Q(49); endIHA=Q(50); doseIHA=Q(51);

RP_LH=data_in(1);
LH=data_in(2);
RP_FSH=data_in(3);
FSH=data_in(4);
MsF=data_in(5);
SeF=data_in(6);
PrF=data_in(7);
Sc1=data_in(8);
Sc2=data_in(9);
Lut1=data_in(10);
Lut2=data_in(11);
Lut3=data_in(12);
Lut4=data_in(13);

E2=e0+e1*SeF+e2*PrF+e3*Lut4 ...
    +doseE2*(heaviside(t-startE2)-heaviside(t-endE2));
P4=p0+p1*Lut3+p2*Lut4 ...
    +doseP4*(heaviside(t-startP4)-heaviside(t-endP4));
IHA=h0+h1*PrF+h2*Lut2+h3*Lut3+h4*Lut4 ...
    +doseIHA*(heaviside(t-startIHA)-heaviside(t-endIHA));

E2old=e0+e1*Z(6,1)+e2*Z(7,1)+e3*Z(13,1) ...
    +doseE2*(heaviside(t-d_E-startE2)-heaviside(t-d_E-endE2));
P4old=p0+p1*Z(12,2)+p2*Z(13,2) ...
    +doseP4*(heaviside(t-d_P-startP4)-heaviside(t-d_P-endP4));
```

```
IHAold=h0+h1*Z(7,3)+h2*Z(11,3)+h3*Z(12,3)+h4*Z(13,3)...
    +doseIHA*(heaviside(t-d_P-startIHA)-heaviside(t-d_P-endIHA));


syn_LH=(v_0_LH + v_1_LH*(E2old/Km_LH)^a/(1+(E2old/Km_LH)^a))/ ...
    (1+P4old/Ki_LH_P);
rel_LH=k_LH*(1+c_LH_P*P4)*RP_LH/(1+c_LH_E*E2);
d_RP_LH=syn_LH - rel_LH;
d_LH=rel_LH/V - r_LH*LH;
d_RP_FSH=(v_FSH_A/(1+IHAold/Ki_FSH_IHA))...
    -(k_FSH*(1+c_FSH_P*P4)*RP_FSH)/(1+c_FSH_E*E2^2);
d_FSH=1/V*(k_FSH*(1+c_FSH_P*P4)*RP_FSH)/(1+c_FSH_E*E2^2)...
    -a_FSH*FSH;
d_MsF=b*FSH+(c1*FSH-c2*LH^alpha)*MsF;
d_SeF=c2*LH^alpha*MsF+(c4*LH^beta-c5*LH)*SeF;
d_PrF=c5*LH*SeF-c8*LH^gamma*PrF;
d_Sc1=c8*LH^gamma*PrF-d1*Sc1;
d_Sc2=d1*Sc1-d2*Sc2;
d_Lut1=d2*Sc2-k1*Lut1;
d_Lut2=k1*Lut1-k2*Lut2;
d_Lut3=k2*Lut2-k3*Lut3;
d_Lut4=k3*Lut3-k4*Lut4;

d_merge=[d_RP_LH d_LH d_RP_FSH d_FSH d_MsF d_SeF d_PrF ...
         d_Sc1 d_Sc2 d_Lut1 d_Lut2 d_Lut3 d_Lut4]';
```

C.6 err_lsq.m

```
%Least-squares total error for five-hormone model
%
% Inputs:
% Q = parameter set
% IC = initial conditions (13)
% thedata = Welt data to measure model against (84 x 7)
%    Order is as follows: day, IHB, IHA, FSH, LH, E2, P4
%    Note that the first two columns are optional
%
% Output: total scaled error (across 84 days, five hormones)
%
% Since the units are different for each hormone,
%     they are all scaled to have a maximum point of 1,
%     for error-computation purposes.

function tot_err=err_lsq(Q,IC,thedata)
global t_0; %Starting day number (usually 0)
global t_f; %Ending day number (suggested at least 120)
global dt; %Days between mesh points (usually 0.01, but could be 0.1)
n=round(1/dt);
final=1+n*t_f;
t=[t_0:dt:t_f];

IHA=thedata(:,3);
FSH=thedata(:,4);
LH=thedata(:,5);
E2=thedata(:,6);
P4=thedata(:,7);

maxdata=[max(IHA) max(FSH) max(LH) max(E2) max(P4)]';
%avgdata=[mean(IHA) mean(FSH) mean(LH) mean(E2) mean(P4)]';

E2model=zeros(length(t),1);
P4model=zeros(length(t),1);
IHAmodel=zeros(length(t),1);

sol=dde23('mergede2',Q(40:42),IC',[t_0, t_f],[],Q);
OV_out=deval(sol,t)';

RP_LH_model=OV_out(:,1);
LHmodel=OV_out(:,2);
FSHmodel=OV_out(:,4);
SeF=OV_out(:,6);
PrF=OV_out(:,7);
Lut2=OV_out(:,11);
Lut3=OV_out(:,12);
Lut4=OV_out(:,13);

for i=1:length(t)
```

```
    E2model(i)=Q(28)+Q(29)*SeF(i)+Q(30)*PrF(i)+Q(31)*Lut4(i);
    P4model(i)=Q(32)+Q(33)*Lut3(i)+Q(34)*Lut4(i);
    IHAmodel(i)=Q(35)+Q(36)*PrF(i)+Q(37)*Lut2(i)+Q(38)*Lut3(i)...
        +Q(39)*Lut4(i);
end;

[junk,peaktime]=max(LHmodel(final-83*n:final-43*n));
peaktime=peaktime+final-83*n-1; %Day of a late LH peak

sqerr=zeros(5,1);
for i=1:84
    j=peaktime+n*(i-42); %Center to LH peak
    sqerr(1)=sqerr(1)+(IHA(i)-IHAmodel(j))^2;
    sqerr(2)=sqerr(2)+(FSH(i)-FSHmodel(j))^2;
    sqerr(3)=sqerr(3)+(LH(i)-LHmodel(j))^2;
    sqerr(4)=sqerr(4)+(E2(i)-E2model(j))^2;
    sqerr(5)=sqerr(5)+(P4(i)-P4model(j))^2;
end;

%adjsqerr=sqerr./(avgdata.^2); %Scale adjusted errors to avg data values
adjsqerr=sqerr./(maxdata.^2); %Scale adjusted errors to max data values
tot_err=sum(adjsqerr);
```

C.7 E2fun.m

```
function y=E2fun(t);
%Input: t = time, in days (ideally 0 <= t <= 56)
%Output: time-dependent E_2 concentration to match the Welt data

v0=55; %Baseline E2 level
v(1)=135; %125; %Peak added amount
d(1)=13; %13.2; %Peak day
s(1)=4; %2; %Spread of peak
v(2)=60; %60;
d(2)=11; %12;
s(2)=15; %20;
v(3)=110;
d(3)=22;
s(3)=15;
for j=4:9 %Take one 28-day cycle to three cycles
    v(j)=v(j-3);
    d(j)=d(j-3)+28;
    s(j)=s(j-3);
end;
for j=10:12
    v(j)=v(j-9);
    d(j)=d(j-9)-28;
    s(j)=s(j-9);
end;

y=v0;
for j=1:12
    y=y+v(j)*exp(-(t-d(j)).^2./s(j));
end;
```

C.8 P4fun.m

```
function y=P4fun(t);
%Input: t = time, in days (ideally 0 <= t <= 56)
%Output: time-dependent P_4 concentration to match the Welt data

v0=0.4; %Baseline P4 level
v(1)=17.5; %Peak added amount
d(1)=21; %Peak day
s(1)=21; %Spread of peak
for j=2:3 %Take one 28-day cycle to three cycles
    v(j)=v(j-1);
    d(j)=d(j-1)+28;
    s(j)=s(j-1);
end;
v(4)=v(1);
d(4)=d(1)-28;
s(4)=s(1);

y=v0;
for j=1:4
    y=y+v(j)*exp(-(t-d(j)).^2./s(j));
end;
```

C.9 IHAfun.m

```
function y=IHAfun(t);
%Input: t = time, in days (ideally 0 <= t <= 56)
%Output: time-dependent IhA concentration to match the Welt data

v0=1; %Baseline IHA level
v(1)=10; %Peak added amount
d(1)=19.5; %Peak day
s(1)=30; %Spread of peak
for j=2:3 %Take one 28-cycle to three cycles
    v(j)=v(j-1);
    d(j)=d(j-1)+28;
    s(j)=s(j-1);
end;
v(4)=v(1);
d(4)=d(1)-28;
s(4)=s(1);

y=v0;
for j=1:4
    y=y+v(j)*exp(-(t-d(j)).^2./s(j));
end;
```

C.10 LHfun.m

```
function y=LHfun(t)
%Input: t = time, in days (ideally 0 <= t <= 56)
%Output: time-dependent LH concentration to match the Welt data
v0=10; %Baseline LH level
v(1)=100; %Peak added amount
d(1)=14; %13.2; %Peak day
s(1)=0.8; %2; %Spread of peak
v(2)=12; %60;
d(2)=13.5; %12;
s(2)=50; %20;
for i=3:6 %Take one 28-cycle to three cycles
    v(i)=v(i-2);
    d(i)=d(i-2)+28;
    s(i)=s(i-2);
end;
for j=7:8
    v(j)=v(j-6);
    d(j)=d(j-6)-28;
    s(j)=s(j-6);
end;


y=v0;
for j=1:8
    y=y+v(j)*exp(-(t-d(j))^2/s(j));
end;
```

C.11 FSHfun.m

```
function y=FSHfun(t)
%Input: t = time, in days (ideally 0 <= t <= 56)
%Output: time-dependent FSH concentration to match the Welt data

v0=4; %Baseline FSH level
v(1)=8.5; %Peak added amount
d(1)=5; %13.2; %Peak day
s(1)=40; %2; %Spread of peak
v(2)=11; %60;
d(2)=14; %12;
s(2)=1; %20;
v(3)=4.5;
d(3)=16.5;
s(3)=20;
for i=4:9 %Take one 28-cycle to three cycles
    v(i)=v(i-3);
    d(i)=d(i-3)+28;
    s(i)=s(i-3);
end;
for j=10:12
    v(j)=v(j-9);
    d(j)=d(j-9)-28;
    s(j)=s(j-9);
end;


y=v0;
for j=1:12
    y=y+v(j)*exp(-(t-d(j))^2/s(j));
end;
```

Appendix D

MATLAB Codes for the Six-Hormone Model

The time-dependent input function files E2fun.m, P4fun.m, IHAfun.m, LHfun.m, and FSHfun.m also apply to the unmerged six-hormone model, together with IHBfun.m.

D.1 merge6.m

```
clear;
close all;

load('welt_data');
t_data=day;

global t_0; global t_f; global dt;
t_0=0;
t_f=150;
dt=0.01;
n=round(1/dt);

%Constants
global V; V=2.5;
global a_FSH; a_FSH=8.21;
global r_LH; r_LH=14;
global a; a=8;

%RP_LH LH RP_FSH FSH PrA1 PrA2 SeF1 SeF2 PrF OvF Sc1 Sc2 Lut1 Lut2 ...
%    Lut3 Lut4
IC=[67 8.5 90 10.9 0.158 0.759 20.7 108 23.2 14.3 30 87 296 175 ...
    1376 2563];
%IC(3)=2403.96 or higher (for normal parameters) causes "blow up" case

%Parameter values for younger women data
Q(1,1:8)=[0.80 0.19 0.1818 0.0912 0.0245 0.5 0.9837 0.7145];
Q(9:16)=[0.7485 0.6672 1.62 0.605 1.0137 0.2613 0.1285 575.19];
Q(17:25)=[3888 188.02 12.36 0.015 2.44E-3 2.8128 756 1.973 107.28];
Q(26:37)=[0.601 63.34 0.3023 2.5 1.004 1 1 1 10 10.864 2.994 3.199];
Q(38:44)=[0.0835 51.77 5.10E-3 5.54E-3 1.55E-2 0.6215 2.916E-4];
Q(45:51)=[2.05E-3 0.9 3.726E-4 9.104E-4 4.149E-4 2.434E-4 29.78];
Q(52:58)=[48.48 0 6.42E-3 0.8825 0.5086 0.9156 10];

t=[t_0:dt:t_f]';
```

```
sol=dde23('newde6',[Q(56) Q(57) Q(29) Q(30)],IC',[t_0, t_f],[],Q);
OV_out=deval(sol,t)';

RP_LH_model=OV_out(:,1);
LHmodel=OV_out(:,2);
FSHmodel=OV_out(:,4);
PrA2=OV_out(:,6);
SeF2=OV_out(:,8);
PrF=OV_out(:,9);
OvF=OV_out(:,10);
Lut2=OV_out(:,14);
Lut3=OV_out(:,15);
Lut4=OV_out(:,16);

for i=1:length(t)
    E2model(i)=Q(39)+Q(40)*SeF2(i)+Q(41)*PrF(i)+Q(42)*Lut4(i);
    P4model(i)=Q(43)+Q(44)*Lut3(i)+Q(45)*Lut4(i);
    IHAmodel(i)=Q(46)+Q(47)*PrF(i)+Q(48)*Lut2(i)+Q(49)*Lut3(i)...
                +Q(50)*Lut4(i);
    IHBmodel(i)=Q(51)+Q(52)*PrA2(i)+Q(53)*PrF(i)+Q(54)*OvF(i);
end;

en=1+(t_f-t_0)*n;
[junk,LHpk2]=max(LHmodel(en-40*n:en));
LHpeak2=LHpk2+(en-40*n-1); %Frame number
[junk,LHpk1]=max(LHmodel(LHpeak2-40*n:LHpeak2-5*n));
LHpeak1=LHpeak2-40*n-1+LHpk1;
LHper=(LHpeak2-LHpeak1)*dt

%Repeat with parameter change
%Make any desired changes to parameter set Q here
Q(1)=0.85; %Example of such a change

sol=dde23('newde6',[Q(56) Q(57) Q(29) Q(30)],IC',[t_0, t_f],[],Q);
OV_out=deval(sol,t)';

RP_LH_model_rep=OV_out(:,1);
LHrep=OV_out(:,2);
FSHrep=OV_out(:,4);
PrA2_rep=OV_out(:,6);
SeF2_rep=OV_out(:,8);
PrF_rep=OV_out(:,9);
OvF_rep=OV_out(:,10);
Lut2_rep=OV_out(:,14);
Lut3_rep=OV_out(:,15);
Lut4_rep=OV_out(:,16);

for i=1:length(t)
    E2rep(i)=Q(39)+Q(40)*SeF2_rep(i)+Q(41)*PrF_rep(i)+Q(42)*Lut4_rep(i);
    P4rep(i)=Q(43)+Q(44)*Lut3_rep(i)+Q(45)*Lut4_rep(i);
    IHArep(i)=Q(46)+Q(47)*PrF_rep(i)+Q(48)*Lut2_rep(i)...
              +Q(49)*Lut3_rep(i)+Q(50)*Lut4_rep(i);
```

```
    IHBrep(i)=Q(51)+Q(52)*PrA2_rep(i)+Q(53)*PrF_rep(i)+Q(54)*OvF_rep(i);
end;

[junk,LHpk2rep]=max(LHrep(en-40*n:en));
LHpeak2rep=LHpk2rep+(en-40*n-1); %Frame number
[junk,LHpk1rep]=max(LHrep(LHpeak2rep-40*n:LHpeak2rep-5*n));
LHpeak1rep=LHpeak2rep-40*n-1+LHpk1rep;
LHper_rep=(LHpeak2rep-LHpeak1rep)*dt %Period length

%Center to data for plotting 84 days
[junk,tc]=max(LHmodel(n*(t_f-72):n*(t_f-42)));
tc=tc+n*(t_f-72)-1;
[junk,tcrep]=max(LHrep(n*(t_f-72):n*(t_f-42)));
tcrep=tcrep+n*(t_f-72)-1;
txa=tc-42*n;
txb=tc+42*n;
txc=tcrep-42*n;
txd=tcrep+42*n;

figure(1);
plot(t_data(1:84),E2data(1:84),'k.',[0:dt:84],E2model(txa:txb),'k-.');
hold on;
plot([0:dt:84],E2rep(txc:txd),'k-');
axis([0 84 0 260]);
title('\fontsize{14} \bf E_2 Model');
%legend('Data','Model');
xlabel('\fontsize{12} \bf Time (days)');
ylabel('\fontsize{12} \bf E_2 (pg/mL)');

figure(2);
plot(t_data(1:84),P4data(1:84),'k.',[0:dt:84],P4model(txa:txb),'k-.');
hold on;
plot([0:dt:84],P4rep(txc:txd),'k-');
axis([0 84 0 19]);
title('\fontsize{14} \bf P_4 Model');
%legend('Data','Model');
xlabel('\fontsize{12} \bf Time (days)');
ylabel('\fontsize{12} \bf P_4 (ng/mL)');

figure(3);
plot(t_data(1:84),IHAdata(1:84),'k.',[0:dt:84],IHAmodel(txa:txb),'k-.');
hold on;
plot([0:dt:84],IHArep(txc:txd),'k-');
axis([0 84 0 13]);
title('\fontsize{14} \bf IhA Model');
%legend('Data','Model');
xlabel('\fontsize{12} \bf Time (days)');
ylabel('\fontsize{12} \bf IhA (IU/mL)');

figure(4);
plot(t_data(1:84),LHdata(1:84),'k.',[0:dt:84],LHmodel(txa:txb),'k-.');
hold on;
```

```
plot([0:dt:84],LHrep(txc:txd),'k-');
axis([0 84 0 140]);
title('\fontsize{14} \bf LH Model');
%legend('Data','Model');
xlabel('\fontsize{12} \bf Time (days)');
ylabel('\fontsize{12} \bf LH (IU/L)');

figure(5);
plot(t_data(1:84),FSHdata(1:84),'k.',[0:dt:84],FSHmodel(txa:txb),'k-.');
hold on;
plot([0:dt:84],FSHrep(txc:txd),'k-');
axis([0 84 4 21]);
%axis tight;
title('\fontsize{14} \bf FSH Model');
%legend('Data','Model');
xlabel('\fontsize{12} \bf Time (days)');
ylabel('\fontsize{12} \bf FSH (IU/L)');

figure(6);
plot(t_data(1:84),IHBdata(1:84),'k.',[0:dt:84],IHBmodel(txa:txb),'k-.');
hold on;
plot([0:dt:84],IHBrep(txc:txd),'k-');
axis([0 84 0 180]);
title('\fontsize{14} \bf IhB Model');
%legend('Data','Model');
xlabel('\fontsize{12} \bf Time (days)');
ylabel('\fontsize{12} \bf IhB (pg/mL)');
```

D.2 old_vs_young.m

```
clear all;
close all;

load('welt_data_both'); %Younger & older women data
t_data=[1:84];

global t_0; global t_f; global dt;
t_0=0; t_f=150; dt=0.01;
n=round(1/dt);

%Constants
global V; V=2.5;
global a_FSH; a_FSH=8.21;
global r_LH; r_LH=14;

IC=[67 8.5 90 10.9 .158 .76 20.7 108 23.2 14.3 30 87 296 175 1376 2563];

%Older women parameters
Q(1,1:8)=[0.8467 0.19 0.1818 0.0912 0.0245 0.5 0.9837 0.7145];
Q(9:16)=[0.7485 0.6672 1.62 0.605 1.0137 0.2613 0.1285 575.19];
Q(17:25)=[3888 188.02 12.36 0.015 2.44E-3 2.8128 756 1.973 107.28];
Q(26:37)=[0.601 63.34 0.3023 2.5 1.004 1 1 1 10 10.864 2.994 3.199];
Q(38:44)=[0.0835 51.77 3.81E-3 6.85E-3 1.55E-2 0.6215 2.916E-4];
Q(45:51)=[2.05E-3 0.9 2.86E-4 4.16E-4 3.80E-4 2.35E-4 18.32];
Q(52:58)=[34.30 0 3.41E-3 0.8825 0.5086 0.9156 10];

t=[t_0:dt:t_f]';
sol=dde23('newde6',[Q(56) Q(57) Q(29) Q(30)],IC',[t_0, t_f],[],Q);
OV_out=deval(sol,t)';

RP_LH_model=OV_out(:,1);
LHmodel=OV_out(:,2);
FSHmodel=OV_out(:,4);
PrA2=OV_out(:,6);
SeF2=OV_out(:,8);
PrF=OV_out(:,9);
OvF=OV_out(:,10);
Lut2=OV_out(:,14);
Lut3=OV_out(:,15);
Lut4=OV_out(:,16);

for i=1:length(t)
    E2model(i)=Q(39)+Q(40)*SeF2(i)+Q(41)*PrF(i)+Q(42)*Lut4(i);
    P4model(i)=Q(43)+Q(44)*Lut3(i)+Q(45)*Lut4(i);
    IHAmodel(i)=Q(46)+Q(47)*PrF(i)+Q(48)*Lut2(i)+Q(49)*Lut3(i)...
                +Q(50)*Lut4(i);
    IHBmodel(i)=Q(51)+Q(52)*PrA2(i)+Q(53)*PrF(i)+Q(54)*OvF(i);
end;
```

```
terr_base=err6(Q,IC,older_data.all)

en=1+(t_f-t_0)*n;
[junk,LHpk2]=max(LHmodel(en-40*n:en));
LHpeak2=LHpk2+(en-40*n-1); %Frame number
[junk,LHpk1]=max(LHmodel(LHpeak2-40*n:LHpeak2-5*n));
LHpeak1=LHpeak2-40*n-1+LHpk1;
LHper=(LHpeak2-LHpeak1)*dt

%Younger women parameters
Q(1:8)=[0.80 0.19 0.1818 0.0912 0.0245 0.5 0.9837 0.7145];
Q(9:16)=[0.7485 0.6672 1.62 0.605 1.0137 0.2613 0.1285 575.19];
Q(17:25)=[3888 188.02 12.36 0.015 2.44E-3 2.8128 756 1.973 107.28];
Q(26:37)=[0.601 63.34 0.3023 2.5 1.004 1 1 1 10 10.864 2.994 3.199];
Q(38:44)=[0.0835 51.77 5.10E-3 5.54E-3 1.55E-2 0.6215 2.916E-4];
Q(45:51)=[2.05E-3 0.9 3.726E-4 9.104E-4 4.149E-4 2.434E-4 29.78];
Q(52:58)=[48.48 0 6.42E-3 0.8825 0.5086 0.9156 10];


sol=dde23('newde6',[Q(56) Q(57) Q(29) Q(30)],IC',[t_0, t_f],[],Q);
OV_out=deval(sol,t)';

RP_LH_model_rep=OV_out(:,1);
LHrep=OV_out(:,2);
FSHrep=OV_out(:,4);
PrA2_rep=OV_out(:,6);
SeF2_rep=OV_out(:,8);
PrF_rep=OV_out(:,9);
OvF_rep=OV_out(:,10);
Lut2_rep=OV_out(:,14);
Lut3_rep=OV_out(:,15);
Lut4_rep=OV_out(:,16);

for i=1:length(t)
    E2rep(i)=Q(39)+Q(40)*SeF2_rep(i)+Q(41)*PrF_rep(i)+Q(42)*Lut4_rep(i);
    P4rep(i)=Q(43)+Q(44)*Lut3_rep(i)+Q(45)*Lut4_rep(i);
    IHArep(i)=Q(46)+Q(47)*PrF_rep(i)+Q(48)*Lut2_rep(i)...
              +Q(49)*Lut3_rep(i)+Q(50)*Lut4_rep(i);
    IHBrep(i)=Q(51)+Q(52)*PrA2_rep(i)+Q(53)*PrF_rep(i)...
              +Q(54)*OvF_rep(i);
end;

terr_rep=err6(Q,IC,younger_data.all)

[junk,LHpk2rep]=max(LHrep(en-40*n:en));
LHpeak2rep=LHpk2rep+(en-40*n-1); %Frame number
[junk,LHpk1rep]=max(LHrep(LHpeak2rep-40*n:LHpeak2rep-5*n));
LHpeak1rep=LHpeak2rep-40*n-1+LHpk1rep;
LHper_rep=(LHpeak2rep-LHpeak1rep)*dt
%End of repeat
```

```
%Center for 28-day plot
[junk,tc]=max(LHmodel(n*(t_f-72):n*(t_f-42)));
tc=tc+n*(t_f-72)-1;
[junk,tcrep]=max(LHrep(n*(t_f-72):n*(t_f-42)));
tcrep=tcrep+n*(t_f-72)-1;
txe=tc-14*n;
txf=tc+14*n;
txg=tcrep-14*n;
txh=tcrep+14*n;

%Older women have solid circles and solid lines
%Younger women have open circles and broken lines
figure(1);
plot(t_data(28:56)-28,younger_data.E2(28:56),'ok',[28:dt:56]-
28,E2rep(txg:txh),'-.k','MarkerSize',4);
hold on;
plot(t_data(28:56)-28,older_data.E2(28:56),'ok',[28:dt:56]-
28,E2model(txe:txf),'-k','MarkerSize',4,'MarkerFaceColor','k');
axis ([0 28 0 350]);
title('\fontsize{14} \bf E_2 Model');
xlabel('\fontsize{12} \bf Time (days)');
ylabel('\fontsize{12} \bf E_2 (pg/mL)');

figure(2);
plot(t_data(28:56)-28,younger_data.P4(28:56),'ok',[28:dt:56]-
28,P4rep(txg:txh),'-.k','MarkerSize',4);
hold on;
plot(t_data(28:56)-28,older_data.P4(28:56),'ok',[28:dt:56]-
28,P4model(txe:txf),'-k','MarkerSize',4,'MarkerFaceColor','k');
axis ([0 28 0 20]);
title('\fontsize{14} \bf P_4 Model');
xlabel('\fontsize{12} \bf Time (days)');
ylabel('\fontsize{12} \bf P_4 (ng/mL)');

figure(3);
plot(t_data(28:56)-28,younger_data.IHA(28:56),'ok',[28:dt:56]-
28,IHArep(txg:txh),'-.k','MarkerSize',4);
hold on;
plot(t_data(28:56)-28,older_data.IHA(28:56),'ok',[28:dt:56]-
28,IHAmodel(txe:txf),'-k','MarkerSize',4,'MarkerFaceColor','k');
axis ([0 28 0 12]);
title('\fontsize{14} \bf IhA Model');
xlabel('\fontsize{12} \bf Time (days)');
ylabel('\fontsize{12} \bf IhA (IU/mL)');

figure(4);
plot(t_data(28:56)-28,younger_data.LH(28:56),'ok',[28:dt:56]-
28,LHrep(txg:txh),'-.k','MarkerSize',4);
hold on;
plot(t_data(28:56)-28,older_data.LH(28:56),'ok',[28:dt:56]-
28,LHmodel(txe:txf),'-k','MarkerSize',4,'MarkerFaceColor','k');
axis ([0 28 0 160]);
```

```
title('\fontsize{14} \bf LH Model');
xlabel('\fontsize{12} \bf Time (days)');
ylabel('\fontsize{12} \bf LH (IU/L)');

figure(5);
plot(t_data(28:56)-28,younger_data.FSH(28:56),'ok',[28:dt:56]-
28,FSHrep(txg:txh),'-.k','MarkerSize',4);
hold on;
plot(t_data(28:56)-28,older_data.FSH(28:56),'ok',[28:dt:56]-
28,FSHmodel(txe:txf),'-k','MarkerSize',4,'MarkerFaceColor','k');
axis ([0 28 0 26]);
title('\fontsize{14} \bf FSH Model');
xlabel('\fontsize{12} \bf Time (days)');
ylabel('\fontsize{12} \bf FSH (IU/L)');

figure(6);
plot(t_data(28:56)-28,younger_data.IHB(28:56),'ok',[28:dt:56]-
28,IHBrep(txg:txh),'-.k','MarkerSize',4);
hold on;
plot(t_data(28:56)-28,older_data.IHB(28:56),'ok',[28:dt:56]-
28,IHBmodel(txe:txf),'-k','MarkerSize',4,'MarkerFaceColor','k');
axis ([0 28 0 180]);
title('\fontsize{14} \bf IhB Model');
xlabel('\fontsize{12} \bf Time (days)');
ylabel('\fontsize{12} \bf IhB (pg/mL)');
```

D.3 external6.m

```
clear;
close all;

load('welt_data');
t_data=day;

global t_0; global t_f; global dt;
t_0=0;
t_f=128;
dt=0.01;
n=round(1/dt);

%Constants
global V; V=2.5;
global a_FSH; a_FSH=8.21;
global r_LH; r_LH=14;
global a; a=8;

Q(1,1:8)=[0.80 0.19 0.1818 0.0912 0.0245 0.5 0.9837 0.7145];
Q(9:16)=[0.7485 0.6672 1.62 0.605 1.0137 0.2613 0.1285 575.19];
Q(17:25)=[3888 188.02 12.36 0.015 2.44E-3 2.8128 756 1.973 107.28];
Q(26:37)=[0.601 63.34 0.3023 2.5 1.004 1 1 1 10 10.864 2.994 3.199];
Q(38:44)=[0.0835 51.77 5.10E-3 5.54E-3 1.55E-2 0.6215 2.916E-4];
Q(45:51)=[2.05E-3 0.9 3.726E-4 9.104E-4 4.149E-4 2.434E-4 29.78];
Q(52:58)=[48.48 0 6.42E-3 0.8825 0.5086 0.9156 10];

%External introduction of hormones
startE2=0.001; %Day number to start E2 dose
endE2=180.001; %Day number to end E2 dose
doseE2=50; %Dosage amount (bloodstream concentration increase)
startP4=0.001;
endP4=180.001;
doseP4=0;
Q(59:64)=[startE2 endE2 doseE2 startP4 endP4 doseP4]';

IC=[67 8.5 90 10.9 .158 .759 20.7 108 23 14 30 87 296 175 1376 2563];

t=[t_0:dt:t_f]';
sol=dde23('newde_ext',[Q(56) Q(57) Q(29) Q(30)],IC',[t_0, t_f],[],Q);
OV_out=deval(sol,t)';

RP_LH_model=OV_out(:,1);
LHmodel=OV_out(:,2);
FSHmodel=OV_out(:,4);
PrA2=OV_out(:,6);
SeF2=OV_out(:,8);
PrF=OV_out(:,9);
OvF=OV_out(:,10);
Lut2=OV_out(:,14);
```

```
Lut3=OV_out(:,15);
Lut4=OV_out(:,16);

for i=1:length(t)
    E2model(i)=Q(39)+Q(40)*SeF2(i)+Q(41)*PrF(i)+Q(42)*Lut4(i)...
         +doseE2*(heaviside(t(i)-startE2)-heaviside(t(i)-endE2));
    P4model(i)=Q(43)+Q(44)*Lut3(i)+Q(45)*Lut4(i)...
         +doseP4*(heaviside(t(i)-startP4)-heaviside(t(i)-endP4));
    IHAmodel(i)=Q(46)+Q(47)*PrF(i)+Q(48)*Lut2(i)+Q(49)*Lut3(i)...
         +Q(50)*Lut4(i);
    IHBmodel(i)=Q(51)+Q(52)*PrA2(i)+Q(53)*PrF(i)+Q(54)*OvF(i);
end;

en=1+(t_f-t_0)*n;
[junk,LHpk2]=max(LHmodel(en-40*n:en));
LHpeak2=LHpk2+(en-40*n-1); %Frame number
[junk,LHpk1]=max(LHmodel(LHpeak2-40*n:LHpeak2-5*n));
LHpeak1=LHpeak2-40*n-1+LHpk1;
LHper=(LHpeak2-LHpeak1)*dt

%Repeat with no external hormones
Q(61)=0; doseE2=0; Q(64)=0; doseP4=0;

sol=dde23('newde_ext',[Q(56) Q(57) Q(29) Q(30)],IC',[t_0, t_f],[],Q);
OV_out=deval(sol,t)';

RP_LH_model_rep=OV_out(:,1);
LHrep=OV_out(:,2);
FSHrep=OV_out(:,4);
PrA2_rep=OV_out(:,6);
SeF2_rep=OV_out(:,8);
PrF_rep=OV_out(:,9);
OvF_rep=OV_out(:,10);
Lut2_rep=OV_out(:,14);
Lut3_rep=OV_out(:,15);
Lut4_rep=OV_out(:,16);

for i=1:length(t)
    E2rep(i)=Q(39)+Q(40)*SeF2_rep(i)+Q(41)*PrF_rep(i)+Q(42)*...
     Lut4_rep(i)+doseE2*(heaviside(t(i)-startE2)-heaviside(t(i)-endE2));
    P4rep(i)=Q(43)+Q(44)*Lut3_rep(i)+Q(45)*Lut4_rep(i)+doseP4...
             *(heaviside(t(i)-startP4)-heaviside(t(i)-endP4));
    IHArep(i)=Q(46)+Q(47)*PrF_rep(i)+Q(48)*Lut2_rep(i)...
             +Q(49)*Lut3_rep(i)+Q(50)*Lut4_rep(i);
    IHBrep(i)=Q(51)+Q(52)*PrA2_rep(i)+Q(53)*PrF_rep(i)+Q(54)*OvF_rep(i);
end;

[junk,LHpk2rep]=max(LHrep(en-40*n:en));
LHpeak2rep=LHpk2rep+(en-40*n-1); %Frame number
[junk,LHpk1rep]=max(LHrep(LHpeak2rep-40*n:LHpeak2rep-5*n));
LHpeak1rep=LHpeak2rep-40*n-1+LHpk1rep;
LHper_rep=(LHpeak2rep-LHpeak1rep)*dt
%End of repeat
```

```
day_start=28; day_end=128; tot=day_end-day_start;
yy=1+day_start*n;
zz=1+day_end*n;
t=[0:dt:tot];

t_p=min(t_f,84);
figure(1);
plot(t,E2model(yy:zz),'-k',t,E2rep(yy:zz),'-.k');
title('\fontsize{14} \bf E_2 Model');
xlabel('\fontsize{12} \bf Time (days)');
ylabel('\fontsize{12} \bf E_2 (pg/mL)');

figure(2);
plot(t,P4model(yy:zz),'-k',t,P4rep(yy:zz),'-.k');
title('\fontsize{14} \bf P_4 Model');
xlabel('\fontsize{12} \bf Time (days)');
ylabel('\fontsize{12} \bf P_4 (ng/mL)');

figure(3);
plot(t,IHAmodel(yy:zz),'-k',t,IHArep(yy:zz),'-.k');
title('\fontsize{14} \bf IhA Model');
xlabel('\fontsize{12} \bf Time (days)');
ylabel('\fontsize{12} \bf IhA (IU/mL)');

figure(4);
plot(t,LHmodel(yy:zz),'-k',t,LHrep(yy:zz),'-.k');
title('\fontsize{14} \bf LH Model');
xlabel('\fontsize{12} \bf Time (days)');
ylabel('\fontsize{12} \bf LH (IU/L)');

figure(5);
plot(t,FSHmodel(yy:zz),'-k',t,FSHrep(yy:zz),'-.k');
title('\fontsize{14} \bf FSH Model');
xlabel('\fontsize{12} \bf Time (days)');
ylabel('\fontsize{12} \bf FSH (IU/L)');

figure(6);
plot(t,IHBmodel(yy:zz),'-k',t,IHBrep(yy:zz),'-.k');
title('\fontsize{14} \bf IhB Model');
xlabel('\fontsize{12} \bf Time (days)');
ylabel('\fontsize{12} \bf IhB (pg/mL)');
```

D.4 err6.m

```
function tot_err=err6(Q,IC,thedata)
%Compute error of model compared to data
%Input: parameter set Q
%       initial conditions IC
%       data set "thedata"
%Output: a single number indicating total error

IHB=thedata(:,2);
IHA=thedata(:,3);
FSH=thedata(:,4);
LH=thedata(:,5);
E2=thedata(:,6);
P4=thedata(:,7);

global t_0; global t_f; global dt;
n=round(1/dt);
final=1+n*t_f;
t=[t_0:dt:t_f];

maxdata=[max(IHB) max(IHA) max(FSH) max(LH) max(E2) max(P4)]';
%avgdata=[mean(IHB) mean(IHA) mean(FSH) mean(LH) mean(E2) mean(P4)]';

E2model=zeros(length(t),1);
P4model=zeros(length(t),1);
IHAmodel=zeros(length(t),1);
IHBmodel=zeros(length(t),1);

sol=dde23('newde6',[Q(56) Q(57) Q(29) Q(30)],IC',[t_0, t_f],[],Q);
OV_out=deval(sol,t)';

LHmodel=OV_out(:,2);
FSHmodel=OV_out(:,4);
PrA2=OV_out(:,6);
SeF2=OV_out(:,8);
PrF=OV_out(:,9);
OvF=OV_out(:,10);
Lut2=OV_out(:,14);
Lut3=OV_out(:,15);
Lut4=OV_out(:,16);

for i=1:length(t)
    E2model(i)=Q(39)+Q(40)*SeF2(i)+Q(41)*PrF(i)+Q(42)*Lut4(i);
    P4model(i)=Q(43)+Q(44)*Lut3(i)+Q(45)*Lut4(i);
    IHAmodel(i)=Q(46)+Q(47)*PrF(i)+Q(48)*Lut2(i)+Q(49)*Lut3(i)...
                +Q(50)*Lut4(i);
    IHBmodel(i)=Q(51)+Q(52)*PrA2(i)+Q(53)*PrF(i)+Q(54)*OvF(i);
end;
```

```
[junk,peaktime]=max(LHmodel(final-83*n:final-43*n));
peaktime=peaktime+final-83*n-1; %Day of a late LH peak

sqerr=zeros(6,1);
for i=1:84
    j=peaktime+n*(i-42); %Center to LH peak
    sqerr(1)=sqerr(1)+(IHB(i)-IHBmodel(j))^2;
    sqerr(2)=sqerr(2)+(IHA(i)-IHAmodel(j))^2;
    sqerr(3)=sqerr(3)+(FSH(i)-FSHmodel(j))^2;
    sqerr(4)=sqerr(4)+(LH(i)-LHmodel(j))^2;
    sqerr(5)=sqerr(5)+(E2(i)-E2model(j))^2;
    sqerr(6)=sqerr(6)+(P4(i)-P4model(j))^2;
end;
%adjsqerr=sqerr./(avgdata.^2); %Scale errors based on avg data values
adjsqerr=sqerr./(maxdata.^2); %Scale errors based on max data values
tot_err=sum(adjsqerr);
```

D.5 newde6.m

```
function d_merge=mergede2(t,data_in,Z,Q);

global V;
global r_LH;
global a_FSH;

alpha=Q(1); c1=Q(2); c2=Q(3); c3=Q(4); c4=Q(5); c5=Q(6);
c6=Q(7); d1=Q(8); d2=Q(9); k1=Q(10); k2=Q(11); k3=Q(12);
k4=Q(13); beta=Q(14);  gamma=Q(15); v_0_LH=Q(16); v_1_LH=Q(17);
Km_LH=Q(18); Ki_LH_P=Q(19); c_LH_P=Q(20); c_LH_E=Q(21); k_LH=Q(22);
v_FSH=Q(23); Ki_FSH_IHA=Q(24); Ki_FSH_IHB=Q(25); k_FSH=Q(26);
c_FSH_P=Q(27); c_FSH_E=Q(28); d_IHA=Q(29); d_IHB=Q(30);
exp_IHA=Q(31); exp_IHB=Q(32); exp_E2=Q(33);
b=Q(34); f1=Q(35); f2=Q(36); f3=Q(37); f4=Q(38);
e0=Q(39); e1=Q(40); e2=Q(41); e3=Q(42); p0=Q(43); p1=Q(44);
p2=Q(45); h0=Q(46); h1=Q(47); h2=Q(48); h3=Q(49); h4=Q(50);
j0=Q(51); j1=Q(52); j2=Q(53); j3=Q(54); delta=Q(55);
d_E=Q(56); d_P=Q(57); a=Q(58);

RP_LH=data_in(1);
LH=data_in(2);
RP_FSH=data_in(3);
FSH=data_in(4);
PrA1=data_in(5);
PrA2=data_in(6);
SeF1=data_in(7);
SeF2=data_in(8);
PrF=data_in(9);
OvF=data_in(10);
Sc1=data_in(11);
Sc2=data_in(12);
Lut1=data_in(13);
Lut2=data_in(14);
Lut3=data_in(15);
Lut4=data_in(16);

E2=e0+e1*SeF2+e2*PrF+e3*Lut4;
P4=p0+p1*Lut3+p2*Lut4;
IHA=h0+h1*PrF+h2*Lut2+h3*Lut3+h4*Lut4;
IHB=j0+j1*PrA2+j2*PrF+j3*OvF;

E2old=e0+e1*Z(8,1)+e2*Z(9,1)+e3*Z(16,1); %index 1 means 1st delay, d_E2
P4old=p0+p1*Z(15,2)+p2*Z(16,2);
IHAold=h0+h1*Z(9,3)+h2*Z(14,3)+h3*Z(15,3)+h4*Z(16,3);
IHBold=j0+j1*Z(6,4)+j2*Z(9,4)+j3*Z(10,4);
```

```
syn_LH=(v_0_LH + v_1_LH*(E2old/Km_LH)^a/(1+(E2old/Km_LH)^a))/ ...
    (1+P4old/Ki_LH_P);
rel_LH=k_LH*(1+c_LH_P*P4)*RP_LH/(1+c_LH_E*E2);
d_RP_LH=syn_LH - rel_LH;
d_LH=rel_LH/V - r_LH*LH;
syn_FSH=v_FSH/...
        (1+(IHAold^exp_IHA)/Ki_FSH_IHA+(IHBold^exp_IHB)/Ki_FSH_IHB);
rel_FSH=k_FSH*(1+c_FSH_P*P4)*RP_FSH/(1+c_FSH_E*E2^exp_E2);
clear_FSH=a_FSH*FSH;
d_RP_FSH=syn_FSH-rel_FSH;
d_FSH=1/V*rel_FSH-clear_FSH;

d_PrA1=f2*(FSH/f1)^b/(1+(FSH/f1)^b)-f3*FSH*PrA1;
d_PrA2=f3*FSH*PrA1-f4*LH^delta*PrA2;
d_SeF1=f4*LH^delta*PrA2+[c1*FSH-c2*LH^alpha]*SeF1;
d_SeF2=c2*LH^alpha*SeF1+(c3*LH^beta-c4*LH)*SeF2;
d_PrF=c4*LH*SeF2-c5*LH^gamma*PrF;
d_OvF=c5*LH^gamma*PrF-c6*OvF;
d_Sc1=c6*OvF-d1*Sc1;
d_Sc2=d1*Sc1-d2*Sc2;
d_Lut1=d2*Sc2-k1*Lut1;
d_Lut2=k1*Lut1-k2*Lut2;
d_Lut3=k2*Lut2-k3*Lut3;
d_Lut4=k3*Lut3-k4*Lut4;


d_merge=[d_RP_LH d_LH d_RP_FSH d_FSH d_PrA1 d_PrA2 d_SeF1 d_SeF2 ...
         d_PrF d_OvF d_Sc1 d_Sc2 d_Lut1 d_Lut2 d_Lut3 d_Lut4]';
```

D.6 newde_ext.m

```
function d_merge=newde_ext(t,data_in,Z,Q);
%For testing the effects of external hormones

global V; global r_LH; global a_FSH;

alpha=Q(1); c1=Q(2); c2=Q(3); c3=Q(4); c4=Q(5); c5=Q(6);
c6=Q(7); d1=Q(8); d2=Q(9); k1=Q(10); k2=Q(11); k3=Q(12);
k4=Q(13); beta=Q(14);  gamma=Q(15); v_0_LH=Q(16); v_1_LH=Q(17);
Km_LH=Q(18); Ki_LH_P=Q(19); c_LH_P=Q(20); c_LH_E=Q(21); k_LH=Q(22);
v_FSH=Q(23); Ki_FSH_IHA=Q(24); Ki_FSH_IHB=Q(25); k_FSH=Q(26);
c_FSH_P=Q(27); c_FSH_E=Q(28); d_IHA=Q(29); d_IHB=Q(30);
exp_IHA=Q(31); exp_IHB=Q(32); exp_E2=Q(33);
b=Q(34); f1=Q(35); f2=Q(36); f3=Q(37); f4=Q(38);
e0=Q(39); e1=Q(40); e2=Q(41); e3=Q(42); p0=Q(43); p1=Q(44);
p2=Q(45); h0=Q(46); h1=Q(47); h2=Q(48); h3=Q(49); h4=Q(50);
j0=Q(51); j1=Q(52); j2=Q(53); j3=Q(54); delta=Q(55);
d_E=Q(56); d_P=Q(57); a=Q(58); startE2=Q(59); endE2=Q(60);
doseE2=Q(61); startP4=Q(62); endP4=Q(63); doseP4=Q(64);

RP_LH=data_in(1);
LH=data_in(2);
RP_FSH=data_in(3);
FSH=data_in(4);
PrA1=data_in(5);
PrA2=data_in(6);
SeF1=data_in(7);
SeF2=data_in(8);
PrF=data_in(9);
OvF=data_in(10);
Sc1=data_in(11);
Sc2=data_in(12);
Lut1=data_in(13);
Lut2=data_in(14);
Lut3=data_in(15);
Lut4=data_in(16);

E2=e0+e1*SeF2+e2*PrF+e3*Lut4+doseE2...
   *(heaviside(t-startE2)-heaviside(t-endE2));
P4=p0+p1*Lut3+p2*Lut4+doseP4*(heaviside(t-startP4)-heaviside(t-endP4));
IHA=h0+h1*PrF+h2*Lut2+h3*Lut3+h4*Lut4;
IHB=j0+j1*PrA2+j2*PrF+j3*OvF;

%index 1 represents 1st delay (d_E), 2 for 2nd (d_P), etc.
E2old=e0+e1*Z(8,1)+e2*Z(9,1)+e3*Z(16,1)...
      +doseE2*(heaviside(t-d_E-startE2)-heaviside(t-d_E-endE2));
P4old=p0+p1*Z(15,2)+p2*Z(16,2)...
      +doseP4*(heaviside(t-d_P-startP4)-heaviside(t-d_P-endP4));
```

```
IHAold=h0+h1*Z(9,3)+h2*Z(14,3)+h3*Z(15,3)+h4*Z(16,3);
IHBold=j0+j1*Z(6,4)+j2*Z(9,4)+j3*Z(10,4);

syn_LH=(v_0_LH + v_1_LH*(E2old/Km_LH)^a/(1+(E2old/Km_LH)^a))/ ...
    (1+P4old/Ki_LH_P);
rel_LH=k_LH*(1+c_LH_P*P4)*RP_LH/(1+c_LH_E*E2);
d_RP_LH=syn_LH - rel_LH;
d_LH=rel_LH/V - r_LH*LH;
syn_FSH=v_FSH/...
       (1+(IHAold^exp_IHA)/Ki_FSH_IHA+(IHBold^exp_IHB)/Ki_FSH_IHB);
rel_FSH=k_FSH*(1+c_FSH_P*P4)*RP_FSH/(1+c_FSH_E*E2^exp_E2);
clear_FSH=a_FSH*FSH;
d_RP_FSH=syn_FSH-rel_FSH;
d_FSH=1/V*rel_FSH-clear_FSH;

d_PrA1=f2*(FSH/f1)^b/(1+(FSH/f1)^b)-f3*FSH*PrA1;
d_PrA2=f3*FSH*PrA1-f4*LH^delta*PrA2;
d_SeF1=f4*LH^delta*PrA2+[c1*FSH-c2*LH^alpha]*SeF1;
d_SeF2=c2*LH^alpha*SeF1+(c3*LH^beta-c4*LH)*SeF2;
d_PrF=c4*LH*SeF2-c5*LH^gamma*PrF;
d_OvF=c5*LH^gamma*PrF-c6*OvF;
d_Sc1=c6*OvF-d1*Sc1;
d_Sc2=d1*Sc1-d2*Sc2;
d_Lut1=d2*Sc2-k1*Lut1;
d_Lut2=k1*Lut1-k2*Lut2;
d_Lut3=k2*Lut2-k3*Lut3;
d_Lut4=k3*Lut3-k4*Lut4;


d_merge=[d_RP_LH d_LH d_RP_FSH d_FSH d_PrA1 d_PrA2 d_SeF1 d_SeF2 ...
         d_PrF d_OvF d_Sc1 d_Sc2 d_Lut1 d_Lut2 d_Lut3 d_Lut4]';
```

D.7 ovary6.m

```
clear;
close all;

load('welt_data');
t_data=day;

global t_0; global t_f; global dt;
t_0=0; t_f=28; dt=0.1;

alpha=0.7736; c1=0.173; c2=0.144; c3=0.012;
c4=.0115; c5=0.7; c6=2; d1=0.672; d2=0.568;
k1=0.550; k2=1.3; k3=1.3; k4=1.3; beta=0.157;
gamma=0.1; delta=alpha;
a=8; f1=11; f2=1.5; f3=1/2; f4=1/20;
e0=55; e1=0.005; e2=0.0083; e3=0.019;
p0=0.6; p1=0; p2=0.0042;
h0=1; h1=0.00047; h2=0.0023; h3=0; h4=0;
j0=30; j1=55; j2=0; j3=0.013;

Q=[alpha c1 c2 c4 c5 d1 d2 k1 k2 k3 k4 c3 beta gamma a f1 f2 ...
   delta f3 f4 c6];
IC=[0.04 0.15 1 1 1 1 1 1 1 1 1 1]'; %Initial conditions
[t,OV_out]=ode15s('ovary6de',[t_0:dt:t_f],IC,[],Q);

PrA1=OV_out(:,1);
PrA2=OV_out(:,2);
SeF2=OV_out(:,4);
PrF=OV_out(:,5);
OvF=OV_out(:,6);
Lut2=OV_out(:,10);
Lut3=OV_out(:,11);
Lut4=OV_out(:,12);

for i=1:length(t)
    E2model(i)=e0+e1*SeF2(i)+e2*PrF(i)+e3*Lut4(i);
    P4model(i)=p0+p1*Lut3(i)+p2*Lut4(i);
    IHAmodel(i)=h0+h1*PrF(i)+h2*Lut2(i)+h3*Lut3(i)+h4*Lut4(i);
    IHBmodel(i)=j0+j1*PrA2(i)+j2*PrF(i)+j3*OvF(i);
end;

figure(1);
plot(t_data(1:28),E2data(1:28),'xk',t,E2model,'k-');
%title('\fontsize{14} \bf E_2 Model');
axis([0 28 0 240]);
xlabel('\fontsize{10} \bf Time (days)');
ylabel('\fontsize{10} \bf E_2 (pg/mL)');
```

```
figure(2);
plot(t_data(1:28),P4data(1:28),'xk',t,P4model,'k-');
%title('\fontsize{14} \bf P_4 Model');
axis([0 28 0 20]);
xlabel('\fontsize{10} \bf Time (days)');
ylabel('\fontsize{10} \bf P_4 (ng/mL)');

figure(3);
plot(t_data(1:28),IHAdata(1:28),'xk',t,IHAmodel,'k-');
%title('\fontsize{14} \bf IhA Model');
axis([0 28 0 12]);
xlabel('\fontsize{10} \bf Time (days)');
ylabel('\fontsize{10} \bf IhA (IU/mL)');

figure(4);
plot(t_data(1:28),IHBdata(1:28),'xk',t,IHBmodel,'k-');
%title('\fontsize{14} \bf IhB Model');
axis([0 28 0 200]);
xlabel('\fontsize{10} \bf Time (days)');
ylabel('\fontsize{10} \bf IhB (pg/mL)');
```

D.8 ovary6de.m

```
function d_ovary=ovary6de(t,data_in,flag,Q);

alpha=Q(1); c1=Q(2); c2=Q(3); c4=Q(4); c5=Q(5);
d1=Q(6); d2=Q(7); k1=Q(8); k2=Q(9); k3=Q(10);
k4=Q(11); c3=Q(12); beta=Q(13); gamma=Q(14); b=Q(15);
f1=Q(16); f2=Q(17); delta=Q(18); f3=Q(19); f4=Q(20); c6=Q(21);

PrA1=data_in(1);
PrA2=data_in(2);
SeF1=data_in(3);
SeF2=data_in(4);
PrF=data_in(5);
OvF=data_in(6);
Sc1=data_in(7);
Sc2=data_in(8);
Lut1=data_in(9);
Lut2=data_in(10);
Lut3=data_in(11);
Lut4=data_in(12);

d_PrA1=f2*(FSHfun(t)/f1)^b/(1+(FSHfun(t)/f1)^b)-f3*FSHfun(t)*PrA1;
d_PrA2=f3*FSHfun(t)*PrA1-f4*LHfun(t)^delta*PrA2;
d_SeF1=f4*LHfun(t)^delta*PrA2+[c1*FSHfun(t)-c2*LHfun(t)^alpha]*SeF1;
d_SeF2=c2*LHfun(t)^alpha*SeF1+(c3*LHfun(t)^beta-c4*LHfun(t))*SeF2;
d_PrF=c4*LHfun(t)*SeF2-c5*LHfun(t)^gamma*PrF;
d_OvF=c5*LHfun(t)^gamma*PrF-c6*OvF;
d_Sc1=c6*OvF-d1*Sc1;
d_Sc2=d1*Sc1-d2*Sc2;
d_Lut1=d2*Sc2-k1*Lut1;
d_Lut2=k1*Lut1-k2*Lut2;
d_Lut3=k2*Lut2-k3*Lut3;
d_Lut4=k3*Lut3-k4*Lut4;

d_ovary=[d_PrA1 d_PrA2 d_SeF1 d_SeF2 d_PrF d_OvF d_Sc1 d_Sc2 ...
         d_Lut1 d_Lut2 d_Lut3 d_Lut4]';
```

D.9 IHBfun.m

```
function y=IHBfun(t);

%t=mod(t,28);

v0=30; %Baseline IHB level
v(1)=117; %Peak added amount
d(1)=15; %Peak day
s(1)=2; %Spread of peak
v(2)=125;
d(2)=7;
s(2)=35;

for j=3:6 %Take one 28-day cycle to three cycles
    v(j)=v(j-2);
    d(j)=d(j-2)+28;
    s(j)=s(j-2);
end;
for j=7:8
    v(j)=v(j-6);
    d(j)=d(j-6)-28;
    s(j)=s(j-6);
end;

y=v0;
for j=1:8
    y=y+v(j)*exp(-(t-d(j)).^2./s(j));
end;
```